Tacrine, trolox and tryptoline as lead compounds for the design and synthesis of multi-target drugs for Alzheimer's disease therapy.

Gerard A. Kenfack Teponnou

A dissertation submitted in partial fulfilment of the requirements for the degree
MASTER IN PHARTMACEUTICAL CHEMISTRY.

Supervisor: Prof Sarel F. Malan

Co-supervisor: Prof J. Joubert

April 2016

UNIVERSITY *of the*
WESTERN CAPE

PHARMACEUTICAL CHEMISTRY, SCHOOL OF PHARMACY, UNIVERSITY
OF THE WESTERN CAPE, PRIVATE BAG X17, BELLVILLE, 7535.

Dedicated to my late grandmothers, Makougou Christine, my late aunt's husband, Tiegoh Jean de Dieu and my late brothers and sisters: Makeugue Alliance Belise, Yougang Pascal, Tchebonssou Celine and Kenfack Raymon.

KEYWORDS

Alzheimer's disease

Amyloid Beta

Cholinesterases

Molecular docking

Multifactorial disease

Multifunctional drugs

Multi-target directed ligand

Reactive oxygen species

Tacrine

Trolox

Tryptoline

DECLARATION

I declare that "*Tacrine, trolox and tryptoline as lead compounds for the design and synthesis of multi-target drugs for Alzheimer's disease therapy"* is my own work and that it has not been submitted for any other degree or examination at any other university, and that all the sources I have used or quoted have been indicated and acknowledged by complete reference.

Full name researcher…………………………………………………………..

Date……………………………………….

UNIVERSITY *of the*

WESTERN CAPE

ii

ABSTRACT

The cascade of neurotoxic events involved in the pathogenesis of Alzheimer's disease may explain the inefficacy of currently available treatment based on acetylcholinesterase inhibitors (AChEI - donepezil, galantamine, rivastigmine) and N-methyl-D-aspartate (NMDA) antagonists (memantine). These drugs were designed based on the "one-molecule-one-target" paradigm and only address a single target. Conversely, the multi-target drug design strategy increasingly gains recognition. Based on the versatile biological activities of tacrine, trolox and β-carboline derivatives, the attention they have received as lead structures for the design of multifunctional drugs for the treatment of Alzheimer's disease, and the topology of the active site of AChE, we have designed tacrine-trolox and tacrine-tryptoline hybrids with various linker chain lengths. The aim with these hybrids was to provide additive or synergistic therapeutic effects that might help overcome the limitation of current anti Alzheimer's disease drugs.

All synthesized compounds were designed from lead structures (tacrine, tryptoline and trolox) to obtain cholinesterase (ChE) multisite binders and multifunctional AD agents. The study was rationalized by docking all structures in the active site of TcAChE using Molecular Operating Environment (MOE) software before proceeding with the synthesis. ChE inhibition was assessed in a UV enzyme inhibition assay using Ellman's method. Anti-oxidant activities were assessed using the 2, 2-diphenyl-1-picrylhydrazyl (DPPH·) absorbance assay.

The hybrids containing the trolox moiety (compounds **8a-e**) showed moderate to high AChE inhibitory activity in the nano to micro molar range (IC_{50}: 17.37 - 2200 nM), BuChE inhibition was observed in the same range (IC_{50}: 3.16 – 128.82 nM), and free radical scavenging activities in micro molar range (IC_{50}: 11.48 – 49.23 µM). These are comparable or slightly higher than their reference compounds donepezil (AChE IC_{50} = 220 nM), tacrine (BuChE IC_{50}: 14.12 nM), and trolox (DPPH IC_{50}: 17.57 µM). The hybrids with longer linker chain lengths, 6 and 8 carbons (**8d** and **8e**), showed better ChE inhibitory activity than the shorter ones, 2, 3, and 4 carbons (**8a-c** respectively). This correlates well with literature. Free radical scavenging activities, however, seems not to be significantly affected by varying linker chain lengths. The hybrid compound (**14**) containing the tryptoline moiety linked with a 7 carbon spacer displayed the best AChE and BuChE inhibitory activity (IC_{50} = 17.37 and

iii

3.16 nM) but poor free radical scavenging activity. Novel anti-Alzheimer's disease drugs with multi-target neuroprotective activities were thus obtained and hybrid molecules that exhibit good ChE inhibition (**8d**, **8e** and **14**) and anti-oxidant (**8d** and **8e**) activity were identified as suitable candidates for further investigation.

UNIVERSITY *of the*

WESTERN CAPE

ACKNOWLEDGEMENTS

To conclude my thesis, I would like to thank all the people who made this work possible and an unforgettable experience for me.

I would like to express my gratitude to my supervisor Prof Sarel F. Malan and my co-supervisor Prof Jacques Joubert for the useful comments, remarks, patience, motivation and engagement through the learning process of this program.

My sincere gratitude also goes to the following people Dr Edith Beukes for assisting in Nuclear Magnetic Resonance processing, Mr Yunus Kippie for assisting in Mass spectrometry and Infra-Red processing and Mrs Audrey Ramplin for introducing me in the pharmaceutical laboratory and for her support all the way.

I would also like to extend my profound gratitude to Mr Sharma Rajan for all guidance in the Laboratory and all his helpful advice during my masters' study.

I am thankful to my family, my parents, my brothers and sisters for supporting me throughout writing this thesis and my life in general.

I thank my fellow laboratory mates for the stimulating discussions, for all the fun we have had in the last two years, and for providing me with unfailing support and continuous encouragement throughout my two years of study and through the process of researching and writing this thesis. This accomplishment would not have been possible without them. Thank you.

A special thanks to H. Moyo Lindelwe and Irene Denya, all in School of Pharmacy / University of the Western Cape, for helping in first editing of my thesis. Wish you good luck for your project.

I acknowledge the School of Pharmacy, University of the Western Cape for the conducive environment they provide for my study. I am very thankful for that.

TABLE OF CONTENTS

viii

UNIVERSITY *of the*

WESTERN CAPE

ix

LIST OF FIGURES

LIST OF TABLES

ABBREVIATIONS

^{13}C-NMR	carbon 13 Nuclear Magnetic Resonance
AAs	amino acids
ACE	Angiotensin Converting Enzyme
Ach	acetylcholine
AChE	acetylcholinesterase
AChEI	acetylcholinesterase inhibitors
AD	Alzheimer's disease
AICD	APP intracellular domain
APP	amyloid precursor protein
ATR	Attenuated Total Reflectance
Aβ	amyloid β peptide
BACE	β-site APP cleaving enzyme
BBB	Blood Brain Barrier
bs	broad singlet
BuChE	butyrylcholinesterase
CAS	catalytic active site
Cdk5	cyclin dependant kinase 5
ChAT	choline acetyltransferase
ChE	cholinesterase
ChEI	cholinesterase inhibitor
CNS	central nervous system
CSF	cerebrospinal fluid
CuBD	copper / metal binding domain
d	doublet
dd	doublet of doublet
DNA	Deoxyribonucleic Acid
dt	doublet of triplet
FDA	Food Drugs Administration
GPI	Glycogen phosphatidyl inositol anchored
GPX	glutathione peroxidase
GSK 3	glycogen synthase kinase 3

HACU	high affinity choline-uptake
HBD	heparin binding domain
HD- SCAs	Huntington's disease spinal cerebellar ataxia
Hz	Hertz
IC_{50}	inhibition concentration to halt 50 % activity
IR	Infra-Red radiation Spin-Spin
J	spin-spin coupling constant (Hz)
KPI	Kunitz-type protease inhibitor
LRP1	Low density Lipoprotein Receptor-Related 1
m/s	mass to charge ratio
MAO	monoamine oxidase
MAO-A	monoamine oxidase A
MAO-B	monoamine oxidase B
MAOI	monoamine oxidase inhibitor
MAP	microtubule-associated protein
MAPKs	Mitogen-Activated Protein Kinase
MCI	mild cognitive impairment
MOE	Molecular Operating Environment.
MOP	myeloperoxidase
MRI	magnetic resonance imaging
MS	mass spectrometry
MT	microtubules
MTDLs	multi-target directed ligand
NADH	Nicotinamide Adenine Dinucleotide plus Hydrogen
NFTs	neurofibrillary tangles
NMDA	N-methyl-D-aspartate
NMJ	neuromuscular junction
P^{25}	protein 25
P^{35}	protein 35
PAS	peripheral anionic site
PHF	paired helical filaments
PNS	peripheral nervous system
PP2A / 1 / 5	phosphatase 2A / 1 / 5

ppm	parts-per-million
PTM	Post Translational Modification
RAGE	Receptor for Advance Glycation and End product
Rf	retention factor
ROS	reactive oxygen species
rt	room temperature
SOD	superoxide dismutase
SPs	senile plaques
t	triplet
TAP 43	TAR DNA-binding protein 43
*Tc*AChE	*Torpedo californica* AChE
TLC	thin layer chromatography
TMD	transmembrane domain
α / β-CTF	α / β-secretase cleaved C-terminal fragment

UNIVERSITY *of the*

WESTERN CAPE

CHAPTER 1.

INTRODUCTION

1.1 Alzheimer's disease

Alzheimer's disease (AD) is a chronic, multifactorial disease of the central nervous system (CNS). It was first described by the German neuropsychiatrist Alois Alzheimer in 1906 (**Ricerca, 2009**). Its characteristic symptoms include short-term memory impairment at the beginning, which worsens as the disease progresses and eventually leads to severe cognitive and physical disability (**Silvestrelli *et al.,* 2006**). AD represents the main cause of dementia and no curative drug is available. To date, it is estimated that 36.6 million people worldwide are suffering from the disease. This number is expected to double or triple by 2030 and 2050 respectively if aggressive, exceptional and well-funded efforts to prevent, diagnose and cure the disease are not made (**Duthey, 2013**). The sequence of molecular events that underlies the occurrence of AD is still a mystery. Current hypotheses from many investigations suggest a decrease in the level of the neurotransmitter acetylcholine (ACh) in the brain regions involved in learning and memory, β-amyloid plaque formation (Aβ), oxidative stress, neuroinflammation and aggregation of tau protein (τ-protein) (**Skovronsky *et al.,* 2006; Crews and Masliah, 2010**).

The current treatment of AD is limited to acetylcholinesterase inhibitor (AChEI) drugs (donepezil, galantamine and rivastigmine) and an *N*-methyl-D-aspartate (NMDA) antagonist (memantine). These drugs have been identified based on the "one-molecule-one target" paradigm and they offer only symptomatic treatment but do not stop the progression of the disease (**Capurro *et al.,* 2013**). In light of the different mechanisms involved in the pathogenesis of AD, this strategy has been questioned recently. Considerable efforts are now devoted to search for single drugs with multifunctional activities. So far, none of the innovative candidate drugs have survived clinical trials due to lack of satisfactory efficacy and toxicity issues (**Capurro *et al.,* 2013**). Therefore, the identification of safer and cost-effective disease-modifying drugs remains an open challenge for drug discovery.

1

1.2   Rational for the design of tacrine-tryptoline and tacrine-trolox hybrids

1.2.1 Lead compounds: Tacrine, Tryptoline and Trolox

Tacrine was the first AChEI drug approved by the US Food Drug Administration (FDA) for the treatment of AD before being withdrawn from the market due to toxicity issues **(Thiratmatrakul *et al.,* 2014).** Its therapeutic effect normalizes the levels of acetylcholine (ACh) in the synaptic cleft. Recent studies have demonstrated that lead optimization of tacrine in the design of novel AD drugs can improve its biological profile and alleviate its hepatotoxicity. Based on these studies, tacrine appears to be a suitable lead compound for the design of multitarget drugs because of its privileged structure, its efficacy and its low molecular weight **(Inglot *et al.,* 2013)**.

Trolox is an analogue of Vitamin E (α-tocopherol) with well documented antioxidant capacity. Besides this therapeutic virtue, trolox has the ability to prevent neurotoxicity induced by Aβ and hydrogen peroxide (H_2O_2) **(Radesätera *et al.,* 2003)**. Another source revealed that trolox could inhibit glycogen synthase kinase3β (GSK 3β) whose hyperactivity causes neurofibrillary tangle (NFTs) formation **(Mun *et al.,* 2002)**. These different biological activities of trolox acknowledge and consolidate its neuroprotective capacity and make it an excellent lead for the design of multifunctional drugs for treating AD.

Tryptoline is a β-carboline derivative. Beta-carbolines are a group of alkaloids first discovered in plants. Later, it was found that they could be formed in the human body from tryptamine derivatives **(Baiget *et al*., 2011)**. Previous research has shown that they have a large range of biological activities associated with target proteins involved in the pathogenesis of AD **(Herraiz *et al.,* 2010)**. The conjugation of tacrine to tryptoline with an appropriate spacer may thus provide a novel multitarget strategy for the treatment of AD.

1.2.2 Multitarget Directed Ligand design strategy - Cholinesterase dual binders

The multitarget directed ligand paradigm is based on the design of a single molecule with the ability to modulate multiple targets simultaneously **(Simoni *et al., 2012)*.** Acetylcholinesterase (AChE) and butyrylcholinesterase (BuChE) are the major

cholinesterases in vertebrates. They are so called due to their higher selectivity to acetylcholine (Ach) and butyrylcholine respectively. Their function is to hydrolyse the cholinergic neurotransmitter acetylcholine after it has terminated its activity (**Greig *et al*., 2001**). The depletion of ACh level in AD due to inability of the cholinergic system to maintain constant the level of ACh has legitimized cholinesterase inhibitors as a useful option for the symptomatic treatment of AD. Accumulation of evidence have demonstrated that cholinesterase play a double role in AD pathology defined by the topology of their active sites. Cholinesterase have got two distinct binding sites (**Agis-torres *et al*., 2014**): The peripheral anionic site (PAS) which is believed to induce Aβ aggregation and the catalytic anionic site (CAS) which is involved in the hydrolysis of Ach (**Figure 1.1) (Agis-torres *et al*., 2014**). Currently, accumulation of Aβ in specific regions of the brain is believed to be the main factor that triggers the cascade of neurotoxic conditions leading to AD. Therefore, a molecule that can span both the PAS and CAS may achieve symptomatic treatment and also stop disease progression.
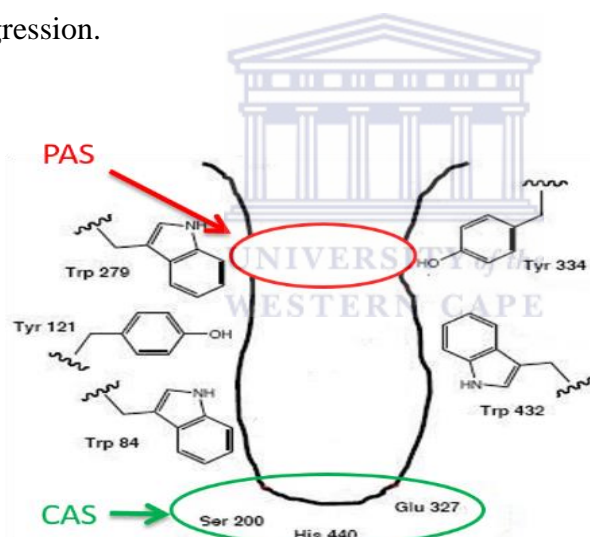
Figure 1.1: Illustration of the binding sites of *Torpedo californica* AChE (*Tc*AChE) and selected conserved aromatic residues: Ser200, His440 and Glu327 are the catalytic triad amino acid residues responsible for the hydrolysis of choline substrate while Trp279, Tyr334 are aromatic residues involved in the binding interaction (Tedwilliams, 2006).

The multifactorial aspect of AD questions the design strategy of the current treatments. Drugs that affect only a single target are not capable of modifying disease progression. Multitarget drugs are thus increasingly gaining recognition. Tacrine is a very attractive lead compound that has successfully been used in the multitarget design strategy. It has ChEI activity and additional biological activity such as monoamine oxidase inhibition (MAOI) and ion channel modulating ability (**Kozurkova *et al.*, 2011**). Trolox possesses potent antioxidant activity and it is also capable of reducing neurotoxicity induced by Aβ and H_2O_2 (**Radesätera *et al.*,**

2003). Tryptoline is a β-carboline derivative, therefore could modulate ChE, MAO, CdK5, DYRK1A and NMDAR activity **(Frost *et al.,* 2011)**. Based on the topology of the active site of ChE we hypothesized that the combination of tacrine with trolox or tryptoline through linkers of varied chain lengths may yield two series of multisite binder hybrid compounds (tacrine-trolox and tacrine-tryptoline) with the ability to interfere with a large spectrum in the disease network. It is expected that in both cases, tacrine's pharmacophore will undergo stacking interaction with conserved aromatic residues in the CAS of ChE necessary for ChE inhibition while trolox or tryptoline will undergo H-π or stacking interaction respectively with conserved aromatic residues in the PAS necessary for the prevention of ChE-induced Aβ aggregation (**Figure 1.1**).   Varying the linker chain length seeks the appropriate fitting of pharmacophores in the active site of the ChE target that will achieve useful activity. The aim with these hybrids is to provide additive or synergistic therapeutic effects that might help overcome the limitation of current anti-Alzheimer's disease drugs **(Figure 1.2).** The study was rationalized by docking all structures in the active site of AChE using Molecular Operating Environment software (MOE) before proceeding with the synthesis.
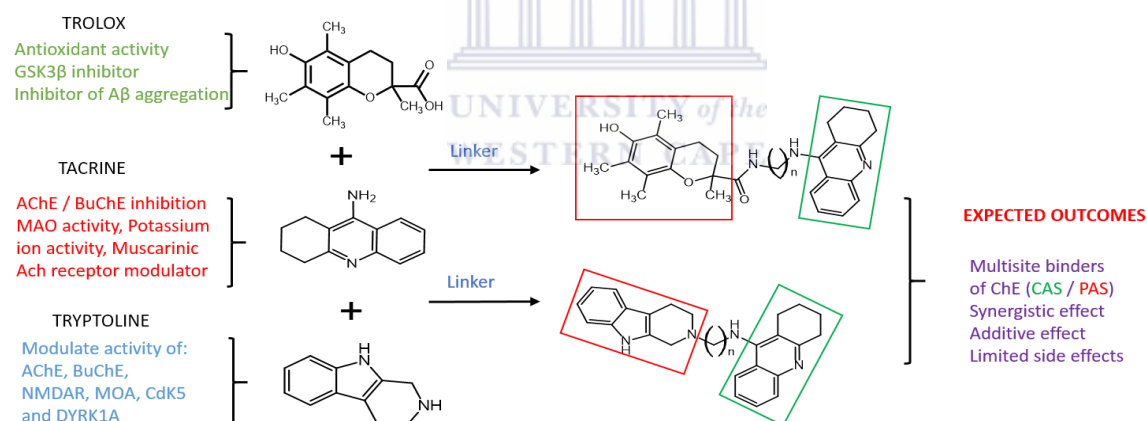
Figure 1.2: Diagram illustrating the rational of the hybridization of tacrine-trolox, tacrine-tryptoline and expected outcomes.

1.3   Aim of the study

Referring to recent hypotheses, Alzheimer's disease results from the disturbance of many signalling pathways in the nervous system. Therefore, disease modifying drugs should be developed with the ability to interfere with or to modulate these multiple pathways with limited harmful effects. The study will be articulated around the following points:

- Selection of the lead compounds from the literature.

- Design of the hybrid compounds (lead optimization).

- Modelling studies to rationalize the study using molecular modelling.

- Synthesis of the hybrid compounds.

- Biological evaluation of the capacity of the synthesized (**Figure 1.3**) compounds to inhibit ChE and to scavenge free radicals.
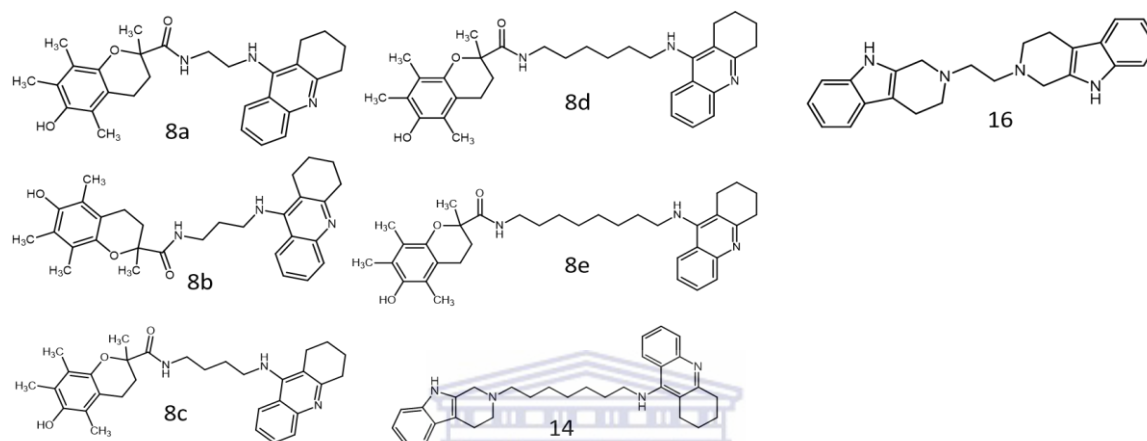
Figure 1.3: Structures of synthesized and tested compounds according to the synthesis procedure.

It is presumed that each of these hybrid compounds will display multifunctional activity on target proteins involved in the pathogenesis of AD. Regarding the present study, the biological evaluation of these hybrids will be limited to acetylcholinesterase and butyrylcholinesterase inhibitory activity and free radical scavenging ability.

CHAPTER 2.

LITERATURE REVIEW

2.1 Introduction

In this chapter, the risk factors of AD and distribution will be discussed. In addition, the pathophysiology and current hypothesis explaining the aetiology of AD, which is the basis of therapeutic intervention, will be assessed. Multitarget directed ligand paradigms as alternative drug design strategies to overcome the limitation of current treatment options of AD will also be evaluated. This chapter will be concluded with arguments that guided the choice of lead compounds of the study namely tacrine, trolox and tryptoline.

2.2 Epidemiology

Epidemiological studies are concerned with the investigation of the occurrence of the disease or health-related conditions in a defined population (**Bartlett and Judge, 1997**). The principle of epidemiological studies is based on the measurement of disease frequency and distribution, precisely, its prevalence and its incidence in a given population. Data generated from epidemiological findings provides evidence that aids public health or community decision makers in designing new approaches for controlling, preventing and treating diseases (**Ray, 2010**). To date, it is estimated that 36.6 million people over 65 years of age worldwide are suffering from AD. This number is expected to double or triple by 2030 and 2050 respectively (**Duthey, 2013**). Old age is the major risk factor for AD. The proportion of patients with AD in the United States in 2015 (**Figure 2.1**) shows age-related increases in the prevalence of AD of 4% (65 years); 15% (< 65-74 years); 48% (75-84 years) and 38% (85+) (**Alzheimer's Association, 2015**).
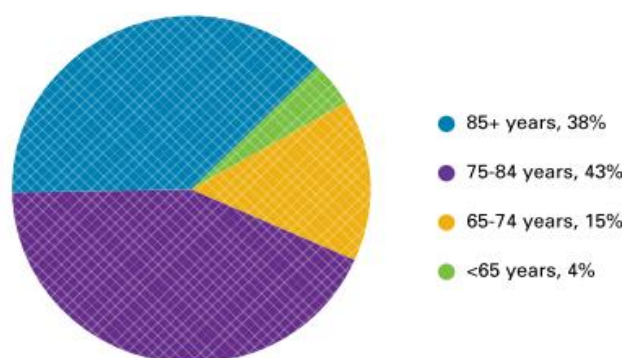
Figure 2.1: Circular diagram showing ages of patients suffering from AD in the United States of America in 2015 (Alzheimer's Association, 2015).

The reason is that at senescence, random effects (chronic internal or external stress) cause gradual increase in non-repair cellular damage, which weakens the cellular repair mechanism and perturbs the equilibrium in cell homeostasis (**Kent, 1983**). These events accumulate over time and are believed to increase the vulnerability of predisposed individuals to the development of AD (**Hindle, 2010; Swerdlow, 2011**). As aging is the strongest risk factor for AD, women are disproportionately affected. One of the explanations may be associated to their higher longevity. The biological explanation may be associated to inherent differences between sexes such as anatomy, genetics and hormones. This includes women's brain anatomy and physiology being more open to pathological lesions with lower cognitive reserve (**Carter *et al.,* 2012**). Moreover, the depletion of oestrogen levels in post-menopausal women increase their risk of AD, since, oestrogen has been found to up-regulate the expression of anti-oxidative enzyme in pre-menopausal women (**Carter *et al.,* 2012**). This finding is supported by the efficacy of oestrogen usage for the prevention or delay of AD in early post-menopausal women (**Simpkins *et al*., 2009**). Data from epidemiological studies have revealed low level of education as another risk factor for AD (**Tyas *et al*., 2001**). These studies are supported by the cognitive reserve hypothesis (**Alzheimer's Association, 2013**). Others risk factors for AD include cardiovascular diseases, type 2 diabetes, brain injuries, genetic factors such as mutations on genes like β-amyloid precursor protein gene (APP), presenilin genes (involved in the early-onset of AD) and inheritance of the isoform ε_4 allele of the apolipoprotein E (involved in the late-onset of AD) (**Reitz *et al.*, 2012**) .

2.3 Pathophysiology

Pathophysiology is a branch of human biology that studies the physiology of the diseased body or that seeks to know how the diseased body works. Thorough comprehension of

7

pathophysiology is indispensable in understanding the disease progression and its mechanism. It is useful, moreover, in helping to assess non-specific toxicity of therapeutic intervention **(Jackson-Siegal, 2005)**. More research still needs to be done to fully comprehend the pathophysiology of AD and the mechanism that promises to uncover new strategies for diagnosing, preventing, or finding novel molecules that could stop the disease progression. Extracellular deposition of β-amyloid (Aβ) fibrils in senile plaques (SPs), accumulation of hyperphosphorylated τ-protein filaments in NFTs and death of neuronal cells are well-documented mean factors that characterize the neurodegenerative process on a micro level **(Morrison and Lyketsos, 2005; Morley and Farr, 2014; Hong-qi *et al.,* 2012).** These molecular events are distributed in particular regions within the brain, which are believed to be involved in memory (hippocampus) and cognition (cerebral cortex) as depicted in **Figure 2.2**.
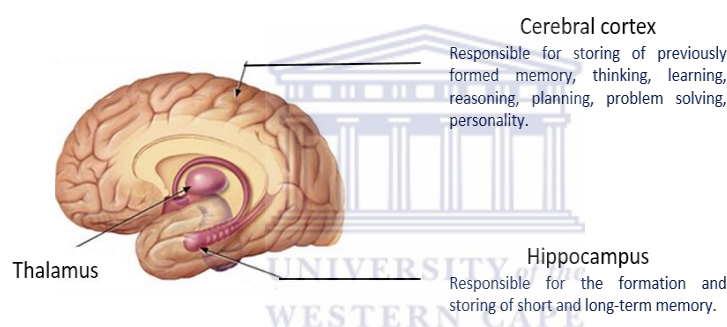
Figure 2.2: Side view of the brain showing major areas affected in AD. Adapted from (Alzheimer's Society, 2012).

Death of neuronal cells which may commence years before memory disturbance, on a macro level, is characterized by histopathological changes studied by magnetic resonance imaging (MRI) or positron emission tomographic (PET), and include shrinking of the brain, enlargement of ventricle and presence of cerebrospinal fluid in empty space created by brain atrophies **(Wang *et al*., 2006) (Figure 2.3)**.
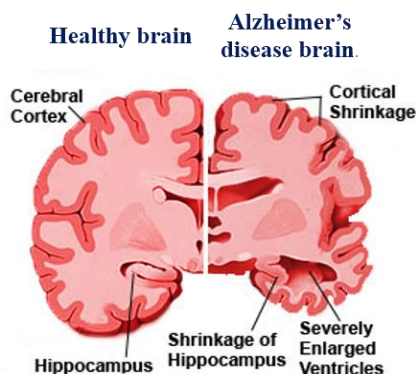
Figure 2.3: Histopathological changes in AD brain compared to healthy brain (Medindia, 2013).

These structural changes expand as the disease progress to other regions of the brain and are generally accompanied by the presence of τ-protein and Aβ in the blood or cerebrospinal fluid **(Medindia, 2013).** These pathological conditions are responsible for the progressive clinical symptoms displayed by AD patients, from mild or early stage, to severe stage as described in **Table 2-1**.

Table 2-1: Description of different stages of AD and their clinical symptoms associated. MCI stands for mild cognitive impairment (Chetelat and Baron, 2003).

AD stages	Clinical symptoms
MCI or early stage	Difficulties in remembering familiar places, people, and time; misplacing things, difficulties in deciding; mood changes; communication problem.
Moderate or middle stage	Difficulties in accomplishing complex tasks (cooking, shopping, driving etc.); communication problem worsens; become aggressive and agitated, personality change.
Severe or late stage	Ignore time and place; cannot recognize relatives and friends, objects, experience difficulties in swallowing become totally dependent (eating, moving) on care support and supervision, incontinence.

2.4 Aetiology

The mystery that surrounds the cause of AD has not been totally uncovered since its discovery and numerous hypotheses have been suggested to explain how the disease occurs **(Kent, 1983)**. The most influential of these hypotheses, specifically those that pay the

9

greatest attention to the prevention and diagnosis of AD, as well as the development of safe and effective pharmacological treatments will be discussed in the following section.

2.4.1 Cholinergic hypothesis

The term cholinergic refers to that part of the neuronal system involved in the synthesis, storage and hydrolysis of the neurotransmitter acetylcholine (ACh). The period 1960s to 1980s witnessed combined research efforts in different domains of neurosciences leading to the discovery and the characterization of the cholinergic and other important neuronergic systems. Based on evidence from these global research efforts, the correlation between the alteration of the neurotransmitter systems and neuropathology has gained full recognition (**Contestabile, 2010**). Evidence from this research approach have revealed that characteristic symptoms caused by degeneration of cholinergic neurones in selective regions (cortex, hippocampus and amygdala) in the brain of AD patients, is as a result of the reduction in the activity of choline acetyltransferase (ChAT), an enzyme involved in the synthesis of acetylcholine. It is also due to a decrease in the activity of the high affinity choline-uptake (HACU) system which functions as a precursor of the substrate choline for the synthesis of acetylcholine in the neuronal cell, a decrease in the level of the neurotransmitter ACh and an alteration of the functions of other components of the cholinergic system (**Kasa *et al.,* 1997**). The results of these studies substantiate the role of ACh in cognition. Studies in human and non-human primates demonstrating that memory loss induced by blocking the cholinergic system with scopolamine can be reversed by an AChEI such as physostigmine, together led to the development of the "cholinergic hypothesis" (**Craig *et al*., 2011**). In light of these studies, and though the cholinergic hypothesis is not the primary cause of AD, depletion of acetylcholine levels appears to contribute significantly to cognitive impairment in AD. This explains the rationale of inhibiting cholinesterase as an important aspect of therapeutic intervention.

2.4.1.1 Acetylcholinesterase: structure, localization, function and mechanism of action

Acetylcholinesterase (AChE) is a member of the cholinesterase family of proteins that hydrolyse cholinesters more rapidly than other substrates. There are two major cholinesterases in vertebrates: AChE and butyrylcholinesterase (BuChE). AChE derives its

name from its higher specificity in hydrolysing acetylcholine. AChE, like other cholinesterases, is reversibly and irreversibly inhibited by natural carbamate alkaloids (physostigmine) and organophosphates such as diisopropylflurophosphate (DFP) respectively (**Massoulié *et al.,* 1993**).

2.4.1.1.1 Structure

AChE was first purified and crystalized in 1991 from the *Torpedo California (Tc).* electric organ (**Dvir *et al*., 2010**). This electric organ was chosen as source of enzyme because of its capacity to hydrolyse amounts of acetylcholine equivalent to up to three times its weight in an hour (**Mortimer *et al*., 1947**), hence an abundant source of AChE. *Tc*AChE displays structural characteristics common to alpha / beta hydrolase fold enzymes that consist essentially of beta sheets connected by alpha helices (**Figure 2.4**). In the active site of *Tc*AChE is found a catalytic triad consisting of Ser200, His440 and Glu327 or aspartate. This catalytic triad is involved in the hydrolysis of the substrate acetylcholine and is buried at the bottom of a 20 Å deep aromatic gorge. This aromatic gorge is highly conserved in different species (**Tripathi *et al.,* 2015**).
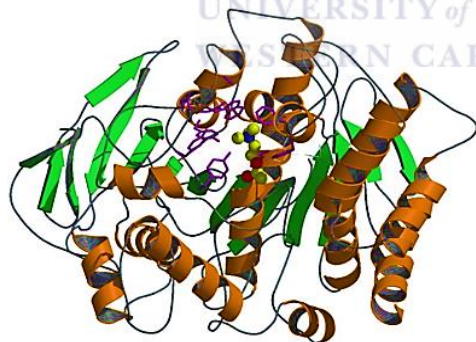
Figure 2.4: Ribbon diagram of *Tc*AChE showing anti-paralleled beta sheets (Green) connected by alpha helices (Brown) with conserved aromatic residues (purple) and its natural substrate ACh in space-filling model docked in its active site (Sussman and Silman, 2009).

These features of *Tc*AChE have been shown to be similar to human, drosophila and mouse AChE. Affinity labelling revealed cation-π interaction between the quaternary group of choline and the indole ring of Trp84. This particular residue, among other conserved residues (Phe330, Phe331), has been demonstrated to play a key role in stabilizing the charged part of the substrate entering the active gorge. AChE also possesses a secondary binding site called the peripheral anionic site (PAS) localized at the entrance of the cavity, which contains

another group of conserved aromatic residues including Trp279, Tyr121, Tyr70 and Asp72 (**Pohanka, 2011**). Its major role is to trap the substrate. A modelling study has revealed that Trp279 is highly flexible and this feature contributes to stabilizing interactions between an inhibitor that is bound to the PAS site through π-π stacking or cation-π interaction (**Xu *et al*., 2008**).

Further studies revealed that the axis of the active-site gorge of *Tc*AChE possesses a singularly large dipole moment pointed in the active-site gorge direction in such a way that it forces the positive charge of ACh down to the active site (**Sussman and Silman, 2009**). The role played by the PAS site Trp279 and CAS site Trp84 of AChE (**confer Figure 1.1**) in ligands' interaction plus studies that have demonstrated the role of the PAS site of AChE in Aβ aggregation, have led to profound changes in the design strategies of new molecules for AD therapy (**Inestrosa *et al*., 1996**). The design strategy has moved from single target drugs that bind to the CAS site to dual target compounds that span the CAS and the PAS site with double therapeutic effects that is; the prevention of Aβ aggregation and increasing the concentration of neurotransmitter ACh in the synaptic cleft (**Savini *et al*., 2003; Rook *et al*., 2010**).

2.4.1.1.2 Localization and function of AChE

A study conducted to understand the molecular and cellular biology of AChE has enabled the identification, in vertebrates and invertebrates, of different molecular forms of AChE sharing common catalytic properties, but different in their type of oligomerization, mode of adherence to the cell surface, level of expression, their localization and function (**Massoulié *et al*., 1993**). In mammals, AChE is expressed by a single gene that undergoes alternative splitting of its H (for hydrophobic) and T (for tailed) subunits to generate many forms as shown in **Figure 2.5**.
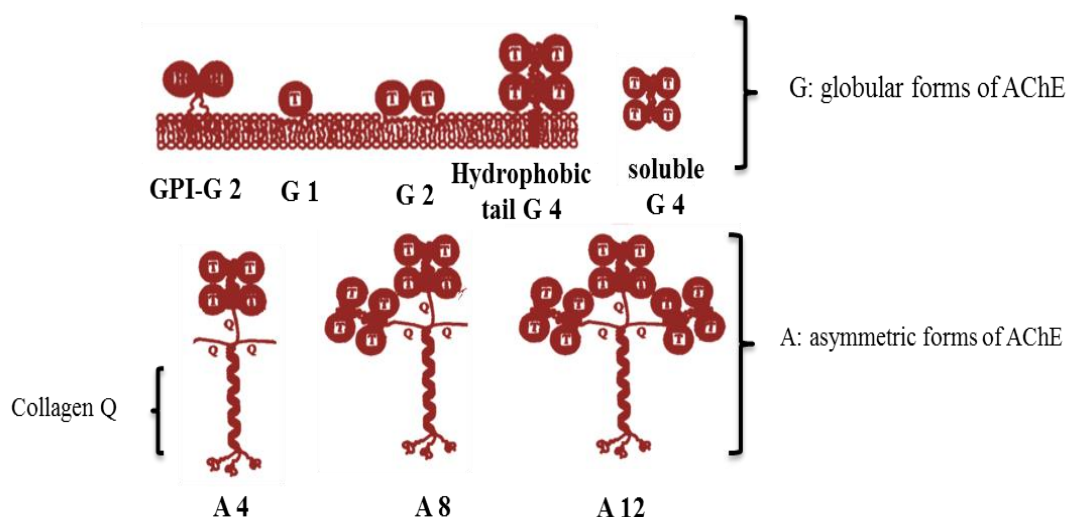
Figure 2.5: Different molecular forms of AChE splice variants (Massoulié *et al*., 1993).

The $AChE_H$ subunit generates the glycogen phosphatidyl inositol-anchored (GPI) dimers (GPI-G2). Immunohistochemistry studies have revealed the expression of this form in mammalian red blood cells (RBC), white blood cells (WBC), embryonic muscle and liver. Their localization in RBC and WBC is believed to indicate the implication of the cholinergic system in detoxication and the regulation of the immune function respectively **(Gouri, 2004; Chacko and Cerf, 1960)**. The $AChE_T$ subunit generates monomer G1, dimer G2, hydrophobic tail tetramer G4, soluble tetramer G4 and the collagen-tailed (Col Q) form. The hydrophobic tail tetramer G4 is membrane anchored and is predominantly present in the synaptic space of the mammalian brain. It is believed to be responsible for 80 to 90% AChE activity, that is, the termination of ACh activity **(Gouri, 2004)**. The decrease of AChE activity in AD patients has been correlated with decrease of the hydrophobic tail tetramer G4 form in the frontal cortex with a relative increase in the level of monomer G1, dimer G2 and soluble tetramer G4 forms, the likely intracellular precursors of mature hydrophobic tail tetramer G4 form. The collagen-tailed form results from the association of the $AChE_T$ subunit with Col Q found principally in the neuro-muscular junction (NMJ). The Col Q is the product of unit gene, which, based on the level of expression and availability of $AChE_T$ defines which type of collagen-tailed will be produced: A4, A8, or A12 (**Figure 2.5**). The A12 form is expressed in NMJ where they are involved in nerve innervation whereas A4 and A8 are expressed both in NMJ and extra junction. A study done to establish the physiological role of Col Q has revealed that a defect of expression of Col Q results in abnormal build-up of $AChE_T$ in NMJ, which desensitizes acetylcholine receptors resulting in the symptoms

13

characteristic of myasthenia **(Massoulié *et al*., 1993)**. The remarkable affinity of AChE for acetylcholine, its high activity in the cholinergic system and its implication in Aβ aggregation makes it the most attractive target for therapeutic intervention for the treatment of AD **(Lane *et al*., 2006)**.

2.4.1.1.3 Mechanism of action

The neurotransmitter acetylcholine is responsible for transmission of action potential across the cholinergic system and in the neuromuscular synapse. The physiological function of AChE in the CNS and the peripheral nervous system (PNS) is to hydrolyse ACh and terminate its action. The catalytic triad Glu327, His440 and Ser200, controls the hydrolysis as shown in **Figure 2.6**. It follows two steps; the first step involves acylation of the AChE and the second step requires one molecule of water and involves deacylation of the AChE by fast hydrolysis of acylated AChE with liberation of choline and acetic acid and regeneration of glutamate and deprotonated histidine.
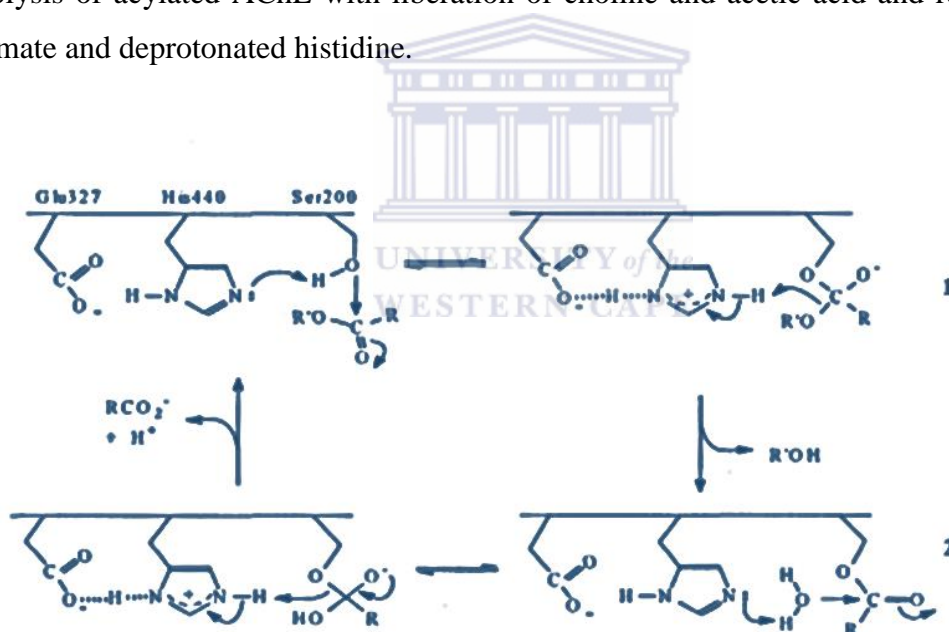
Figure 2.6: Chemical mechanism of hydrolysis of Ach by AChE with residue number of *Torpedo California* (Zhou *et al*., 2010).

2.4.1.2 Butyrylcholinesterase: structure, localisation, function and mechanism of action

BuChE derives its name from its specificity for the substrate butyrylcholine. BuChE and AChE are members of the cholinesterase family of proteins. As such, they share some common features, molecular forms, mechanisms of action (**Figure 2.6**) (observed in serine

14

hydrolase) and often an overlapping localization pattern. They also display some characteristic differences including their substrate specificity and function.

2.4.1.2.1 Structure

BuChE has a similar structure to AChE, but some important differences have been demonstrated in their substrate specificity. These enzymes share 65% amino acid sequence homology and are encoded by two different genes on human chromosome 7 (7q22, AChE) and chromosome 3 (3q26, BuChE) (**Lane *et al*., 2006**). The reason for the substrate specificity difference resides within the 35% other amino acids in their primary structure, which determine the three-dimensional size and shape of their binding and catalytic pocket (**Lane *et al*., 2006**). For instance, crystallographic studies have shown that amino acids residues Phe 288 and Phe 290 lining the gorge (acyl-binding pocket) of *Tc*AChE, are replaced by hydrophobic amino acid residues Leu286 and Val288 in BuChE. These changes have been suggested to increase the volume of the acyl-binding pocket and partly explain the capability of BuChE to accommodate bulkier substrates such as butyrylcholine (**Nicolet *et al*., 2003**). Furthermore, a similar PAS described in BuChE have been demonstrated *via* site-directed ligand mutagenesis and photo-affinity labelling studies to be localised half way between the peripheral and the acylation sites and is formed by two amino acid residues, Asp70 and Tyr332 (**Nicolet *et al.,* 2003; Lane *et al.,* 2006**).

2.4.1.2.2 Localization and function

AChE is responsible for approximately of 80% of ChE activity in the healthy brain, while only 20% is attributed to BuChE activity. This is related to the low level of BuChE in neuronal cells (**Greig *et al.,* 2001**). BuChE in the brain is mostly associated with the region receiving cholinergic innervation, notably glial cells and endothelial cells where it modulates neurotransmission (**Lane *et al.,* 2006**). In the PNS, BuChE is localized in the heart and liver where it serves as drug metabolisers and antitoxins (**Bono *et al*., 2015**). As for AChE, BuChE is expressed by a single gene; however, unlike AChE, it does not go through alternative splitting. All soluble globular tetrameric forms (in the plasma) or membrane bound forms in the synapses (brain and muscle) are encoded by unique BuChE mRNA (**Bono *et al.,* 2015**). Accumulation of evidence in recent literature highlights the neurobiological importance of BuChE and its implication in the progression of AD. A review study done to comprehend the distribution and the role of BuChE in the CNS has revealed that transgenic mice exhibited no

15

abnormality of the cholinergic system in the CNS during a period of 3-4 months after birth. However, they showed high sensitivity to a selective inhibitor of BuChE, bambutol. Similar studies have shown that 10% of ChE positive neurones express BuChE in the human hippocampus and amygdala of an AD brain; moreover, high activity of BuChE has been detected mainly in the temporal cortex and hippocampus, which are areas regularly affected by AD (**Greig** *et al.*, **2001**). A separate study also revealed that the level of the form G4 AChE and BuChE may decrease by nearly two-thirds while the level of the G1 form of AChE, which has low affinity for ACh, remains unchanged and the G1 form for BuChE, in mitigation, increases 30% - 60% in the AD brain (**Greig** *et al.*, **2001**). The results of these studies emphasized the key role played by BuChE in the cholinergic system as a co-regulator of ACh with AChE. Further studies have demonstrated that selective BuChE inhibition can increase ACh levels in a rat's cortex and also improve memory in elderly rats, ruling out speculations about the role of BuChE in the cholinergic system (**Greig** *et al.*, **2001**). These studies, coupled with the decreased sensitivity of BuChE to substrate inhibition as compared to AChE, and other studies supporting the role of AChE and BuChE in promoting the formation of toxic β-amyloid peptide in tissue culture legitimise BuChE as a suitable target for the development of new AD drugs (**Yan and Feng, 2004**).

2.4.2 Amyloid hypothesis

2.4.2.1 History of amyloid fibrils

The term amyloid is derived from the expression "corpora amylacea" introduced the first time in 1854 by the German physician scientist Rudolph Virchow (**Figure 2.7**) to denote small corpuscles with atypical microscopic appearance detected around the blood vessel in the CNS of subjects at old age (**Sipe and Cohen, 2000**). As these corpuscles colour pale blue in the presence of iodine, a property common to starch, Virchow compared the amyloid content to starch and named them "corpora amylacea". Later in 1859, subsequent

Figure 2.7: Rudolph Virchow (1821-1902).

investigations demonstrated that the amyloid content is not of a carbohydrate nature, but has a high nitrogen content. These discoveries shifted the study of amyloids to a new direction. Amyloids were no longer studied as carbohydrates but as proteins susceptible to conformation change forming amyloid fibrils (**Sipe and Cohen, 2000**). In the early nineties, the necessity to discover new therapeutic approaches to slow, avoid, reverse or halt amyloid

formation gained some success with advances in molecular biology research and the development of biophysics tools including solid phase Nuclear Magnetic Resonance (NMR) and other techniques. This progress has enabled the understanding of the molecular deposition and composition of amyloid fibrils (**Rambaran and Serpell, 2008**). Recent convincing evidence now shows that amyloid fibrils are extracellular deposits of insoluble misfolded native proteins (**Figure 2.8),** structurally dominated by β-sheet structure. They are detectable by apple green birefringence when treated with Congo Red and examined under polarized light (**Rambaran and Serpell, 2008; Sipe and Cohen, 2000**).
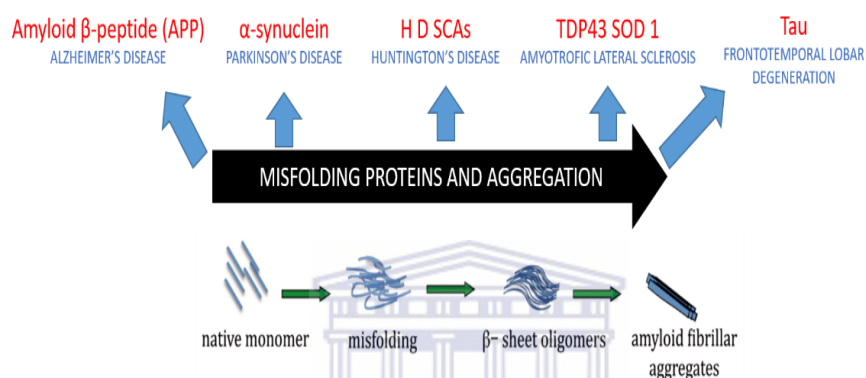
Figure 2.8: Native protein due to some intrinsic factors or drastic conditions might undergo conformation change and aggregate. The type of neurodegeneration depend on the region of accumulation of misfolded protein and its nature (Di Carlo *et al*., 2012).

Factors that accelerate the misfolding and aggregation of proteins are not well understood. Nevertheless, currently proposed explanations include amino acid sequence composition of the protein, mutations, aging, defects in the chaperones' function (chaperones are proteins that assist in proteins folding) and environmental changes (pH variation, agitation, ionic force, sudden variation etc.) (**Herczenik and Gebbink, 2008).** These misfolded proteins that form amyloid fibrils are responsible for many neurodegenerative diseases including AD (**Figure 2.8**). They are grouped in the general term of amyloidosis. The type of amyloidosis provoked is mostly influenced by the site of accumulation of the amyloid fibrils and the nature of the protein precursor of that amyloid fibril formation (**Figure 2.8**). Amyloid precursor protein (APP) was confirmed as precursor of Aβ after it was cloned in 1987 (**Rambaran and Serpell, 2008**).

A specimen containing insoluble abnormal intracellular accumulation of amyloid fibril and neuritic plaques was isolated and purified in 1984, and was similar to a special substance discovered in the brain tissues of an autopsy performed on a 55 year old woman called

17

Auguster Deter earlier in 1907. Auguster was Alois Alzheimer's patient and died from a behavioural disturbance and cognitive impairment **(O'Brienand Wong, 2011)**. Alzheimer hypothesized at this time that histopathological changes in his patient's brain might be the cause of disease symptoms. The prediction of Alzheimer was soon correlated with many more people with the same symptoms and was named AD. It is important to underline that before the case of Auguster D as documented by Alois Alzheimer, dementia was considered as a disease of normal aging along with its histopathological abnormality (neuritic plaques and neurofibrillary tangles). Thanks to Alzheimer's work, it was understood and recognized that APP plays a role in AD forming Aβ that accumulate to form neuritic plaque and neurofibrillary tangle derivatives. Therefore, the biological function of APP and its metabolic products have been a continued subject of attention in research.

2.4.2.1.1   APP: structure and physiological functions
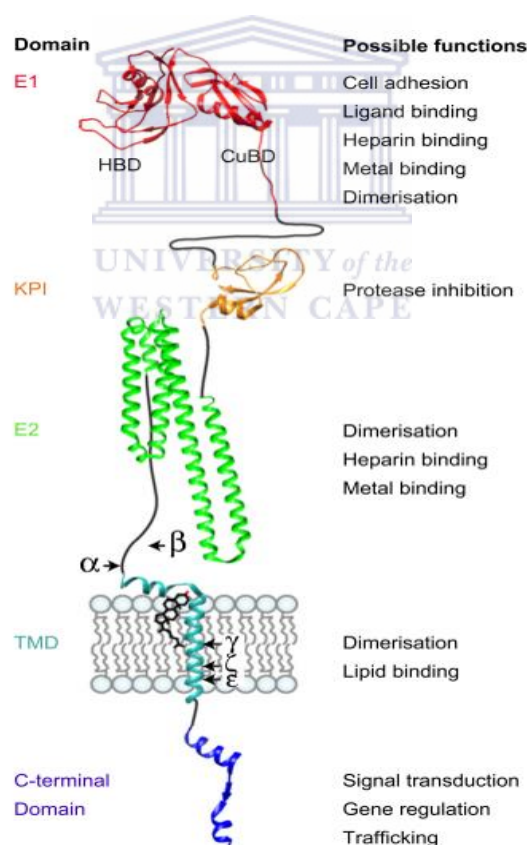
Figure 2.9: Proposed 3D structure of APP showing its different domains and functions and the sites of post-translational processing by α, β, γ, ζ and ε secretases (Dawkins and Small, 2014).

The APP is a single pass transmembrane protein best known as a precursor molecule. The gene encoding for APP is located on chromosome 21q21.3 in humans. In addition, it contains 18 exons and can undergo alternative splitting leading to the expression of three isoforms

with 695, 751 and 770 amino-acids. The complete 3D structure of APP is not yet resolved, however, the crystallized structure of individual domains have been achieved as shown in **Figure 2.9**. The structure contains a large extracellular portion formed by a cysteine rich domain or E1 domain comprising the Heparin-binding domain (HBD) and the Copper or metal Binding Domain (CuBD), the Kunitz-type Protease inhibitor (KPI) domain, E2 domain and the cleavage sites of β, and α secretase; the Intracellular domain or C-terminal domain is linked to the extracellular domain through the Transmembrane Domain (TDM) bearing the cleavage sites of others secretases. Many studies have been done to comprehend the physiological function of APP and its role as precursor of Aβ formation. Though the normal biological function off APP is not totally clear, some published data provide evidence of its role in cell growth and proliferation. Additionally, APP act as trophic factors, therefore may control molecular events including outgrowth, synaptogenesis and signal transduction **(Dawkins and Small 2014; Müller and Zheng, 2013).**

2.4.2.1.2 Metabolic processing of APP and its role in AD

Amyloid precursor protein, after transcription into mRNA in the nucleus and its migration into the cytoplasm where it is translated into protein, undergoes post-translational modification (PTM) including glycosylation, phosphorylation, sialylation and tyrosine sulfation. This is required for the proper folding of the newly expressed protein into its native form **(De Strooper and Annaert, 2000)**. Besides these PTM, APP undergoes sequential proteolytic cleavage considered as an activation process inside or outside the cell by the secretases family of proteins; notably α-secretase, β-secretase, and γ-secretase generating peptide fragments, which, are responsible for its proposed normal physiological functions as mentioned in the preview session (**Gervais *et al*., 2007**).

In the normal brain, the activation of APP by sequential processing is tightly controlled by three membrane proteases: α-secretase, β-secretase and γ-secretase. All of the three proteins, when in close proximity with APP, are able to recognize their normal cleavage site on APP sequence (**Figure 2.10**).
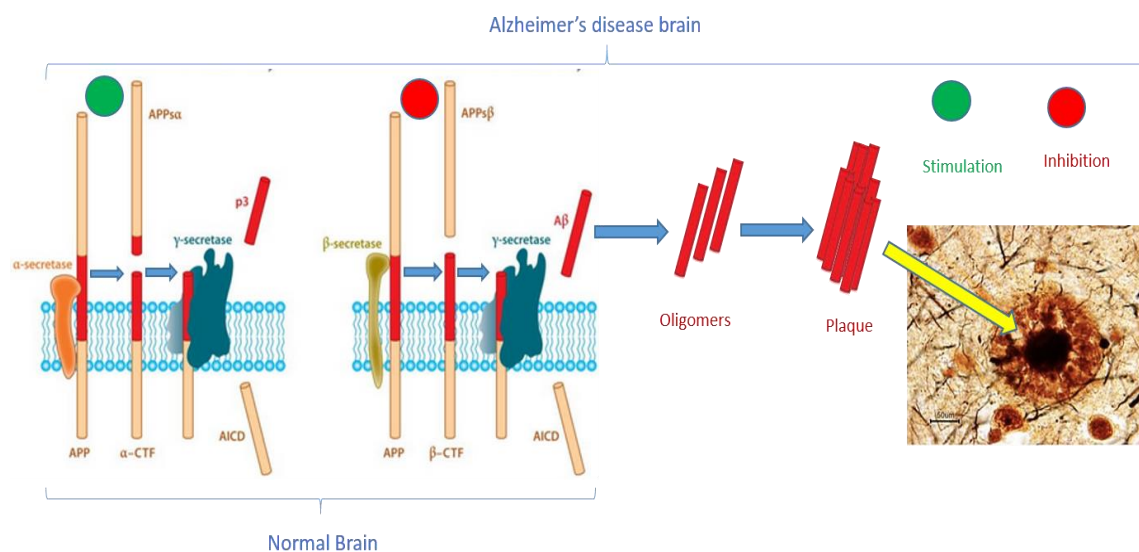
Figure 2.10: Post-translational processing of APP in normal and pathological conditions leading to plaque formation. The green and red are circles indicating possible points of regulation of APP processing (Cell biology of disease and exercise, 2012).

If APP is first recognized and cleaved by α-secretase, it generates an α-secretase cleaved C-terminal Fragment (α-CTF) and an α-secretase cleaved soluble APP (APPsα) fragment; then the α-CTF can be recognized and cleaved by γ-secretase to generate protein 3 (p3) and APP Intracellular Domain (AICD). However, if APP is first recognized and cleaved by β-secretase, it generates a β-secretase cleaved C-terminal Fragment (β-CTF) and β-secretase cleaved APP soluble (APPsβ) fragment; then β-CTF can be recognized and cleaved by γ-secretase to finally generate an amyloid beta (Aβ) fragment and APP Intracellular Domain (AICD) fragment. This pathway is also considered as the amyloidogenic pathway since it leads to the production of Aβ **(O'Brien and Wong, 2011; Zheng and Koo, 2011).** Products of these sequential processing in both cases, as already mentioned in the previous section, have poorly understood physiological function. The Aβ fragment is the most known and documented to be susceptible to oligomerization and aggregation, therefore the most suspected product in disease conditions. However, a study done to understand the role of Aβ in the regulation of memory has revealed that at physiological concentration (Pico molar (pM) or Nano molar nM), Aβ may enhance memory and only impair cognition in higher concentration **(Morley and Farr, 2014)**. Factors known as the driving forces responsible for the cause of Familial Alzheimer's Disease (FAD), also known as early onset AD or inheritance form of AD, as we shall describe in the next section, might support this study. The build-up of Aβ in the brain has been demonstrated to be the pathological hallmark of both types of AD **(Mondragón-Rodríguez *et al*., 2012)**.

20

2.4.2.1.2.1 Sporadic AD

The argument put forward so far to explain the role of Aβ in sporadic AD is the disturbance in the mechanism controlling the rate at which Aβ is generated versus clearance (**Tanzi** *et al.,* **2004**). Two pathways are retained to describe how the levels of Aβ are normalized or cleared from the brain. Included are proteolytic degradation and receptor-mediated transport from the brain. The level of Aβ in brain is normalized or regulated by amyloid degrading enzymes such as insulin-degrading enzyme (IDE) and Neprilysin (NEP), which are more specific for degrading Aβ monomer types. Additional amyloid degrading enzymes are the angiotensin converting enzyme (ACE) and plasmin (**Dries** *et al.,* **2012**). The activity of IDE is inhibited by insulin, supporting diabetes mellitus as a risk factor for AD disease (**Bates** *et al.,* **2009**). The receptor-mediated transport across the Blood Brain Barrier (BBB) includes the multiligand cell surface Receptor for advance glycation and end product (RAGE) that mediates the influx of Aβ into the brain and Low-density Lipoprotein Receptor-related 1 (LRP 1) protein that mediates efflux of the Aβ from the brain to the peripheral system through endocytosis where it is targeted for degradation in the liver (**Tanzi** *et al.,* **2004**) (**Figure 2.11**).
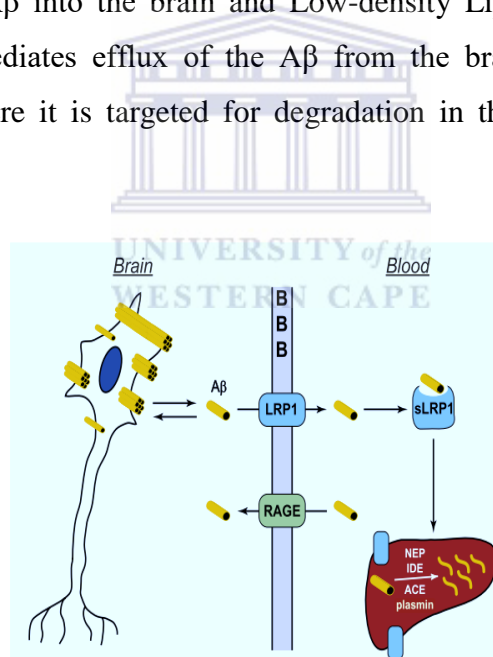
Figure 2.11: Flux of Aβ between the brain and the peripheral system and its target degradation in the liver (Dries, Yu, and Herz, 2012).

The expression of LRP 1 decreases in AD whereas the expression of RAGE increases (**Dries** *et al.,* **2012**)**,** and an age-related defect of Aβ transport across the BBB (**Bates** *et al.,* **2009**)**,** are believed to be responsible of accumulation of Aβ which, disrupt neuronal integrity, interfere in nerve transmission and triggers a multiple cascade neurotoxic events leading to AD. The major risk factor of sporadic AD is associated with the presence of the isoform of ApoE ε4 in the genome (**Liu** *et al.,* **2013**).

2.4.2.1.2.2 Early onset of AD or FAD

The dysregulation in the metabolic processing of APP is believed to orchestrate the build-up, oligomerization and aggregation Aβ leading to FAD (**Shimizu *et al.*, 2008**). γ-Secretase that cleaves APP after β-secretase is able to cleave APP at several sites, which results in the production of Aβ with various fragments. Under normal conditions, the sequential processing of APP produces $A\beta_{38-43}$ residues with the more common ones $A\beta_{40}$ and $A\beta_{42}$ (**Rang *et al*., 2012).** Many studies have demonstrated that $A\beta_{40}$ is produced in relative higher proportion than $A\beta_{42}$. $A\beta_{40}$ is more soluble and less toxic whereas $A\beta_{42}$ is insoluble and more susceptible to aggregation, therefore more toxic (**LaFerla *et al*., 2007**). In other words, the ratio of $A\beta_{42}$ / $A\beta_{40}$ is low in healthy brain and the equilibrium between the production of Aβ and the clearance pathways is well controlled (**Bates *et al.,* 2009**). However, in the AD brain, mutation of the gene encoding APP coupled with the mutation of presenilin (part of γ-secretase complex protein comprising: Presenilin 1, presenilin 2, Nicastin and Anterior Pharynx-defective 1 (APH 1)) is believed to shift the preferable cleavage site of γ- secretase towards high production of $A\beta_{42,}$ increasing the $A\beta_{42}$ / $A\beta_{40}$ ratio which is supported by many studies as a pathological hallmark of FAD (**Rang *et al*., 2012; Pachaiyappan and Boobalan, 2011**).

In light of the information provided by these data, it can be retained that although the pathological process leading to both forms of AD are different, the accumulation of Aβ appear to be the starting point that trigger the cascade of neurotoxic events, for instance, neuroinflammation, production of reactive oxygen species (ROS), ion dyshomeostasis, tau-hyperphosphorylation, synaptic dysfunction and neuronal loss leading to dementia. These compelling arguments have been at the base of the Amyloid hypothesis and is strengthened by the observation that immunotherapy that reduces the Aβ level in mice, improve cognitive impairment (**Elder *et al.,* 2010**).

In conclusion, of all secretases involved in the APP processing are points of regulation that may help decrease the level of Aβ in the brain, either by stimulating or inhibiting α-secretase and β-secretase activity respectively (**Figure 13) (Dries *et al.,* 2012).** Additionally, accelerated degradation or promoting clearance of Aβ from the brain by modulation of LRP 1, RAGE and enzymes that degrade Aβ may also contribute in reducing Aβ in the brain. However, β-secretase also called BACE (β-site APP Cleaving Enzyme), the preponderant

transmembrane aspartyl protease, is the immediate and primary cause of Aβ production. Therefore, it seems to be the most attractive target for the design of drugs that can stop the disease progression **(Shimizu *et al*., 2008)**.

2.4.3 Tau protein hypothesis

Tau protein is a member of the Microtubule-Associated Protein (MAP) family, so called due to their ability to promote the assembly of tubulin into microtubules (MT). Microtubules are part of the neuronal cytoskeleton, which provide structural support that are essential for the physiological function of neurones. Tau protein discovery dated from 1975 in Marc Kirschner's Laboratory at Princeton University **(Mandelkow and Mandelkow, 2012)**. Nine years later, it was demonstrated that the degree of phosphorylation of tau-protein determines its capacity to promote microtubule assembly. Many years after, subsequent studies found that Paired Helical Filaments (PHFs) forming NFTs in AD brain is a result of hyper-phosphorylation of the tau protein. This finding and the discovery that tau deposits were linked to other neurodegeneration independently to Aβ peptide aggregation, attracted the curiosity of researchers and increased their interest in understanding how Tau protein is post-translationally regulated after its synthesis and also to establish the molecular mechanism leading to NFTs **(Mandelkow and Mandelkow, 2012)**.

Molecular biology studies, biophysical studies and NMR have enabled the location of Tau protein on the human genome and the determination of its 3D conformation. The gene encoding human tau protein is located on chromosome 17q21. It contains 16 exons, which undergo alternative splitting to produce 6 isoforms with various numbers of amino acids ranging from 352 to 441. The variation in AAs contained is linked to either no insert or the presence of one or two inserts (E2, E3) of 29 amino acids in their *N*-terminal region and a three or four repeat-region in the *C*-terminal region (**Figure 2.12**). The longest isoform, 441 amino acids, is present in the CNS and it contains four repeat-regions (R1, R2, R3 and R4) and two inserts E2 and E3 **(Lim *et al.,* 2014)**.

They are naturally heat resistant and less sensitive to degradation in acidic medium. These characteristics are attributed to their "natively unfolded" protein nature **(Tenreiro *et al.,* 2014)**. The activities of tau proteins are tightly regulated by multiple kinases and

phosphatases, which can add or remove a phosphate group to specific residues (Threonine / serine), **(Gong *et al.,* 2006)**.
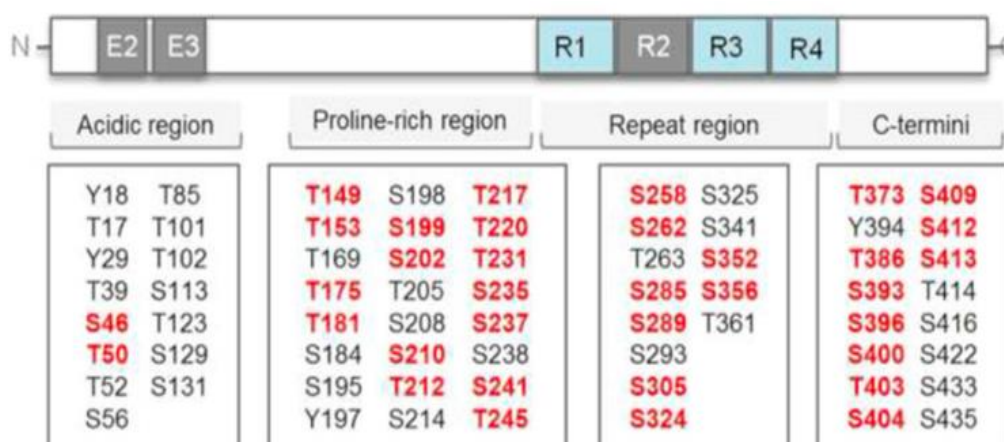
Figure 2.12: Longest (441 AAs) isoform of Tau protein present in the CNS showing its different regions. Residues in red coloured are site-specific phosphorylation mediated by GSKβ3. The phosphorylation of grey residues is mediated by others kinase (Lim *et al*., 2014).

Tau protein function depends on degree of phosphorylation and also aging factors. In normal conditions, tau proteins promote tubulin assembly to microtubules, providing them structural support, which assist axonal transport of nutrients, nerve impulses and other important substances away from nerves cells **(Johnson, 2004)**. In the light of this information, we can conclude that tau proteins are indispensable for communication between nerve cells. In AD, tau proteins are hyperphosphorylated due to unbalanced tau kinase and phosphatase activities. Hyperphosphorylation of tau proteins induce conformation changes unfavourable to their continued attachment to microtubules. Therefore, they detach from microtubule and spontaneously self-associate into insoluble PHFs, which further aggregate to form NFTs causing the break-down of neural functions **(Figure 2.13)**. This pathological consequence, interrupt communication between neurones in regions regularly associated with AD **(Chung, 2009)**.

Protein phosphatase 2A (PP2A), Protein phosphatase 1 (PP1) and 5 (PP5) are the major serine / threonine tau phosphatases whose activities are crucial for tau dephosphorylation **(Billingsley and Kincaid, 1997)**. The hyperphosphorylation of tau protein is suspected to be the result of a decrease in their activities in many neurodegenerative diseases, and particularly in AD. This assumption somewhat correlates with previous studies which show that activities

of both PP2A, PP5 and PP1 decrease in AD brain patients due to an endogenous phosphatase inhibitor (**Chung, 2009; Billingsley and Kincaid, 1997**).
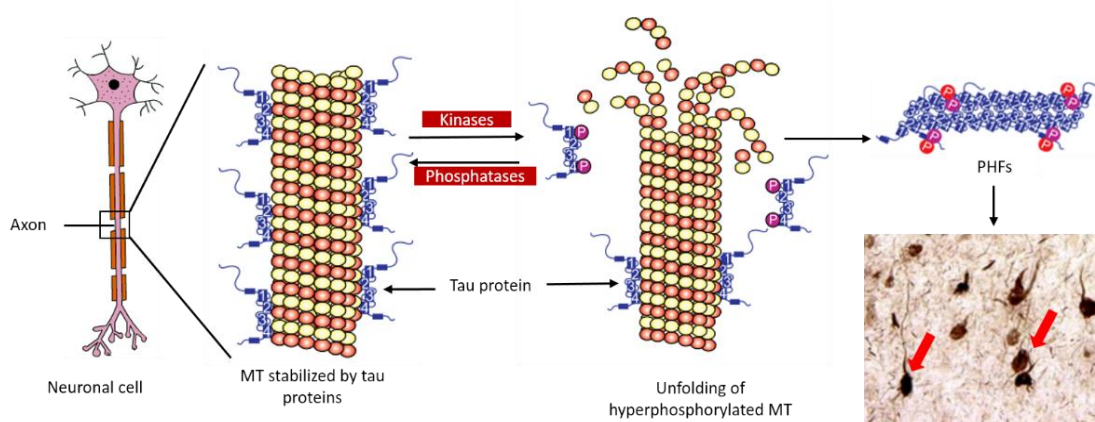
Figure 2.13: Propose process of NFTs formation: hyperphosphorylation of tau protein causes disassembly of MT leading to NFTs (red arrows) formation in AD (Drewes, 2004).

Glycogen synthase kinase β3 (GSKβ3), Cyclin-dependent kinase 5 (CdK5), Dual-specific Tyrosine (Y)-Regulated Kinase 1A (Dyrk1A), Mitogen-Activated Protein Kinase (MAPKs) and many others are serine / threonine tau proteins kinase capable of phosphorylating tau protein at specific sites (**Mietelska-Porowska *et al*., 2014**). CdK5 and GSKβ3 are known to have some overlapping phosphorylation sites, for instance Ser199, Thr181 (**Mietelska-Porowska *et al*., 2014**). Accumulation of evidence confirms hyperactivity or higher expression of these kinases in AD (**Chung, 2009; Gong *et al*., 2006**). The autophosphorylation of Tyr216 is believed to be one of the reasons that explains the hyperactivity of GSKβ3 in AD (**Johnson, 2004**). On the other hand, the increase of CdK5 activity is associated with increased overexpression of protein 25 (p25), a protein resulting from the cleavage of protein 35 (p35) mediated by calcium-dependent protease Calpain in neurotoxic conditions like Aβ (**Johnson, 2004**). The imbalance in the activities of key proteins (protein kinases and phosphatases) responsible for phosphorylation and dephosphorylation of tau proteins are suggested by the tau hypothesis of aetiology of AD to be the main cause of misfolding and further aggregation of tau protein into NFTs which interferes in synaptic function leading to neuronal death (**Desai and Chand, 2009**). The tau hypothesis is also supported by the observation that decreased tau levels in transgenic mice reduces neuronal dysfunction and the extent of tau disease, which is associated to cognitive impairment in humans (**Chesser *et al*., 2013**). In line with these observations, preventing or

reducing hyperphosphorylation of Tau protein by modulating kinase and phosphatase activities appear as tau-based strategy for the treatment of AD.

2.4.4 Other neurotoxic events

The formation of senile plaques and aggregation of tau protein into NFTs are believed to be the major upstream molecular factors that trigger a cascade of neurotoxic events including; disturbance of metal ion homeostasis, mitochondrial and endoplasmic dysfunction, neuroinflammation, oxidative stress, collapse of neurotransmission system, stimulation of programmed cell death and atrophy of the brain observed in AD patient (**Yamasaki *et al.,* 2012**). In this section, we will discuss only the role played by oxidative stress in the pathogenesis of AD, which is believed by some sources to be a contributor to the early stages of AD (**Pereira *et al*., 2005; Zhao and Zhao, 2013**), while emphasizing their relevance for therapeutic intervention.

2.4.4.1 Oxidative stress

Oxidative stress can be defined as a physiological reaction of the body in response to cumulative damage orchestrated by free radicals improperly neutralized by endogenous antioxidants that is believed to be linked to aging or diseases. Free radicals are compounds that contain one or more unpaired electrons and are generally more reactive. For instance (**Figure 2.14**), the superoxide radical ($O_2^{\cdot-}$) which results from the reaction of oxygen (O_2) with one electron escaped from the electron transport chain in the mitochondrial membrane (**Halliwell, 2001**). The reaction is catalysed by the enzymatic complex Nicotinamide Adenine Dinucleotide plus Hydrogen (NADH), ubiquinone reductase and ubiquinone cytochrome C-reductase. Hydrogen peroxide (H_2O_2), the least harmful ROS, results from the conversion of superoxide (more harmful) catalysed by an antioxidant enzyme superoxide dismutase (SOD) and H_2O_2 in turn can interact either with copper (Cu^+) or iron (Fe^{2+}) (by Fenton reaction) to produce the potent oxidant species, hydroxyl radical ($\cdot OH$). Alternatively, they can interact with chlorine (catalysed by myeloperoxidase (MPO) to produce hypochlorous acid (HOCl). H_2O_2 can also be converted into water (H_2O) by the antioxidant enzyme catalase (CAT) or Glutathione peroxidase (GPX). Nitric oxide (NO) interacts with superoxide to produce peroxinitrite ($ONOO\cdot$) (**Lü *et al*., 2010**).

26
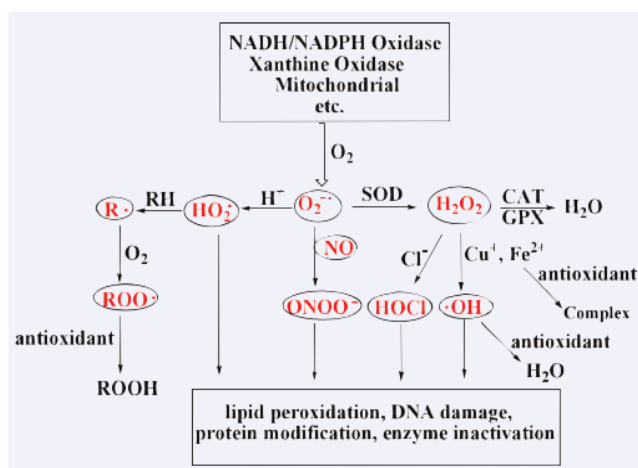
Figure 2.14: Diagram showing different sources of ROS and sites of antioxidant activities (Lü *et al*., 2 010).

In the healthy body, these ROS have antimicrobial activities and play a vital role in degrading foreign matter **(Nimse and Pal, 2015)**. Generally, excess ROS are neutralized by antioxidant enzymes as mentioned above and antioxidant compounds such as carotenoids, α-tocopherol (Vitamin E), glutathione and ascorbic acid (Vitamin C). Therefore, the diseases associated with ROS, particularly AD, usually results from an imbalance between free radical generation and neutralization. Excess free radicals cause the peroxidation and damage of biological molecules, for instance peroxidation of lipids (ROO·), protein modification, DNA damage and enzyme inactivation. If the damage is too great, the cell might undergo apoptosis or programmed cell death **(Uttara *et al.,* 2009)**.

 Another's factor responsible for ROS production that have been revealed in AD and neurodegeneration is associated with β-amyloid formation; interaction of β-amyloid with transition metals ions ($Cu^{2+,}$ Fe^{3+} and Zn^{2+}) generates Cu^+ / Fe^{2+} / Zn^+ which further reacts with H_2O_2 to produce very harmful ·OH **(Uttara *et al.,* 2009)**. Additional sources of ROS production are by-products of monoamine oxidase (MAO) activities. MAO are Flavin enzymes present in the outer mitochondrial membrane where they accelerate oxidative deamination or degradation of monoamine neurotransmitters, neuromodulators and hormones thus preventing their neuro and cardio-toxicity **(Outcomes and Monoamine, 2012).** H_2O_2 is one of many by-products of MAO activities which when converted into other ROS provokes mitochondrial and cytoplasmic dysfunction or damage **(Sturza *et al.,* 2013)**. It has also been demonstrated that exposure of the cell to glutamate reduces mediation of cystine into the cell and cystine is the precursor of glutathione synthesis; Glutathione is an antioxidant, therefore

reduction of its synthesis impair the ability of the cell to protect against oxidative damage (**Maher and Davis, 1996**).

Many other lines of evidence indicate oxidative stress in the pathology of AD: the presence of numerous traces of free radical attack, mitochondrial dysfunction, nucleic acid damage and protein oxidation. The build-up of free radicals has also been demonstrated in the brain of old age AD patients and is associated with an increase of transition metal anion copper, and Zinc, both precursors of free radical production (**Pereira *et al.,* 2005**). In light of these findings, enhancing cellular defences against oxidative stress using antioxidants might be of therapeutic value.

2.4.5 Conclusion from the aetiology of AD

Recent studies demonstrated that aging remains the principal risk factor of sporadic AD dominated mainly by the build-up of β-amyloid peptide, a result of imbalance of generation and clearance. Early onset AD results from genetic mutation of APP, presenilin 1 / 2 (part of BACE complex) which cause the dysregulation of metabolic processing of APP with the pathological consequences of accumulation of β-amyloid peptide. The accumulation of β-amyloid is believed to be the primary factor that triggers downstream events including dysregulation of tau protein phosphorylation leading to aggregation of PHFs into NFTs, oxidative stress and death of the nerve cells leading to dementia (**Figure 2.15**).
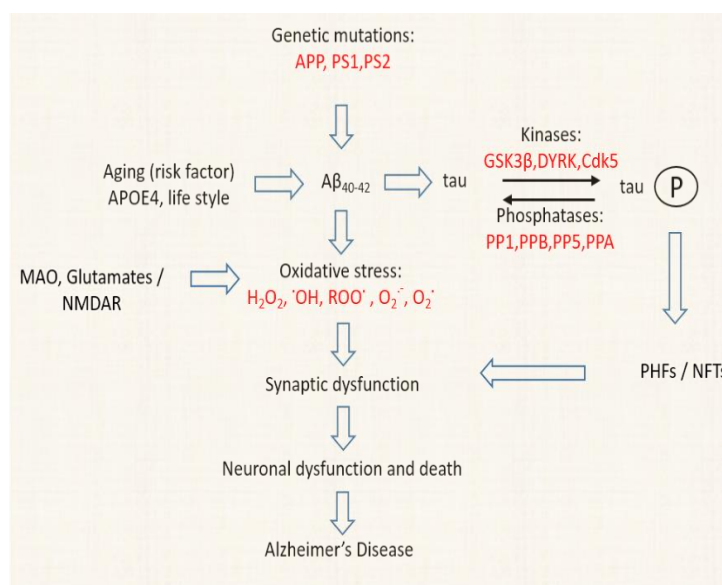
Figure 2.15: Proposed diagram of the chronology of toxic events involved in AD (Mao and Reddy, 2011).

The multiple molecular events leading to AD partly explain the limitation of the current treatment, but also explains why combined therapy are continuously gaining more attention as alternative strategy for stopping the disease progression.

2.5 Therapy of Alzheimer's disease and limitation

The pathogenesis of AD covers a complex network of dysfunction involving processing of proteins interacting with each other (**Zheng *et al*., 2014**). This complexity poses a serious challenge in designing safer drugs that can stop the disease progression and up to now, the challenge is still open. The current drugs approved for treatment of AD are symptomatic and limited to cholinesterase inhibitors drugs (donepezil, galantamine and rivastigmine) designed to address abnormally decreased levels of the neurotransmitter ACh and a glutamatergic receptor modulator (Memantine) (**Soininen, 2010**).

Donepezil   Rivastigmine   Galantamine   Memantine
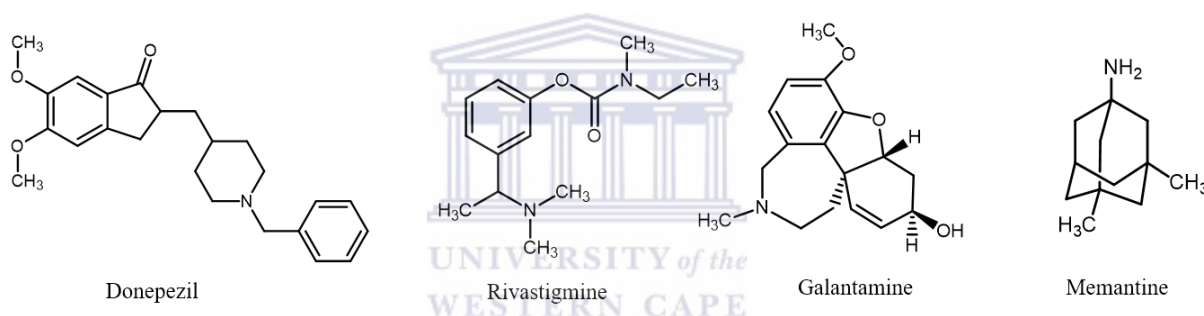
Although these drugs have demonstrated some beneficial effects in the treatment of AD, (**Table 2-2**), they interfere only on a single level in disease pathways with marginal effects. Cholinesterases promote survival of ACh in the synapse junction when bound to CAS or reduce ChE-induce β-amyloid aggregation when able to bind both the PAS and CAS (Donepezil particularly), hence improved cognition and daily life. Memantine modulates Ca^{2+} influx in the cell, limiting excitotoxicity, hence preventing damage of nerve cells (**Parsons *et al.,* 2013**). AD is a multifactorial disease and bodies of evidence suggest that a single drug with multiple effects or that can interfere at different levels of the disease pathway may synergistically improve the therapeutic effect and stop disease progression (**Agis-torres *et al.,* 2014; Fern *et al.,* 2010**).

Table 2-2: Summary of pharmacological characteristics of current AD drugs.

	Donepezil	**Galantamine**	**Rivastigmine**	**Memantine**
Therapeutic class	Piperidine derivative	Alkaloid	Carbamate	Adamantane or diamanoid
FDA approved	1996	2001	2000	2003
Use	Palliative treatment mild-to moderate AD	Palliative treatment mild-to moderate AD	Palliative treatment mild-to moderate AD	Palliative treatment Moderate –to severe AD
Targets	AChE and negligible BuChE	AChE	AChE / BuChE	NMDAR
Benefits	Improve cognitive function and speech	Improve cognitive function and speech	Improve cognition, daily life activity	Decrease emergency of behavioural symptoms such as cognition,
Side effects	Gastro international abnormalities, nausea, anorexia, abdominal pain	Nausea, vomiting, anorexia, diarrhoea	Nausea, vomiting, anorexia, diarrhoea, head ache	Head ache, dizziness, confusion, somnolence, Infrequent hallucination
Mechanism of action	Binds to the PAS and CAS of AChE and inhibits acetylcholinesterase activities	Binds to the CAS of AChE and inhibits acetylcholinesterase activities	Binds to the PAS of AChE / BuChE and inhibits cholinesterase activities	Uncompetitively binds with moderate and voltage dependent to NMDAR and antagonizes NMDAR activity
Half life	70 hours	7 hours	10	60-80 hours
References	**(Mehta *et al.,* 2012)**	**(Soininen, 2010)**	**(Soininen, 2010)**	**(Parsons *et al*., 2013)**

2.6 Multitarget Directed Ligand (MTDL) paradigm

The accumulation of evidence on the complex nature and the diverse causes (dysfunction of the cholinergic system, ChE-induced Aβ aggregation, Aβ accumulation into neurotic plaque, NFT formation, ROS, excitotoxicity, neuroinflammation and apoptosis) involved in the pathogenesis of AD clearly explains the draw-back of the current treatment limited to AChEIs and NMDA receptor modulators. In fact, these drugs have been designed based on "one-drug-one-target" paradigm and only address a single target **(Ricerca, 2009)**. More recently, this design strategy has been questioned and substituted by a poly-pharmacology

30

approach. Poly-pharmacology is the combination of drugs to treat disease with pathophysiology involving multiple target proteins **(Simoni *et al.,* 2012)**. The objective is a synergistic effect with enhanced efficacy and reduced individual toxicity associated with each drug, thus overcoming the limitation of the current treatment. However, this strategy proved ineffective on the treatment of certain diseases such as hypertension and the difficulty of patient in adherence to the treatment **(Agis-torres *et al.,* 2014)**.

The Multitarget directed ligand paradigm is based on the design of a single molecule with the ability to act on multiple targets simultaneously (**Figure 2.16**) (**Nepovimova *et al*., 2014***)*. The strategy offers diverse advantages, for instance improved efficacy associated with synergistic effect and a single drug is safer than poly-pharmacology due to the reduced doses. Pharmacokinetic studies of a single drug are also easier to predict, drug-drug interaction is minimized, and compliance of patients is increased **(Simoni *et al., 2012)*.**
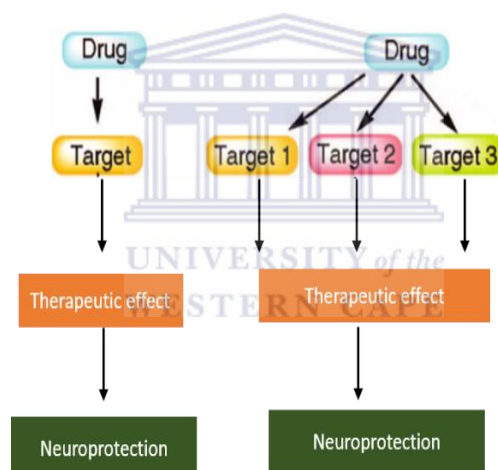
Figure 2.16: Drug development strategy for AD. Shifted from "one-drug-one target" paradigm (current treatment) on the left to one-drug multiple targets paradigm (current approach for the discovery of drug modifying disease drugs) on the right (Agis-torres *et al.,* 2014).

Numerous examples of drug candidates have already been developed and published in a recent review that supports the validity of MTDL, with pharmacological profile offering promise of slowing or stopping the disease progression **(Simone *et al.,* 2014)**. However, none of these innovative candidate drugs have so far survived clinical trials due to lack of satisfactory efficacy and toxicity issues **(Capurro *et al.,* 2013).**

31

2.7   Strategy for designing multitarget ligand drugs for AD therapy.

The most widely used strategy in the design of novel drug-like compounds against AD is the dual binders of ChE. It consists of hybridizing pharmacophore subunits (or lead compounds) of molecules currently used for the symptomatic treatment of AD and include AChEI (Tacrine, Galantamine, Rivastigmine and Donepezil) and NMDAR modulators (Memantine). For example the Bis-7-tacrine dimer, galantamine-memantine hybrid **(Simoni *et al*., 2012)** or the attachment, *via* a spacer with appropriate chain length, to a bioactive synthetic or natural product displaying versatile biological activities on other target proteins involved in the aetiology of AD to produce a hybrid compound; like the phenylthiazole-tacrine hybrids **(Simone *et al.*, 2014)**.

Galantamine-memantine hybrid   Phenylthiazole-tacrine hybrid   Bis-7-tacrine dimer   Bivalent β-carboline
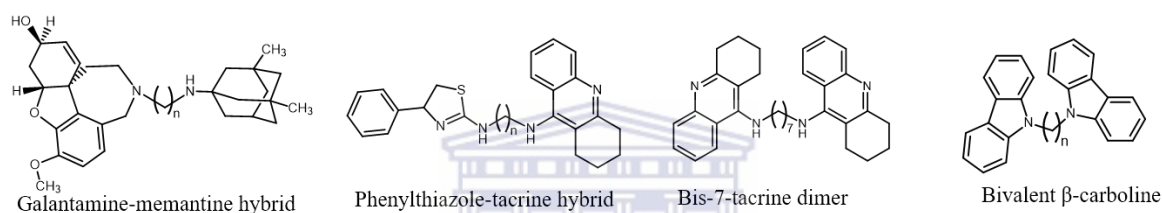
These compounds are capable of modulating more than one pathophysiological pathway leading to neurodegeneration for instance, β-secretase activity, hyperphosphorylation of tau-protein and ROS activities **(Cavalli *et al.*, 2008)**. Another successfully applied type of hybridization involves natural products with diverse neuroprotective activities, for example bivalent β-carboline **(Rook *et al*., 2010)**. An alternative design approach is the optimization of existing AChEI, with the aim to enlarge their spectra of activity regarding target proteins involved in AD **(Cavalli *et al.*, 2008)**.

2.8   Lead compounds for novel multitarget AD drug design.

A lead compound can be defined as a compound with one or more recognized therapeutic useful properties. In the context of the MTDL drug development strategy for AD treatment, attractive lead compounds are those that can interfere in multiple pathophysiological networks, and therefore, their lead optimization might yield novel compounds with the ability to reverse the situation. For the purposes of our study, we have selected the lead compounds described in the following section.

32

2.8.1 Tacrine (9-amino-1,2,3,4-tetrahydroacridine)

Tacrine was first synthesized in 1945 while investigating antibacterial properties of acridine derivatives (**Kozurkova *et al.*, 2011**). Tacrine was the first drug approved to reverse cognitive impairment in 1993 by the FDA in US, Canada and parts of Europe, but its hepatotoxicity limited its clinical application
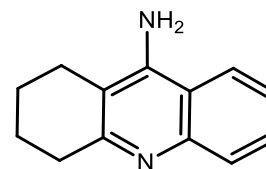

Tacrine

(**Thiratmatrakul *et al.*, 2014**). Tacrine is a potent inhibitor of AChE and BuChE and its therapeutic effect normalizes the levels of acetylcholine (ACh) in the synaptic cleft. Further biological activities include MAOI activity, the ability to decrease neuronal uptake of 5-hydroxytryptamine and dopamine, modulation of muscarinic ACh receptors and certain potassium ion channel activities (**Kozurkova *et al.*, 2011**). Recent studies have demonstrated that, lead optimization of tacrine in the design of novel AD drugs can improve its biological profile and alleviate its hepatotoxicity. Based on what precedes, tacrine appears to be a suitable lead compound for the design of multitarget drugs because of its privileged structure, its efficacy and its low molecular weight (**Inglot *et al.*, 2013**).

2.8.2 Tryptoline (pyrido[3,4-b]indoles)

Tryptoline belong to a family of β-carboline compounds. They are alkaloids with structures dominated by a core indole structure and a pyrrolidine ring (**Frost *et al.*, 2011**) and were first discovered in plants. Previous studies have shown that they have a large range of biological activities associated with target
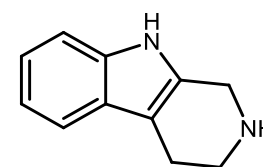
Tryptoline

proteins involved in the pathogenesis of AD (**Herraiz *et al.*, 2010**). β-carbolines have also been demonstrated to improve memory in low concentration (0.3mg / kg) in mice (**Venault and Chapouthier, 2007**). Additional studies have shown that β-carbolines can inhibit AChE and BuChE activities, which are first choice targets for the symptomatic treatment of AD (**Schott *et al.*, 2006; Becher *et al.*, 2005**). Furthermore, β-carboline can influence the activities of the NMDA receptor, MAO and also inhibits CdK5 (**Song *et al.*, 2002**). Harmine, one of the β-carboline derivatives in particular has been shown to be a potent inhibitor of DYRK1A. As described earlier, DYRK1A overexpression and CdK5 deregulation are linked

33

to NFT formation in AD (**Frost *et al.,* 2011**). These versatile biological activities of β-carbolines suggests that tryptoline could modulate AChE, BuChE, NMDAR, MAO, CdK5 and DYRK1A activities. Therefore, tryptoline appears as legitimate lead compound for the development of multifunctional AD drugs.

2.8.3 Trolox (6-hydroxy- 2,5,7,8-tetramethylchromane-2-carboxylic acid)

Reactive oxygen species are one of the major factors that contribute to AD by overproducing free radicals that exceed the antioxidant capacity of neuronal cells, thus compromising their viability (**Hamad, 2010**). This excess of free radicals can be neutralized using exogenous antioxidant compounds
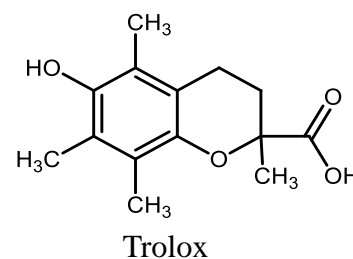
Trolox

such as Vitamin C, Vitamin E (α-tocopherol) and a Vitamin E analogue, 6-hydroxy-2,5,7,8-tetramethylchromane-2-carboxylic acid (Trolox) (**Hamad, 2010**). All these compounds exhibit good free radical scavenging and other neuroprotective activities to different degrees. Comparative studies have demonstrated that trolox possess greater antioxidant effect than Vitamin C and vitamin E (**Mun *et al.,* 2002**). Trolox has an additional advantage over its analogue, Vitamin E, in that it has capacity to incorporate into the lipid and the water soluble compartment of cells. Moreover, trolox has the ability to prevent neurotoxicity induced by Aβ and H_2O_2 (**Radesätera *et al.,* 2003**). The same study suggests that trolox prevents neurotoxicity induced by H_2O_2 by decreasing permeability to H_2O_2. A separate study revealed that trolox can inhibit GSK3β whose hyperactivity causes NFT formation (**Mun *et al.,* 2002**). Considering the ability of trolox to protect neuronal cells using a different mechanism, and the large advantage it offers over other antioxidant compounds (Vitamin C and Vitamin E), it was selected as the third lead compound.

2.9 Conclusion

In light of the current hypothesis underlining the cause of AD, aging, and some genetic predisposition interplay leading to Aβ aggregation into neurotic plaque and hyperphosphorylation of tau-protein that accumulates to form NFTs. These events create a complex network of neurotoxic conditions responsible for the disease progression. The multifaceted nature of the aetiology involving interconnected multiple signalling pathways explain the marginal effects of the current treatment that is limited to cholinesterases

34

inhibitors (Donepezil, Galantamine, Rivastigmine) and NMDA receptor modulators (Memantine). This supports the need of the MTDL paradigm as an alternative strategy for the development of novel drug compounds capable of overcoming limitations attributed to the "one-drug-one target" paradigm. Lead compounds (tacrine, trolox and tryptoline) were identified based on their multiple biological activities on target proteins involved in the pathophysiology of AD. It is hypothesized that connecting tacrine-trolox and tacrine-tryptoline with an appropriate linker chain length might yield hybrids with promising disease modifying drug potency.

UNIVERSITY *of the*

WESTERN CAPE

35

CHAPTER 3.

MOLECULAR MODELLING AND SYNTHESIS

3.1 Molecular Modelling Study

3.1.1 Introduction

Molecular modelling also referred to as computer aided-drug design can be defined as all techniques which use computerized methods to explore the three dimensional conformation change that small molecules (ligands) or macromolecules (proteins) undergo during any kind of intermolecular interaction (**Ferreira *et al.,* 2015**). One of the most used techniques is molecular docking. It assists in estimating the binding interaction between drugs and specific target proteins. It has the ability to provide useful information regarding the different conformations adapted by the drugs in the active site such as, the binding energy, the type of interactions, the affinity of binding, and the stability, which are helpful in predicting molecular recognition (**Durrant and McCammon, 2011**).

3.1.2 Method

Modelling was performed using the Molecular Operating Environment (MOE 2014.0901) software package. The X-ray crystal structure of the acetylcholinesterase / bistacrine complex (code: 2cmf) was downloaded from the protein data bank (PDB) and loaded in the working environment. The ligand was removed and the structure was protonated ignoring water molecules and heteroatoms. The structure was protonated in "generalized born" implicit solvated environment before importing the ligands. Hybrid compounds were accurately drawn in Chemsketch and saved as MDL mole file (V3000) for import into the Database. The structures were energy minimized in implicit solvated environment under AMBER99 force field and docked into the active site of the protein. The binding site was defined with the conserved aromatic residues Trp279 and Trp84. All other parameters were left as default values. Finally, the conformation with the lowest docking score was selected for analysing the interactions between the AChE and the hybrid compounds.

3.1.3 Results and discussion

Docking was performed using MOE 2014.0901 and the 3D and 2D images depicting interactions of selected lowest docking score conformations of each compound with *Tc*AChE (PDB code: 2cmf) are included below **(Figure 3.1).** The results of the docking revealed that selected conformations of the tacrine-trolox hybrids, the tacrine-tryptoline hybrid and the tryptoline dimer show similar binding patterns. The two moieties (trolox-tacrine / tacrine-tryptoline) in both hybrids spanned the CAS and PAS of *Tc*AChE but with different energy scores. Compounds with the short linker chain lengths (2 carbons) tend to have high energy scores of -8.10 **(16)** to -9.84 **(8a)** while **8b**, **8c**, **8d**, **8e** and **14** have relatively lower energy score -10.20, -10.30, -11.43, -11.70 and -10.40 respectively. The difference in energy scores indicate a disparity in how strong / fast / stable the synthesized compounds bind to the active site. This therefore can be a determining factor indicating to which extent they can inhibit the activity of *Tc*AChE activity. Based on this concept, compounds with the longest linker chain length (6 and 8 carbons) followed by (3, 4, and 7 carbons) is expected to display the highest activity. In all experiments, tacrine occupied the CAS and trolox / tryptoline occupied the PAS (**Figure 3.1**), which correlated well with our prediction and also demonstrated the high selectivity of tacrine for the CAS as supported in the literature (**Savini** *et al.,* **2003; Lan** *et al.,* **2014**). In **Figure 3.1**, the ball and stick representations are compounds from **8a** to **16** and dashed lines are interactions between ligands and *Tc*AChE. In pink and cyan are Trp84 (CAS) and Trp 279 (PAS), crucial amino acids regularly involved in inhibition of the *Tc*AChE activity. This binding mode corresponds to that found in the crystallised ligands.
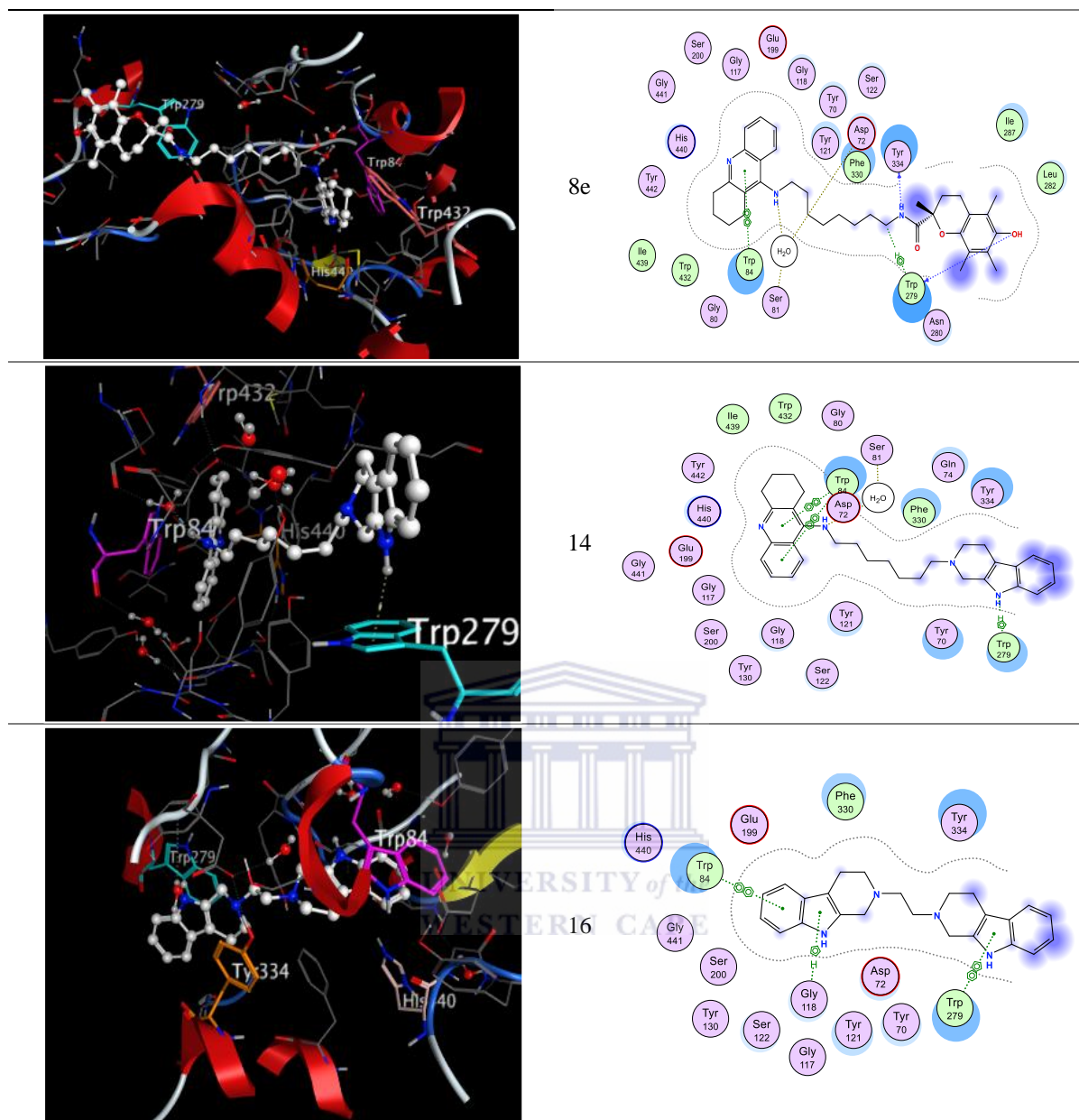
Compounds docked in *Tc*AChE active site (3D)		**Ligand interaction with conserved aromatic residues (2D)**
	8a	
	8b	
	8c	
	8d	

38

Figure 3.1: Compounds docked in the active site of *Tc*AChE (3D) and possible interactions (2D).

It is clear from the images that the quinoline ring of tacrine of all the synthesized hybrids form π-π interactions (green dashed line, 2D) with Trp84 (pink, 3D). Hybrid **8e** also undergoes backbone acceptor interactions (dashed blue line) and side chain interaction (dashed green line) between H of the amide bond and the O of the OH group of trolox with conserved aromatic residues Tyr334 and Trp279 in the PAS. The indole ring of the tryptoline dimer undergoes π-π interaction and H-π interaction with Trp84 and Gly118 in the CAS. The second pyrrole ring undergoes π-π interaction with Trp279 in the PAS. A H-π interaction is also observed with compound (**14**) between 9-H and Trp279. These results suggest the

39

cholinesterase multisite binder ability of these newly designed hybrids and thus support the rational of our design strategy. In this study, due to the high similarity in tridimensional structure of AChE and BuChE, ligands were expected to dock in similar fashion in the BuChE active site

3.2 Instruments

The instruments described below were used for reaction monitoring and to confirm the structure of the synthesized compounds.

3.2.1 Nuclear Magnetic Resonance Spectroscopy (NMR)

^{1}H and ^{13}C NMR spectra were obtained using a Bruker Ascend™ 400 spectrometer at frequency of 400.12247 MHz for proton NMR and 100.1216005 MHz for ^{13}C with tetramethylsilane (TMS) or deuterated solvent used as internal standard. The chemical shifts (δ) were expressed in ppm and coupling constants (J) in Hz.

3.2.2 Infrared Spectroscopy (IR)

IR spectra were recorded on a Perkin Elmer spectrum 400 spectrometer, fitted with a diamond attenuated total reflectance (ATR) attachment.

3.2.3 Mass spectrometry (MS)

An analytical Perkin Elmer Single Quadrupole (SQ) 300 mass spectrometer was used to record mass spectra with Direct Infusion Electrospray Ionization positive Mass Spectrometry (DI-ESI- (+)) as ionization technique.

3.2.4 Thin layer chromatography (TLC)

Analytical TLC were performed on 0.20 mm thick aluminum silica gel sheets (Alugram SIL G / UV254, Kiesegel 60, Macherey-Nagel, Duren, Germany). Visualization was achieved using a Chromto-vue® Cabinet under UV light (254 nm and 366 nm), a spray reagent (containing Ninhydrin in ethanol) or iodine vapours. Mobile phases were prepared on a volume-to-volume basis. All chemical reactions were monitored by TLC.

40

3.2.5 Column Chromatography (CC)

Compounds were purified using a standard open glass column. Silica gel (0.063-0.200 mm / 70-230 mesh ASTM, Macherey-Nagel, Duren, Germany) was used as stationary phase with mobile phases as indicated for each compound.

3.2.6 Melting Point

Melting points were determined using Stuart SMP-10 melting point apparatus in capillary tubes.

3.2.7 Microwave Reactor

CEM Discover^{TM} focused closed vessel reactor was used as source of microwave in some of synthetic procedures.

3.3 Synthesis of selected compounds

All starting materials used were bought from Sigma Aldrich® and Merck® and used without any further purification.

3.3.1 Synthesis of (spiro [2*H*-3,1-benzoxazine-2,1-cyclohexan]-4(1*H*)-one (3)

In 100 ml toluene in a 250 ml round bottom flask was dissolved 50 g (0.36 mol) anthranilic acid (**1**) and 45.3 ml (0.44 mol) cyclohexanone (**2**) was added. The mixture was refluxed for 4 hr using a Dean-Stark trap until approximately 6.8 ml water was collected. The reaction mixture was cooled to room temperature and needle like-crystals formed. The solid was collected by filtration and successively washed with 50 ml toluene and 50 ml ethanol. The solid was then dried *in vacuo* and 72.51 g white crystals were collected which afforded a yield of 90.91% of product (**3**) with physical characteristics similar to that described in the literature (**Chao *et al*., 2012**).

3.3.2 Synthesis of 9-chloro-1,2,3,4-tetrahydroacridine intermediate (4)

In a 250 ml round bottom flask, containing 120 ml (1.30 mol) of $POCl_3$ was added 67 g (0.31 mol) of **3** and the mixture was refluxed on an oil bath at 120° C for 2 hrs. The reaction

41

mixture was then cooled to room temperature and cautiously added to 540 g KOH in 1000 ml ice water while stirred rapidly. 1500 ml CH_2Cl_2 was added to dissolve the solid. The aqueous layer was extracted with 3×1000 ml CH_2Cl_2. The combined organic extracts were dried with anhydrous $MgSO_4$. The mixture was filtered and the solvent was removed on a rotary evaporator to give a yellow solid, which was further recrystallized in acetone to give 64 g of pure yellow clear crystals (**4**) with the physical characteristic as described in the literature (**Lan *et al.*, 2014**). The synthetic procedure is shown in **Figure 3.2.**
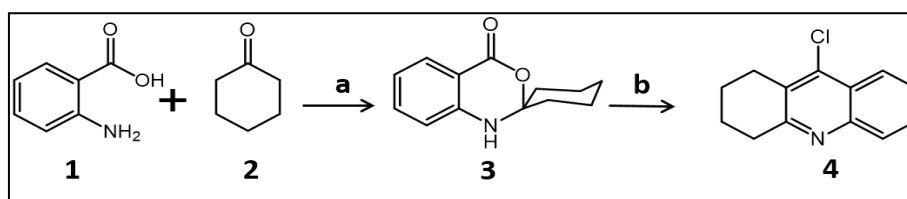

Figure 3.2: Reagents and conditions. a) Toluene, reflux 4 hrs, b) POCl₃, 2 hrs, KOH, Ice H₂O.

3.3.3 Synthesis of N^I(1,2,3,4-tetrahydroacridin-9-yl)alkane-1,w-diamine (w = 2, 3, 4, 6 or 8; alkane = ethane, propane, butane, hexane or octane)

To 0.43 g (2.00 mmol) of **4** contained in a microwave tube, was added 40.10 mmol of the appropriate alkylenediamine (**5n**). The mixture was reacted for 30 minutes at 200 ℃ with 250 W power and maximum pressure. After cooling, 30 ml of CH_2Cl_2 was added to the reaction mixture. Excess alkylenediamine was extracted from the mixture with 3×30 ml of distilled water acidified to pH5-6 with diluted HCl. The organic layer was dried with Na_2SO_4 and filtered through filter paper. The organic solvent was evaporated on a rotary evaporator to yield the final products (**6n**). The physical characteristics of these compounds were exactly the same as described in the literature (**Lan *et al.*, 2014**).

3.3.4 Activation of Trolox and synthesis of Tacrine-Trolox hybrid

To a solution of THF (20 ml) containing 0.75 g (3.20 mmol) of Trolox (**7**) was added 0.54 g (3.30 mmol) of *N,N*-carbanoyldiimidazole. The mixture was stirred at room temperature for 30 minutes before adding 3.00 mmol of the appropriate N^I-(1,2,3,4-tetrahydroacridin-9-yl) alkane-1,w-diamine (**6n**) in 10 ml THF. The resulting solution was reacted overnight at room temperature. Thereafter, the solvent was removed *in vacuo* and the residue was added to

42

DCM (25 ml) and extracted with acidified water (pH 3) 3×25 ml. The organic phase was further extracted with 5 N NaOH (aq) 3×25 ml. The combined organic phase was dried over anhydrous $MgSO_4$ and the solvent was removed *in vacuo* rendering the crude products, which were first purified by flash column chromatography with acetone as mobile phase and then flushed with ethanol (250 ml) to render the impure products (**8n**). A final purification was carried out by column chromatography for each compound with mobile phase ethyl acetate-ethanol (1:1) to yield pure products with similar characteristics to recently published work (**Nepovimova *et al*., 2015**). The synthetic procedure is described in **Figure 3.3**.
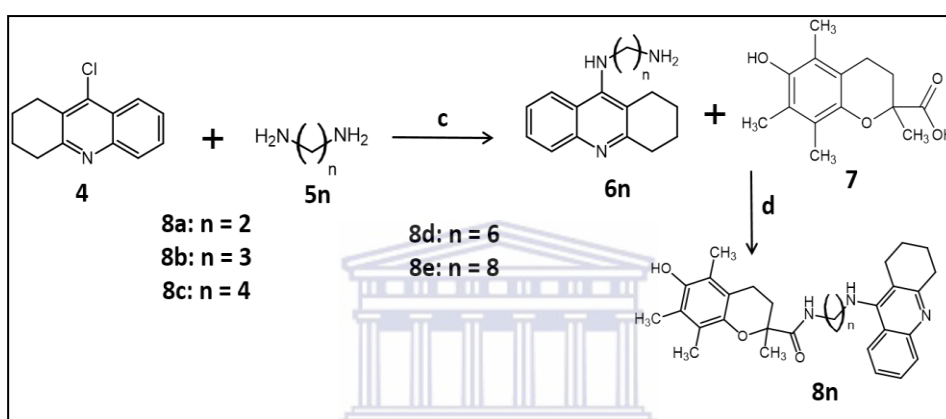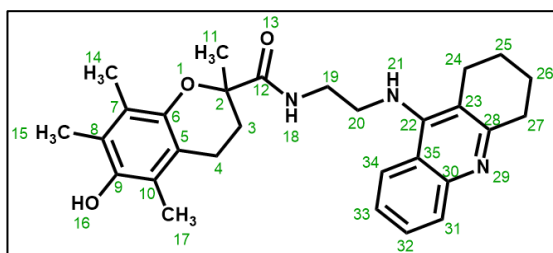

Figure 3.3: Reagents and conditions. c) Microwave radiation at 200 °C, 250 W and maximum pressure for 30 minutes, DCM, NaHCO₃, H₂O, Na₂SO₄, d) *N,N*-**carbonyldiimidazole, tetrahydrofuran (THF).**

3.3.4.1   6-Hydroxy-2,5,7,8-tetramethyl-*N*-{2-[(1,2,3,4-tetrahydroacridin-9-yl)amino]ethyl}-3,4-dihydro-2*H*-1-benzopyran-2-carboxamide (8a)

$C_{29}H_{35}N_3O_3$; **yield 16%**; **Physical data**: **MP**: 33-35 °C; **Rf** 0.3 (ethyl acetate-ethanol / 1:1); **¹H NMR** (400 MHz, CDCl₃), (spectrum 1a) δ_H: 7.95 (d, J = 8.97 Hz, 1H, H-31), 7.87 (d, J = 8.97 Hz, 1H, H-34), 7.55-7.53 (m, 1H, H-32), 7.32-7.26 (m, 1H, H-33), 6.86 (t, J = 5.95 Hz, 1H, H-18), 3.61-3.56 (bs, 4H, H-19, 20), 3.08-3.05 (m, 2H, H-27), 2.67-2.63 (m, 2H, H-24), 2.35-2.31 (m, 2H, H-4), 2.12-2.03 (3s, 9H, H-14, 15, 17), 1.89 (bs, 6H, H-3, 25, 26), 1.52 (s,3H, H-11), **¹³C-NMR** (100 MHz, CDCl₃), (spectrum 1b) δ_C: 176.64, 148.86, 145.86,

43

143.91, 141.47, 133.34, 129.89, 129.65, 129.06, 128.65, 124.37, 122.91, 121.76, 117.74, 78.33, 50.27, 40.22, 31.94, 29.67, 29.40, 25.26, 24.71, 24.43, 22.64, 21.95, 20.44, 14.10, 12.30, 12.03, 11.34.   **MS** (DI-ESI$_{(+)}$ m/z), (spectrum 1c): 474.31 [M + H]$^+$; **IR** (ATR, cm^{-1}) V$_{max}$ (spectrum 1d): 3326, 2924, 1447, 1091, 760.

3.3.4.2   6-Hydroxy-2,5,7,8-tetramethyl-*N*-{3-[(1,2,3,4-tetrahydroacridin-9-yl)amino]propyl}-3,4-dihydro-2*H*-1-benzopyran-2-carboxamide (8b)
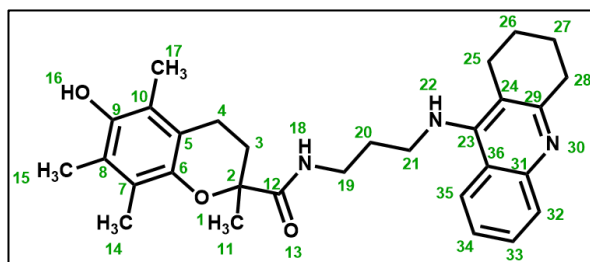
C$_{30}$H$_{37}$N$_3$O$_3$; **Yield 24.85%**; **Physical data**: **MP**: 118-122 ^{o}C **Rf** 0.33 (ethyl acetate-ethanol / 1:1); **^{1}H NMR** (400 MHz, CDCl$_3$), (spectrum 2a) δ$_H$: 7.93-7.87 (m, 2H), 7.51-7.49 (m, 1H), 7.34-7.31 (m, 1H), 6.71 (t, J = 6.26 Hz, 1H), 3.47-3.35 (m, 4H), 3.039 (bs, 2H), 2.68-2.60 (m, 5H), 2.07-2.03 (3s, 9H), 1.87 (bs, 6H), 1.72-1.68 (m, 3H), 1.54 (s, 3H); **^{13}C-NMR** (100 MHz, CDCl$_3$), (spectrum 2b) δ$_C$: 175.62, 157.75, 151.55, 146.03, 144.26, 129.09, 127.53, 124.31, 122.70, 122.13, 121.84, 120.00, 119.59, 118.00, 116,32, 78.58, 45.39, 36.56, 32.99, 31.43, 29.86, 25.07, 24.89, 23.05, 22.59, 20.76, 12.47, 12.15, 12.06, 11.61. **MS** (DI-ESI$_{(+)}$ m/z), (spectrum 2c): 488.39 [M + H]$^+$, **IR** (ATR, cm^{-1}) V$_{max}$, (spectrum 2d): 3326, 2927, 1447, 760.

3.3.4.3   6-Hydroxy-2,5,7,8-tetramethyl-*N*-{4-[(1,2,3,4-tetrahydroacridin-9-yl)amino]butyl}-3,4-dihydro-2*H*-1-benzopyran-2-carboxamide (8c)
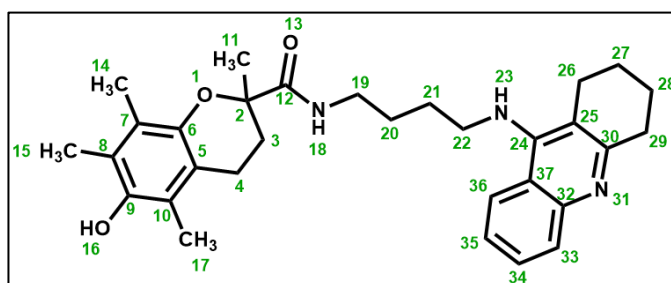
C$_{31}$H$_{39}$N$_3$O$_3$; **yield 13%**; **Physical data**: **MP**: 154-159 ^{o}C **Rf** 0.36 (ethyl acetat-ethanol / 1:1); **^{1}H NMR** (400 MHz, CD$_3$OD), (spectrum 3a) δ$_H$: 8.15 (d, J = 8.45 Hz, 1H), 7.71-7.67 (m, 2H), 7.46-7.42 (m, 1H), 3.59 (bs, 2H), 3.32-3.28 (m, 2H), 3.06 (bs, 1H), 2.94 (bs, 2H),

44

2.62 (bs, 2H), 2.48-2.41 (m, 2H), 2.24 (m, 1H), 2.08-2.05 (2s, 6H), 1.93 (s, 3H), 1.90-1.86 (m, 4H), 1.72-1.70 (m, 1H), 1.45-1.44 (m, 4H), 1.40 (s, 3H); **^{13}C-NMR** (100 MHz, CD$_3$OD), (spectrum 3b) δ$_C$: 174.69, 153.94, 153.62, 145.97, 144.19, 142.00, 130.60, 124.57, 123.74, 123.64, 122.60, 121.56, 120.18, 117.84, 117.54, 113.04, 78.27, 48.09, 38.43, 30.53, 29.65, 28.04, 26.97, 24.52, 24.37, 21.46, 20.60, 12.64, 12.02, 11.68. **MS** (DI-ESI$_{(+)}$ $_{m}$/z) (spectrum 3c): 502.34 [M + H]$^+$; **IR** (ATR, cm^{-1}) V$_{max}$, (spectrum 3d): 3370, 2928, 1520, 1088, 750, 530.

3.3.4.4   6-Hydroxy-2,5,7,8-tetramethyl-*N*-{6-[(1,2,3,4-tetrahydroacridin- 9-yl)amino]hexyl}-3,4-dihydro-2*H*-1-benzopyran-2-carboxamide (8d)
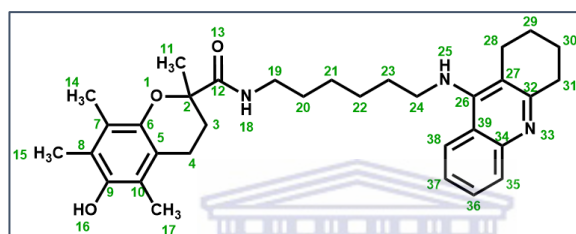
C$_{33}$H$_{43}$N$_3$O$_3$; **yield 12%**; **Physical data**: **MP**: 146-149 ^{o}C **Rf** 0.46 (ethyl acetate-ethanol / 1:1); **^{1}H NMR** (400 MHz, CDCl$_3$), (spectrum 4a) δ$_H$: 8.29 (d, J = 8.55 Hz, 1H), 8.19 (d, J = 8.55 Hz, 1H), 7.61-7.57 (m, 1H), 7.40-7.336 (m, 1H), 6.34-6.31 (m, 1H), 3.77 (t, J = 7.25 Hz, 2H), 3.14 (t, J = 6.29, 2H), 2.68 (t, J = 5.82 Hz, 2H), 2.52-2.43 (m, 4H), 2.17-2.08 (3s, 9H), 1.85-1.77 (m, 6H), 1.62-1.52 (m, 2H), 1.51 (s, 3H), 1.23-1.19 (m, 6H), 0.92-0.90 (m, 2H); **^{13}C-NMR** (100 MHz, CDCl$_3$), (spectrum 4b) δ$_C$: 174.49, 155.42, 151.41, 146.18, 144.41, 139.31, 131.96, 124.98, 124.49, 122.90, 121.48, 120.99, 118.09, 116.14, 11.37, 78.50, 48.24, 38.73, 38.54, 30.96, 29.74, 29.39, 28.83, 26.85, 26.31, 25.77, 25.36, 24.13, 22.12, 20.86, 13.09, 12.94, 11.99; **MS** (DI-ESI$_{(+)}$ m/z), (spectrum 4c): 530.38 [M + H]$^+$; **IR** (ATR, cm^{-1}) V$_{max}$, (spectrum 4d): 3270, 2932, 1520, 1088, 576.

3.3.4.5   6-Hydroxy-2,5,7,8-tetramethyl-*N*-{8-[(1,2,3,4-tetrahydroacridin- 9-yl)amino]octyl}-3,4-dihydro-2*H*-1-benzopyran-2-carboxamide (8e)
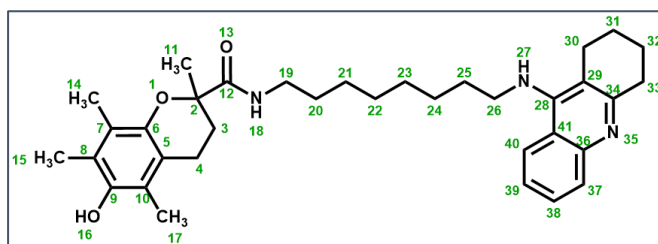
C₃₅H₄₇N₃O₃; **yield 19** ; **Physical data**: **MP**: 63-66 °C **Rf** 0.5 (ethyl acetate-ethanol / 1:1); **¹H NMR** (400 MHz, CDCl₃), (spectrum 5a) δ_H: 8.31 (bs, 1H), 8.19 (d, J = 8.52 Hz, 1H), 7.59 (bs, 1H), 7.43-7.36 (m, 1H), 6.35-6.34 (m, 1H), 3.80 (t, J = 7.15 Hz, 2H), 3.16 (bs, 2H), 2.69 (t, J = 5.32 Hz, 2H), 2.54-2.44 (m, 2H), 2.19-2.09 (3s, 9H), 1.85-1.77 (m, 6H), 1.60 (t, J = 7.21, 2H), 1.52 (bs, 4H), 1,39-1.35 (m, 3H), 1.27-1.21 (m, 4H), 0.91-0.82 (m, 3H); **¹³C-NMR** (100 MHz, CDCl₃), (spectrum 5b), δ_C: 174.50, 155.49, 151.22, 147.70, 146.17, 144.40, 139.00, 132.01, 124.99, 124.49, 122.76, 121.49, 120.46, 118.10, 115.99, 111.16, 78.51, 48.20, 38.56, 30.96, 29.75, 29.40, 28.65, 26.33, 26.04, 25.78, 25.37, 24.12, 22.10, 20.86, 20.82, 14.39, 12.04, 8.83; **MS** (DI-ESI₍₊₎ m/z), (Spectrum 5c): 602.42 [M + 2Na-H]⁺; **IR** (ATR, cm⁻¹) V_max, (spectrum 5d): 3271, 2926, 1521, 760.

3.3.5 Synthesis of *N*-(7-bromoheptyl)-1,2,3,4-tetrahydroacridin-9-amine intermediate (12)

9-Amino-1,2,3,4-tetrahydroacridine (780 mg) (**10**) was obtained by precipitating tacrine hydrochloride (9-amino-1,2,3,4-tetrahydroacridine hydrochloride) 1g (**9**) in a sodium hydrogen carbonate solution. To a solution of CH₃CN (10 ml) containing 400 mg (2.01 mmol) of (**10**) in a 100 ml round bottom flask was added 2.60 g (10.10 mmol) of 1,7-dibromoheptane (**11**) and 224 mg (4.02 mmol) of KOH. The mixture was stirred at room temperature overnight. The reaction was monitored by TLC (mobile phase: ethyl acetate-hexane-TEA (10:10:1). After completion, the reaction mixture was poured into 10 ml of distilled water and extracted with DCM (3×20 ml). The combined organic layer was dried over anhydrous Na₂SO₄, filtered, and the solvent was evaporated under reduced pressure. The residue was purified by silica gel column chromatography using ethyl acetate-hexane-TEA (10:10:1) as eluent to produce 100 mg (13.20%) of a pure yellow oil product (**12**) with the same characteristics as described in the literature (**Savini *et al.*, 2003**).

46

3.3.6 Synthesis of Tacrine-Tryptoline hybrid (14)

In a microwave tube containing 5 ml of DMF was dissolved 70 mg (0.18 mmol) of **12**. 26.30 mg (0.15 mmol) of tryptoline (**13**) and 38.80 mg (0.30 mmol) of K_2CO_3 were added with a catalytic amount of KI. The mixture was irradiated in the microwave at 160 ^{o}C, 250 PSI, 200 W, Ramp 30 s, power max on and high stir for 1 hr. The reaction was monitored by TLC (mobile phase: ethyl acetate-hexane-TEA in a ratio 10:10:1. After completion, the reaction mixture was poured into 5 ml of distilled water and extracted with ethyl acetate (3×10 ml). The combined organic phase was washed with water, and then saturated NaCl solution (3×10 ml). The organic fraction was dried with anhydrous Na_2SO_4 and evaporated under reduced pressure. The residue was purified by silica gel column chromatography using of ethyl acetate-hexane-TEA (10:10:1) to produce 18 mg (25.30%) of a pure dark yellow product (**14**). The synthetic procedure is described in **Figure 3.4**.
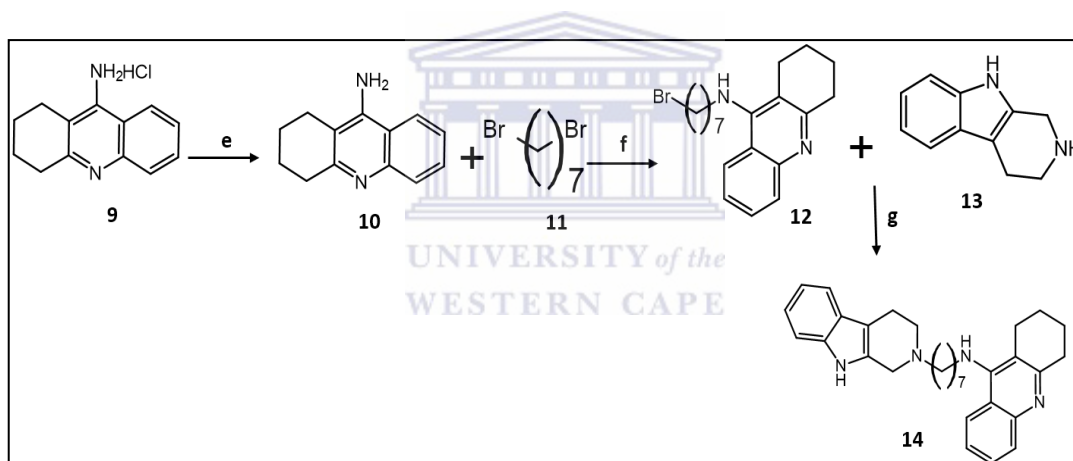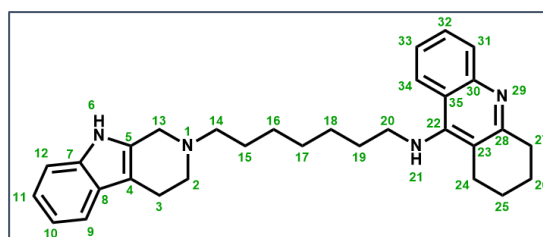

Figure 3.4: Reagents and conditions. e) Sodium hydrogen carbonate, f) CH₃CN, KOH, rt, overnight, g) DMF, K₂CO₃, Microwave 160 ^{o}C, 250 PSI, 200 W, 1h, Ramp 30 S.
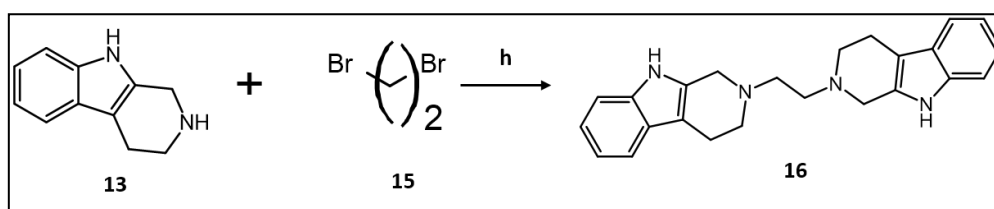
3.3.6.1 *N*-(7-(3,4-dihydro-1*H*-pyrido[3,4-b]indol-2(9*H*)-yl)heptyl)-1,2,3,4-tetrahydroacridin-9-amine (14)

C$_{31}$H$_{38}$N$_4$; **yield 21.43%**; **MP:** 98-101 °C; **Physical data**: **Rf** 0.43 (ethyl acetate-hexane-TEA / 10:10:1); **^{1}H NMR** (400 MHz, CDCl$_3$), (spectrum 6a), δ$_H$: 8.37 (s, 1H, H-6), 7.98 (m, 2H, H-31, 34), 7.59-7.55 (m, 1H, H-32), 7.45 (d, J = 7.29 Hz, 1H, H-12), 7.37-7.30 (m, 2H, H-9, 33), 7.13-7.044 (m, 2H, H-10,11), 3.58-3.54 (m, 4H, H-24, 27), 3.08 (s, 2H, H-13), 2.83-2.80 (m, 4H, H-25, 26), 2.68 (t, J = 6.02 Hz, 2H, H-20), 2.54 (t, J = 7.67 Hz, 2H, H-14), 1.90 (m, 4H, H-3, 2), 1.67-1.65 (m, 2H, H-19), 1.53 (m, 2H H-15), 1.35 (m, 6H, H-16, 17, 18); **^{13}C-NMR** (100 MHz, CDCl$_3$), (spectrum 6b), δc 157.66, 151.60, 136.24, 132.05, 129.04, 127.76, 123.95, 123.15, 121.29, 119.70, 117.99, 115.22, 110.88, 108.33, 57.86, 51.39., 50.43, 49.39, 33.31, 31.72, 29.23, 27.37, 27.29, 26.78, 24.76, 23.01, 22.61, 21.38,, 18.57; **MS** (DI-ESI $_{(+)}$ m/z), (spectrum 6c): 467.35 [M + H]$^+$; **IR** (ATR, cm^{-1}) V$_{max}$, (spectrum 6d): 3214, 2926, 1563, 740.

3.3.7 Synthesis of Tryptoline dimer (16)

To a solution of CH$_3$CN (20 ml) containing 0.4 g (2.32 mmol) of **13** in a 100 ml round bottom flask was added 2.18 g (11.61 mmol) of 1,2-dibromoethane (**15**) and 0.26 mg (4.63 mmol) KOH. The mixture was irradiated in the microwave (130 W, 250 PSI, 100 °C, Ramp 30s, high stir, power max on for 1 hr). The reaction was monitored by TLC (mobile phase: methanol). After completion of the reaction, the solvent was evaporated under reduced pressure and the resulting solid residue was dissolved in methanol and purified by silica column chromatography (mobile phase: methanol) to yield impure powder like-product, which was further subjected to 2 cycles of recrystallization in ethanol to afford 150 mg pure white pale powder **(16).** The synthetic procedure is described in **Figure 3.5**.

Figure 3.5: Reagents and conditions. h) KOH, CH$_3$CN, microwave 100 °C, 250 PSI, 130 W, Ramp 30s, high stirr, power max on, for 1 hr

3.3.7.1 1,2-bis(3,4-dihydro-1*H*-pyrido[3,4-b]indol-2(9*H*)-yl)ethane (16)
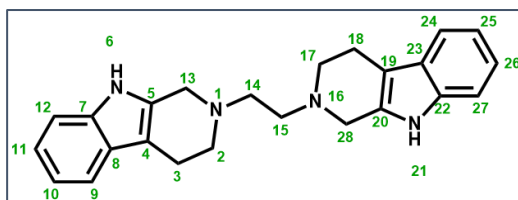
$C_{24}H_{26}N_4$; **yield 17.45%**; **white pale crystals**; **Physical data**: **MP**: 255-260 °C; **Rf** 0.57 (methanol); **^{1}H NMR** (400 MHz, $(CD_3)_2SO$), (spectrum 7a), δ_H: 10.70 (s, 2H, H-6 / 21), 7.35 (m, 4H, H-9, 12 / 24, 27), 6.97(m, 4H, H-10,11 / 25, 26), 3.69 (s, 4H, H-13 / 28), 3.35 (s, 4H, H-3 / 18), 2.80 (bs, 4H, H-2 / 17), 2,68 (s, 4H, H-14 / 15); **^{13}C-NMR** (100 MHz, $(CD_3)_2SO$), (spectrum 7b), δ_C: 135.85, 132.95, 126.70, 120.23, 118.20, 117.30, 110.85, 106.41, 55.33, 51.21, 50.46, 21.26; **MS** (DI-ESI$_{(+)}$ m/z), (spectrum 7c): 371.13 [M + H]$^+$; IR (ATR, cm-1) Vmax, (spectrum 7d): 3374, 2815, 1450, 741.

3.4 Structure elucidation and confirmation

^{1}H NMR spectra of compounds **8a-e** were characterized by 4 strong signals, three singlets at δ 2.18-2.03 and one singlet at δ 1.93-1.60 corresponding to C-14, C-15, C-17, and C-11 of the trolox moiety**.** These strong signals and the integration match with the four methyl groups of trolox present in the final compounds. This characteristic is common to other hybrids containing the trolox moiety (**Nepovimova *et al*., 2015**) . Four downfield aromatic signals with multiplicity caused by variation of the chemical environment at δ 8.31-7.26 were assigned to the quinoline ring of tacrine. Others upfields signals were assigned to the cyclic hydrocarbon of tacrine, trolox and the linker. In the ^{13}C spectra, a signal was observed at δ 176.64-174.49 which is the characteristic signal of the carbonyl and signals at δ 160-110 were assigned to the quinoline ring of tacrine and aromatic ring of trolox. In the IR spectra, a sharp peak appeared at 1589-1692 cm^{-1} due to carbonyl group of the respective compounds. The final structures were confirmed by ESI-MS and molecular ion peaks were observed at m/z 474.31 [M+H]$^+$, 488.39 [M+H]$^+$, 502.34 [M+H]$^+$, 530.38 [M+H]$^+$, and 602.42 [M+2Na-H]$^+$, for **8a-e** respectively.

The ^{1}H NMR spectrum of compound **14** was characterized by nine downfield signals. A weak singlet, which integrated for 1 H at δ 8.37 corresponded to H-6. Overlapping multiplets at δ 7.99-7.97, 7.37-7.34 and 7.30-7.044, which can be clearly distinguished by the

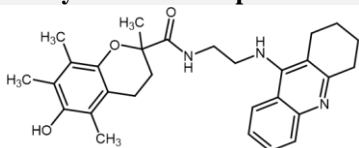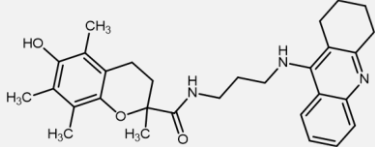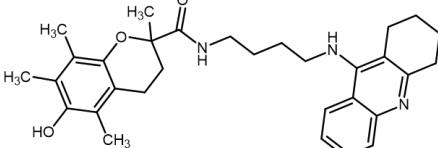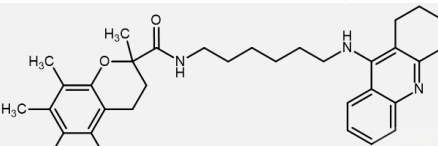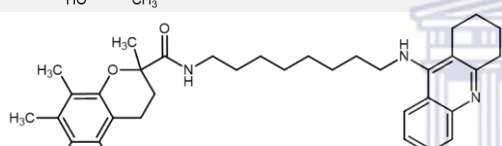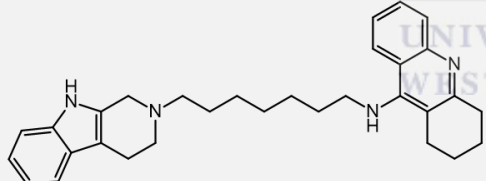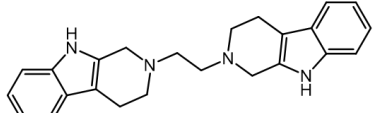integration as six signals and two multiplets at δ 7.59-7.55 and 7.37-7.34 was assigned to the aromatic ring of the quinoline (tacrine) and indole (tryptoline). The final structure was confirmed by ESI-MS and the molecular ion peak appeared at m/z 467.35 [M + H]$^+$.

For compound **16**, the ^{1}H and ^{13}C NMR spectra were characterized by the appearance of a new peak in at the aliphatic region at δ 3.69 / 55.33, corresponding to the C-14 / 15 of the linker which does not appear on the spectrum of tryptoline. The final structure was confirmed by ESI-MS and molecular ion peak at m/z 371.13 [M + H]$^+$.

3.5   Discussion and conclusion

The synthesis of the tacrine-trolox hybrid **(8n)** required intermediate 9-chloro-1,2,3,4-tetrahydroacridine that was obtained from two sequential reactions; Condensation of anthranilic acid and cyclohexanone, followed by a reaction of the Spiro intermediate with phosphoryl chloride. The intermediate (chlorotacrine) was then aminated via microwave with appropriate alkyl diamine linkers followed by conjugation to trolox through an amide bond. The tacrine-tryptoline hybrid **(14)** was synthesized by a two-step reaction including amination of 1,7-dibromoheptane with 9-amino-1,2,3,4-tetrahydroacridine to produce an intermediate, followed by its condensation to tryptoline through a further amination reaction. The tryptoline dimer **(16)** resulted from reaction of tryptoline with excess 1,2-dibromoethane. The yields of all final products were low, ranging from 12 % to 24.85 % (**Table 3-1**).

50

Table 3-1: Final products of synthesis and theirs percentage yield.

Synthesized compounds	Numbers	Percentage yield
	8a	17 %
	8b	24 %
	8c	13 %
	8d	12 %
	8e	19 %
	14	21 %
	16	17.45 %

These reaction methods suffer from degradation products, secondary reaction products and unreacted starting materials that contaminate the desired final product and necessitated lengthy purification and hence low yield. New synthetic methods thus need to be developed with the aim to improve the yield, reduce reaction time and produce relatively pure product.

51

CHAPTER 4.

# BIOLOGICAL ASSAY

4.1 Introduction

It was expected that the newly synthesized multifunctional compounds developed based on MTDL strategy would display the ability to modulate multiple target proteins or multiple pathways, which play crucial roles in the aetiology of AD. To stay in the scope of this study, the biological evaluation was limited to the investigation of cholinesterase inhibitory activity and free radical scavenging activity of synthesized compounds. This would give an indication of the ability of the designed and synthesized compounds to protect neuronal cells.

4.2 Anti-cholinesterase assay

AChE and BuChE are the two major cholinesterases present in vertebrates. Both enzymes have been demonstrated to regulate ACh activity by terminating its physiological action by hydrolyzing it into acetate and choline in the synaptic cleft (**Massoulié *et al.,* 1993**). In healthy brain, choline resulting from the hydrolysis of Ach, is taken up in the presynaptic nerve for use as precursor in the synthesis of new ACh by the cholinergic system. This process maintains a constant level of ACh in cholinergic nerves. In AD, the cholinergic system does not work efficiently. This leads to loss of neuronal cells, and cause depletion of ACh levels in the regions responsible for cognition and memory such as neocortex, hippocampus and basalis of Meynert, leading to dementia (**Francis *et al*., 1999**). Therefore, the inhibition of cholinesterase activity has been proposed in the cholinergic hypothesis as alternative to correct cholinergic system deficits and cells loss by promoting the survival of ACh in the synaptic cleft using cholinesterase inhibitors.

One of the most used techniques for the determination of cholinesterase activity is the colorimetric Ellman's assay. This method offers some advantages such as its simplicity, rapidity and low cost (**Worek and Thiermann, 2012**). The general principle is based on the measurement of the ability of AChE or BuChE to catalyse the hydrolysis of their analogue

52

substrates acetylthiocholine and butyrylthiocholine, generating thiocholine and acetate / butyrate respectively. The thiocholine then reacts with the chromogen 5,5-dithiobis-(2-nitrobenzoic acid) (DTNB) to produce the 5-thio-2-nitrobenzoate anion (TNB⁻) with a yellow colour. The intensity of the coloration is proportional to the quantity of substrate hydrolysed monitored at 405 nm absorbance. **Figure 4.1** illustrates the chemical reaction taking place in the assay.
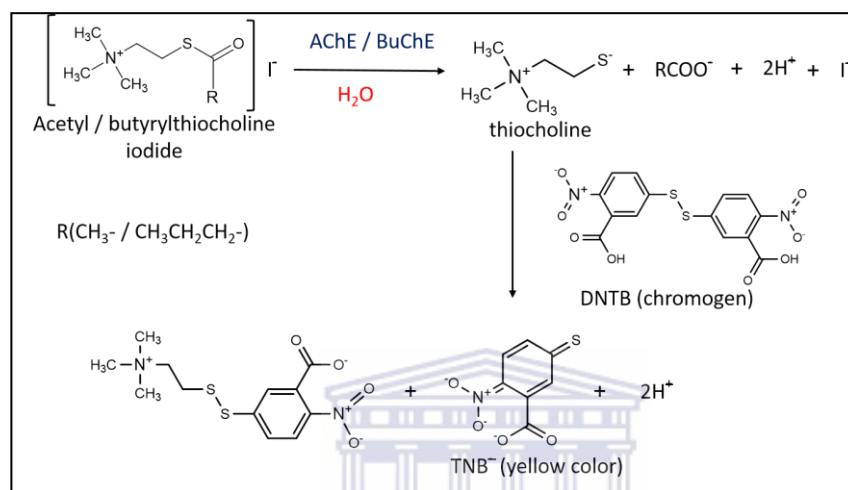
Figure 4.1: Summary of principal chemical reactions taking place in the colorimetric method of determination of cholinesterase activity using Ellman's assay (Worek and Thiermann, 2012).

The principle behind this method was adapted to determine the inhibitory effect of synthesized compounds on cholinesterase activity.

4.2.1 Method and materials

All chemicals were purchased from Sigma Aldrich. Absorbance was recorded at 405 nm using a Rayto 6100 microplate reader. Trizma®-Hydrochloride (2-Amino-2-(hydroxymethyl)-1,3-propanediol hydrochloride) buffer (50 mM) was prepared, the pH adjusted to 8 with NaOH and it was refrigerated until use for no longer than 5 working days. The stock solution of test compounds were dissolved in DMSO and thereafter diluted with DMSO to five different concentrations ranging from 10 mM – 10 nM. The final concentration of DMSO in the working solution was 1%. Acetylthiocholine (15 nM) and butyrylthiocholine (15 mM) solutions were prepared with Tris-HCl buffer pH 8 immediately preceding the assay and protected from light by means of aluminum foil. Stock solutions of *electric eel* AChE / BuChE (12 units/ml) were

prepared and 20 µl were aliquoted in 2 ml Eppendorf tubes and stored at – 60 ⁰C. Each working day, a suitable amount of stock solution 12 units/ml were defrosted and diluted with Tris-HCl buffer to a working concentration of 0.12 units/ml containing 0.1% of Bovine Serum Albumin (BSA).

The in vitro assay was carried on as follows: Into each Eppendorf tube was pipetted 148 µl of the 1.5 mM DTNB solution and to this was added 50 µl of diluted enzyme 0.12 Unit/ml (AChE / BuChE) and 2 µl of the corresponding test compound / DMSO for the blank / reference compounds. The mixture was vortexed vigorously before being transferred into a 96 well plate and incubated for 10 minutes at 37 ℃. 30 µl of the substrate, acetyl / butyrylthiocholine iodide (15 mM) was added using a multipipette and it was mixed by pipetting up and down. The plate was returned into the incubator for 20-30 minutes. Afterwards it was placed in the microplate reader to determine the absorbance at 405 nm. For the blank, 2 µl of DMSO was used in place of test compounds and all other parameters were kept the same. Donepezil and tacrine were used as reference compounds for the acetylcholinesterase and butyrylcholinesterase assay respectively. The procedure is summarized in the **Figure 4.2**. During incubation of test compounds with AChE / BuChE, interaction occurs that determines, in the second incubation time, the concentration of free enzymes available to catalyse hydrolysis of substrates (acetyl / butyrylcholine), liberating thiocholine, which further reacts with DNTB to produce yellow colour TNB⁻ (optical density, 405 nm). The intensity of the yellow colour is proportional to substrate hydrolysed.

The percentage inhibition was obtained by subtracting the absorbance of the blank from the absorbance of test compounds at each concentration, divided by the absorbance of the blank x 100 ((Absorbance blank - Absorbance test compounds) / absorbance blank x 100). Each concentration was run in triplicate.
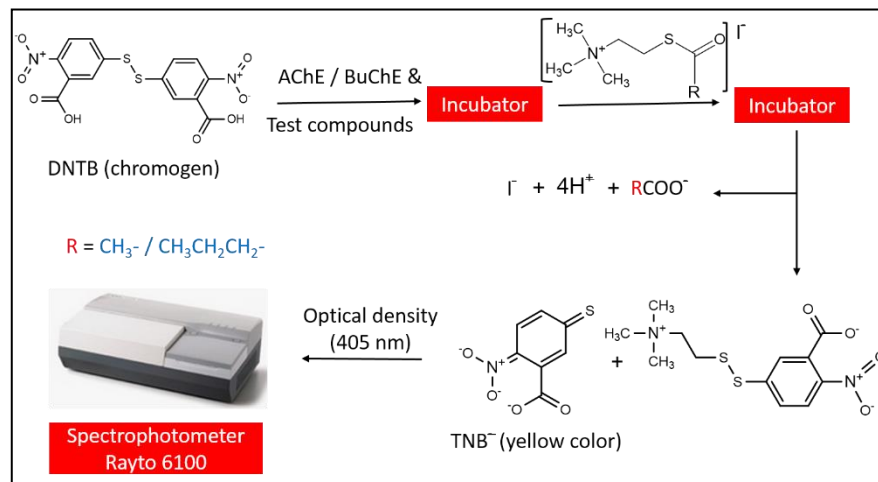
Figure 4.2: Simplified procedure of determination of inhibitory effect of synthesized compounds using Ellman's method.

4.2.2 Results and Discussion

4.2.2.1 Anticholinesterase assay

Five different concentrations of test compounds were run in triplicate. The percentage inhibition was calculated from the absorbance values using Microsoft Excel 13 and expressed as mean and standard deviation (SD). The IC_{50} was determined by non-linear regression using Graphpad Prism® version 6.5 by plotting the Log of concentrations of test compounds versus percentage inhibition of cholinesterase (AChE / BuChE). IC_{50} is defined as the concentration of test compounds required to half the activity of cholinesterase and is useful for comparing the potency of test compounds to each other and to the control. **Figure 4.3** and **Figure 4.4** represent the typical graphs of non-linear regression curve obtained by plotting log concentration of test compounds versus percentages inhibition.

4.2.2.1.1 AChE inhibition assay

Biological evaluation results of AChE inhibitory ability of synthesized compounds are expressed in terms of IC_{50} (**Figure 4.3**).

The tacrine hybrid compounds showed moderate to high AChE inhibitory activities comparable or better than their reference compounds donepezil and tacrine. Compounds **16** displayed no

55

inhibitory activity against AChE. Though tryptoline is not known to have AChE inhibitory activity, it is possible that the short linker chain length (C2 carbon) limited the flexibility of the pharmacophore (tryptoline moieties) and prevented the dimer from adopting a stable conformation for effective activity. This scenario is slightly different from **8a** where the 2 carbon linker chain length is extended by the amide bond. Compounds **8d** and **8e** with 6 and 8 carbon linker chain lengths respectively display higher activities than **8a, 8b** and **8c** with 2, 3 and 4 carbon linker chain lengths. Compound **14** with the 7 carbon linker exhibited the highest activity and this is consolidated by the modelling study that clearly illustrate the interaction of the two pharmacophore moieties (tacrine and tryptoline) with Trp84 and Trp279, which is crucial for AChE activity. It can be deduced from this observation that, hybrids with longer linker chain lengths have increased AChE inhibitory activities compared to the shorter ones. This is in line with predictions from the modelling study and also correlates well with other studies described in the literature **(Simone *et al*., 2014).**

The idea of varying linker chain length seeks to assign to the two linked pharmacophore units, the ability to span the PAS (important for attraction of ACh) and CAS (necessary for the hydrolysis of ACh) of AChE, and obtain the appropriate orientation that would enable them to interact with crucial amino acids in the active site, generating better activities. As confirmed by these results, shorter linker chain lengths (less than 5 carbons) are less favourable for this.
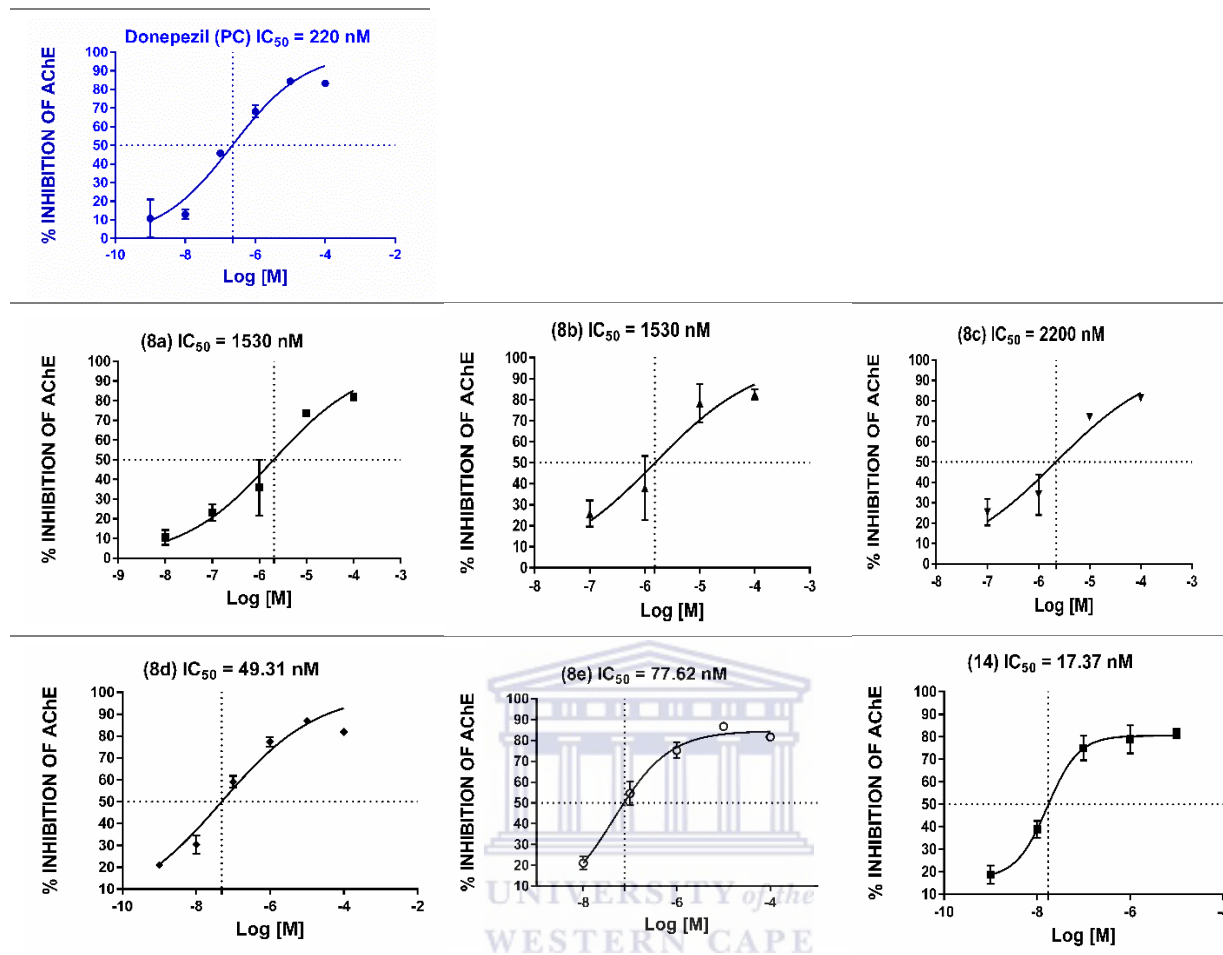
56

Figure 4.3: Graphs showing the inhibitory activity of synthesized compounds against AChE in terms of IC$_{50}$ (compounds 8a-e and 14). The IC$_{50}$ value was calculated using the equation; Log IC$_{50}$ = X (X is the numerical value of LogIC$_{50}$ determined graphically or generated automatically by graph prism 6 as equivalent of the X coordinate of 50% activity on the X axis). The blue graph is the positive control (PC).

4.2.2.1.2   BuChE inhibitory assay

Biological evaluation results of BuChE inhibitory ability of synthesized compounds are included in **Figure 4.4**. These synthesized compounds showed moderate to high BuChE inhibitory activities comparable or higher than their reference compound tacrine. Compound **8d**, **8e** and **14** with 6, 8 and 7 carbon linker chain lengths respectively tend to display higher activities than **8a**, **8b**, and **8c** with 2, 3 and 4 carbons linker chain lengths. It can be deduced from this observation that hybrids with longer linker chain lengths also seem to exhibit increased BuChE inhibitory activities compared to the shorter ones.
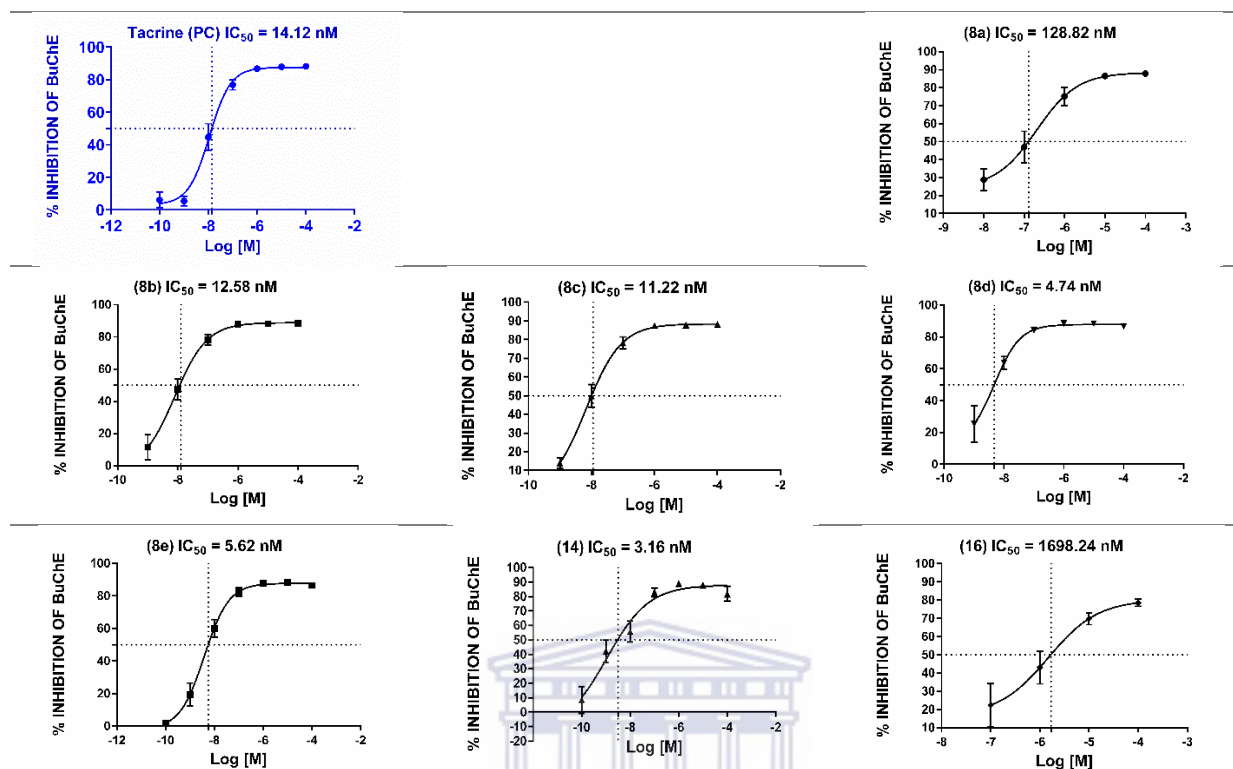
57

Figure 4.4: **Graphs showing the inhibitory activity of synthesized compounds against BuChE in terms of IC$_{50}$** (compounds **8a**-**e**, **14** and **16**).

This similarity of interaction of synthesized compounds and target proteins (AChE / BuChE) is consistent with the similarity of the topology of their active sites. Compounds **8d**, **8e** and **14** exhibited BuChE inhibitor activity almost 4 fold**,** 3 fold and 4 fold higher than tacrine. All the synthesized compounds showed higher inhibitory activity for BuChE than AChE. This might be the result of the higher affinity of synthesized compounds to BuChE. It has been demonstrated that the two proteins share 65% amino acid sequence similarity and the 35% difference in their amino sequence confer to BuChE the ability to accommodate bulkier substrates than AChE (**Nicolet *et al*., 2003**).

The difference in amino acid sequence of AChE and BuChE might prove to be a challenge in effects to design a 100% non-selective cholinesterase inhibitor. The goal of the anticholinesterase assay was to discover new dual inhibitors of cholinesterase since both proteins are believed to contribute, to different degrees, to the depletion of ACh levels in AD brain. Based

58

on this observation, selective inhibitors could be less effective as therapeutic options. The synthesized compounds showed different selectivity index as can be seen in **Table 4-1**.

Table 4-1: Selectivity Index (SI) of synthesized compounds and their Log P values and MW (obtained from ACD / Chemsketch software), nd (not determined).

Compounds	MW (g / mol)	AChE IC$_{50}$ (nM)	BuChE IC$_{50}$ (nM)	AChE / BuChE (SI)	Log P
8a	473.6	1530	128.82	11.87	5.98
8b	487.6	1530	12.58	121.62	6.31
8c	501.7	2200	11.22	196.07	6.70
8d	529.7	49.31	4.74	10.40	7.57
8e	557.8	77.62	5.62	13.81	8.63
14	466.66	17.37	3.16	5.49	8.02
16	370.49	0	1698.24	-	4.21
Tacrine	-	nd	14.12	nd	-
Donepezil	-	220	nd	nd	-

Compounds **8d**, **8e** and **14** showed relatively low SI with inhibition of both enzymes at nano molar concentration, which could make them suitable as dual inhibitors of cholinesterase. Compounds **8a-8c** inhibited AChE in the micro molar range and would be less effective as dual ChE inhibitors. However, they were selective inhibitor of BuChE.

4.2.3 Antioxidant assay

4.2.3.1 Introduction

Free radicals are compounds that contain one or more unpaired electrons (superoxide free radical ($O_2 {}^{\cdot-}$), hydroxyl free radical ($\cdot OH$). etc.) and are generally highly reactive. They are produced in the body by diverse pathways. Their physiological concentration has been demonstrated to protect cells from foreign substances by degradating them and it also dysplay anti-microbial

properties (**Nimse and Pal, 2015**). Neurotoxic conditions such as accumulation of toxic Aβ in AD can cause high production of free radicals that overwhelm endogenous antioxidant activities (Vitamin C, Vitamin E, superoxide dismutase etc.) responsible of maintaining the level of free radicals in the physiological concentration. Inadequate neutralization of excess free radicals can attack biological molecules (proteins , DNA and lipids), leading to oxidative stress. Therefore, enhancing the cellular defence against oxidative stress based on exogenous antioxidants might offer positive therapeutic value.

Multiple methods are used to assess the free radical scavenging or antioxidant effect of given substances. The most frequently used are the 2-azinobis-(3-ethylbenzothiazoline-6-sulfonic acid) (ABTS) and 2,2-diphenyl-1-picrylhydrazyl (DPPH) assays. They offer similar advantages like accessibiliy, cheapness and simplicity (**Shalaby and Shanab, 2013**). DPPH was chosen for the evaluation of free radical scavenging properties of the synthesized compounds. The characteristic absorbance of DPPH˙ is at 517 nm. The principle of DPPH assay consists of monitoring whether the decrease of the absorbance of the DPPH• (purple) is reduced in presence of a free radical scavenging substance to generate DPPH-H (light yellow) (**Shalaby and Shanab, 2013)** as shown in **Figure 4.5**.

4.2.3.2   Method and materials

All chemicals were purchased from Sigma Aldrich. DPPH˙ methanolic solution (0.12 mM) was prepared the day of the assay and was protected from light by means of aliminium foil. Four different concentrations (10 mM, 1 mM, 0.1 mM and 0.01 mM) of test compounds from the Ellman's assay were used. Trolox was used as positive control and the required amount for four different concentrations were disolved in the same solvent (DMSO) as test compounds. 180 µl aliquots of methanolic solution of DPPH˙ were placed in a 96 well microplate using a multiplepipette. 20 µl of the test compounds, positive control or DMSO for the blank were added to the corresponding wells and it was incubated in a dark at room temperature for 30 minutes. The absorbance was then measured at 517 nm (POLARstar omega spectrophotometer (**Figure 4.5**).
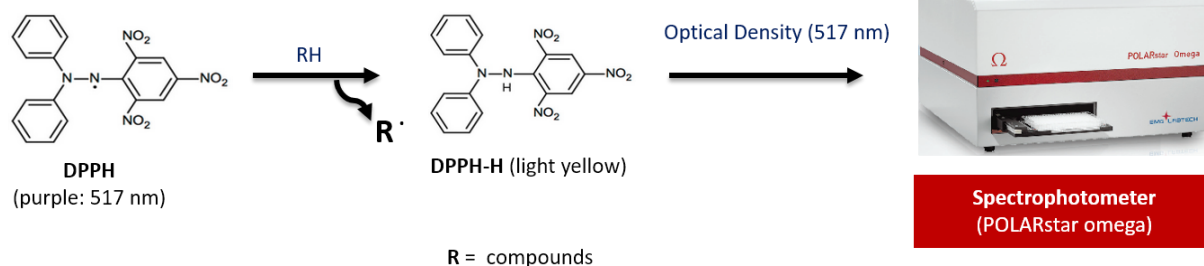
Figure 4.5: Schematic representation of the principle reaction of DPPH assay.

Each concentration was run in triplicate. The percentage activity was calculated using the following equation: (absorbance of blank – absorbance of test compounds) / absorbance of blank × 100). Data analysis and, further calculations, graphs and IC_{50} determination were done using GraphPad Prism 6.5 software as discussed in the results session.

4.2.3.3 Results and discussions

Biological evaluation results for free radical scavenging ability of synthesized compounds were expressed in terms of IC_{50} values **(Figure 4.6)**.

Trolox has well documented antioxidant properties and is regularly used as reference compound in investigating antioxidant or free radical scavenging activity of new drugs. As can be seen in **Figure 4.6**, the conjugation of trolox to tacrine through varying linker chain lengths did not affect its ability to scavenge free radicals.

All the newly synthesized compounds exhibited activity with IC_{50} value in the same range as that of trolox (17.57 µM), 11.48 µM **(8b)**, 14.38 µM **(8c)**, 12.67 µM **(8d)**, and 14.96 µM **(8e)**. The exception is compound **8a** (46.23 µM) which showed free radical scavenging activity of about half that of trolox. Compounds **14** and **16** exhibited lower free radical scavenging activity with IC_{50} values of 129.41 µM and 125.24 µM. This can be expected as the trolox moiety is replaced by the less potent free radical scavenging tryptoline moiety.
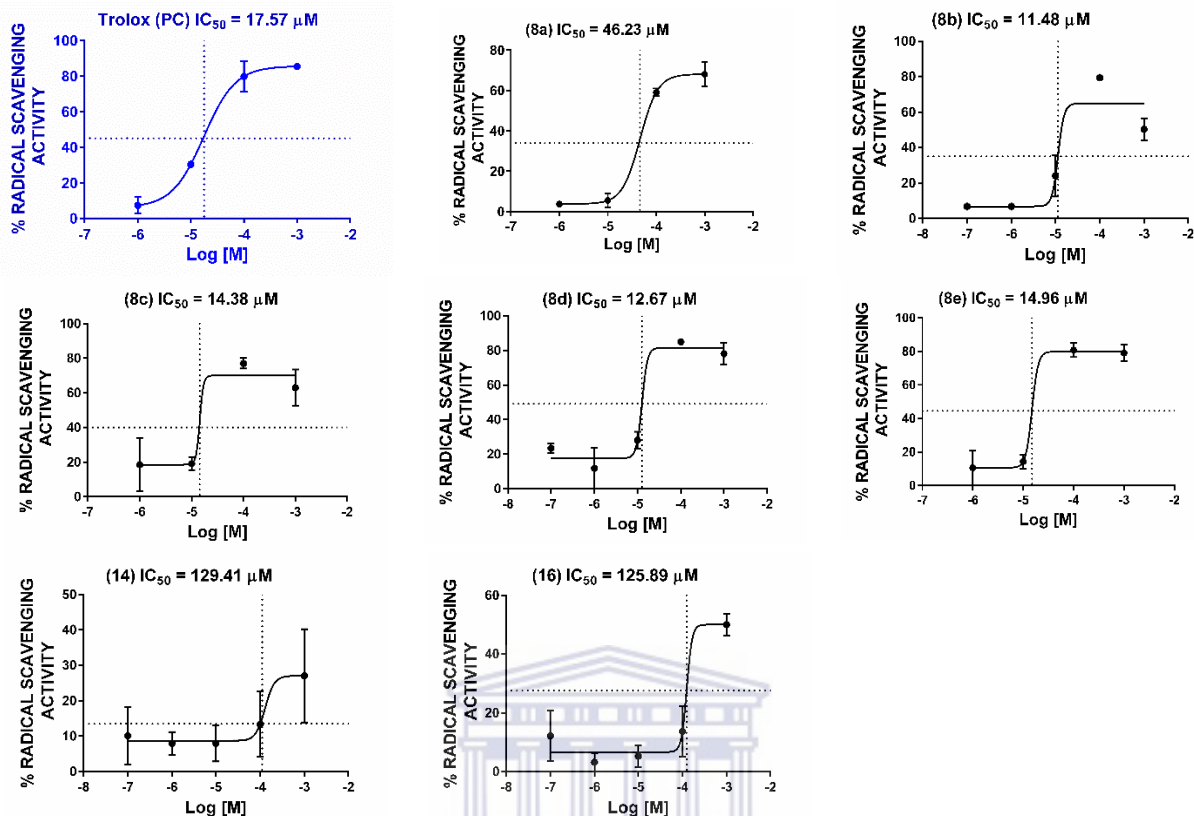
61

Figure 4.6: Graphs showing the free radical scavenging activity of synthesized compounds in terms of IC$_{50}$ (concentrations in μM range of test compounds 8a-e, 14 and 16 required to scavenge 50 % free radical of DPPH).

4.3 Conclusion

All designed, synthesized and tested compounds showed inhibitory activities against AChE, BuChE and antioxidant activities that correlated well with predicted and modelling results. The most potent are compounds **8d** and **8e** and **14.** Compounds **8d** and **8e** demonstrated good activity in all three assays with acceptable SI towards AChE / BuChE. Compound **14** showed the best dual cholinesterase inhibitor activity but with lower free radical scavenging activity. As illustrated in the bar graph in **Figure 4.7**, **8d** and **8e** are the best lead molecules from this study as they demonstrated the best ability to inhibit AChE, BuChE and free radical scavenging activity with IC$_{50}$ values lower than their reference compounds and also good non-selective cholinesterase inhibitory activity. Compounds **14** showed promising activity for ChE inhibition and these hybrid molecules in this series could also be further explored.
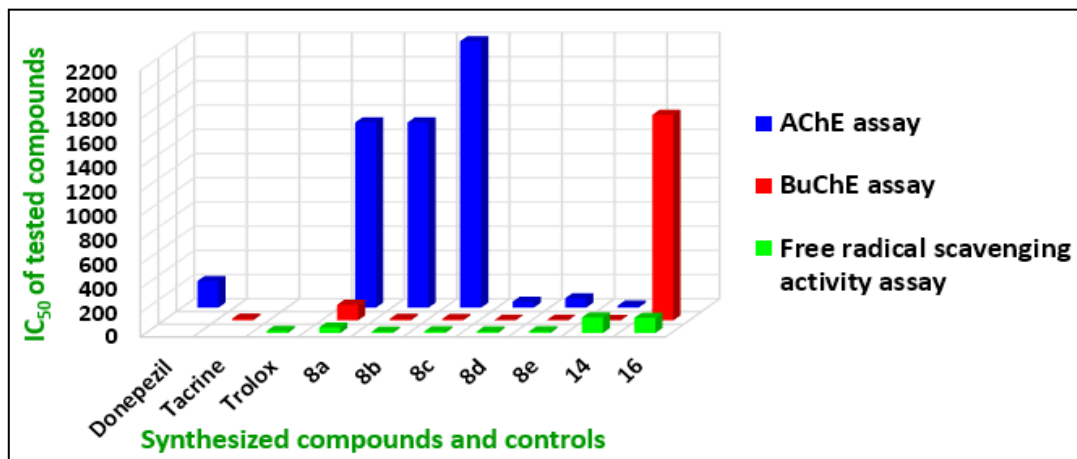
62

Figure 4.7: Bar graph showing comparative study of IC$_{50}$ value depicting the multifunctional ability of synthesized compounds. Cholinesterase assay IC$_{50}$ (nM); Free radical scavenging activity assay IC$_{50}$ (µM).

63

CHAPTER 5.

CONCLUSION

5.1 Introduction

Though the mystery that surrounds the cause of AD is not totally uncovered, accumulation of Aβ, dysregulation of tau protein phosphorylation, free radical production and defects in the cholinergic system are believed to be the main factors that trigger the cascade of neurotoxic events causing the death of neuronal cells, which leads to characteristic symptoms of AD. Evidence gathered from the multifactorial aspects of the pathogenesis of AD explains the limitation of the current treatment, which are drugs designed to modulate single target protein activity. This traditional approach is no longer deemed appropriate to treat this complex disease. Conversely, the MTDLs concept, which is based on the design of a bioactive molecule that can modulate multiple biological pathways, is increasingly believed to be a viable alternative to address the problem. This concept can be exemplified by molecules that have already been developed such as the bis-7-tacrine dimer, galantamine-memantine, the bivalent β-carboline hybrid or phenylthiazole-tacrine hybrids which have shown encouraging pharmacological profiles (**Simone *et al.,* 2014**; **Simoni *et al.,* 2012**).

This study set out to design and synthesize multifunctional drug candidates and assess their biological activity for possible AD therapy. All desired structures (hybrids) were designed from lead structures (tacrine, trolox and tryptoline) to obtain dual binders of ChE and thus multifunctional properties.

5.2 Rationalization of the study

The molecular recognition (docking) study was performed to confirm possible interaction with *Tc*AChE using MOE. From this study, it was predicted that pharmacophores linked by less than five carbons, in terms of chain length, would have lower ChE inhibitory activity compared those with more than five carbon chain lengths. This is in line with published literature (**Savini *et al.,* 2003; Lan *et al.,* 2014**).

64

5.3 Synthesis and characterization

The yield of the synthesized compounds were low due to non-optimized methods used. New synthetic methods thus need to be developed with the aim to improve the yield, reduce reaction time and produce relatively pure product. The synthesized final products were characterized by physical methods (IR, MP, NMR and MS). The investigation of multifunctional ability of the synthesized tacrine-trolox and tacrine-tryptoline hybrids in the case of this study was limited to the screening of their inhibitory effect on cholinesterases (AChE / BuChE) and their ability to scavenge free radicals.

5.4 Cholinesterase and free radical scavenging assay

The ability of the synthesized compounds to inhibit cholinesterase and to scavenge free radicals were tested using Ellman's method and the DPPH· assay respectively. Compounds **8d** and **8e** which exhibited good inhibition of cholinesterase and good free radical scavenging activity with IC_{50} values better than their reference compounds (tacrine, donepezil and trolox) (**Table 5-1**) were identified. These compounds also displayed reasonable non-selectivity toward AChE and BuChE, which is essential in correcting cholinergic system defects as the basis of symptomatic treatment. Compounds **8a**, **8b** and **8c** also showed good BuChE activity, good free radical scavenging activity and reasonable AChE activity. Their selectivity index however impairs their dual cholinesterase inhibitors potency, but they still appear as to be promising lead compounds endowed with multifunctional biological activity regarding the target proteins involved in the aetiology of AD. Compound **14** had the best dual cholinesterase inhibitory activity with IC_{50} values 17.37 and 3.16 nM for AChE and BuChE respectively, but relatively poor free radical scavenging activity IC_{50} value 129.41 µM.

Table 5-1: Summary of IC$_{50}$ values of promising multi-target agents compared to references compounds (nd: not determined).

Compounds / references	AChE IC$_{50}$ (nM)	BuChE IC$_{50}$ (nM)	Free radical scavenging activity IC$_{50}$ (µM)
8d	49.31	4.74	12.67
8e	77.62	5.62	14.96
14	17.37	3.16	129.41
Donepezil	220	nd	nd
Tacrine	nd	14.12	nd
Trolox	nd	nd	17.57

These compounds further show good interaction with PAS of AChE in docking studies and this might be indicative of the ability of **8a-d** and **14** to prevent cholinesterase induced Aβ aggregation. Compound **16** showed no AChE inhibitory activity, poor BuChE IC$_{50}$ 1698.24 nM compared to tacrine IC$_{50}$ 14.12 nM and poor free radical scavenging activity IC$_{50}$ 125.89 µM compared to trolox IC$_{50}$ 17.57 µM.

5.5 Future works and recommendations

The investigation of cholinesterase and free radical scavenging activity of the newly synthesized compounds is part of an ongoing project. Our next goal is to assess the biological activity of the newly developed hybrids on other pathways linked to AD progression. Included are ChE induced Aβ aggregation associated with interaction of toxic Aβ with the PAS of ChE; MAO; NMDA; anti-apoptotic activity and BACE activity. Furthermore, to perform the kinetics studies which are important in defining the type of inhibition and the mechanism of action of the synthesized compounds. Tacrine-tryptoline hybrids have shown the best dual cholinesterase inhibition and expanding the library by conjugating tacrine to other β-carboline structures (Harmane, norharmane, harmine, harmaline) could lead to the discovery of new multifunctional agents for AD therapy.

5.6 Conclusion

In this study, novel multi-target anti-Alzheimer's drugs were designed, synthesized and evaluated for ChE inhibition and free radical scavenging activity. All the hybrid compounds synthesized and tested have shown inhibitory activities against AChE, BuChE and free radical scavenging activities, some even more than their reference compounds. Furthermore, new hybrids designed for ChE dual binder capability should have spacers of at least five carbons to achieve good ChE inhibitory activity. This result is supported and confirmed by recently published work wherein nonhepatoxicity of tacrine-trolox hybrids has been demonstrated as expected (**Nepovimova *et al*., 2015**). Compounds **8d** and **8e** showed AChE, BuChE and free radical scavenging activity with IC_{50} values lower than their reference compounds donepezil, tacrine and trolox respectively. Therefore, **8d** and **8e** were identified as suitable candidates for further investigation. The bioavailability and the ability of the newly synthesized compounds to cross the BBB were analysed based on criteria stipulated by Lipinski rule of five **(Keller, Pichota, and Yin, 2006).** Only compounds **8d** and **8e** violate more than one of the rule with a molecular weight greater than 500 g/mol and Log P value greater than 5 but should still be able to cross the BBB.

REFERENCES

AGIS-TORRES, A.; SOLLHUBER, M., FERNANDEZ, M. and SANCHEZ-MONTERO, J.M. (2014). Multi-Target-Directed Ligands and other Therapeutic Strategies in the Search of a Real Solution for Alzheimer's disease. *Current Neuropharmacology*, 2–36.

ALZHEIMER'S, ASSOCIATION, (2015). "2015 Alzheimer's disease facts and figures." Alzheimer's and dementia: *The Journal of the Alzheimer's Association*. 11(3), 332-384.

ALZHEIMER'S ASSOCIATION. (2013). "2013 Alzheimer's disease facts and figures." *Alzheimer's and Dementia*. 9 (2), 208-245.

ALZHEIMER'S SOCIETY, (2012). Coping with memory loss. 1–9.

BAIGET, J., LLONA-MINGUEZ, S., LANG, S., MACKAY, S. P., SUCKLING, C. J. and SUTCLIFFE, O. B. (2011). Manganese dioxide mediated one-pot synthesis of methyl 9H-pyrido [3, 4-b] indole-1-carboxylate: Concise synthesis of alangiobussinine. *Beilstein Journal of Organic Chemistry*, *7*(1), 1407-1411.

BARTLETT, P.C. and JUDGE, L.J. (1997). The role of epidemiology in public health Types of epidemiological studies. , 16(2), 331–336.

BATES, K. A., VERDILE, G., LI, Q. X., AMES, D., HUDSON, P. and MASTERS, C. L. (2009). Clearance mechanisms of Alzheimer's amyloid-beta peptide: implications for therapeutic design and diagnostic tests. *Molecular Psychiatry*, 14(5), 469–486.

BECHER, P. G., BEUCHAT, J., GADEMANN, K. and JÜTTNER, F. (2005). Nostocarboline: isolation and synthesis of a new cholinesterase inhibitor from Nostoc 78-12A. *Journal of Natural Products*, 68(12), 1793-1795.

BILLINGSLEY, M.L. and KINCAID, R.L. (1997). Regulated phosphorylation and dephosphorylation of tau protein: effects on microtubule interaction, intracellular trafficking and neurodegeneration. *The Biochemical Journal,* 323(3), 577–591.

BONO, G.F., SIMÃO-SILVA, D.P., BATISTELA, M.S., JOSVIAK, N.D., DIAS P.F.R., NASCIMENTO, G.A., SOUZA, R.L.R., PIOVEZAN, M.R., SOUZA, R.K.M. and

FURTADO-ALLE, L. (2015). Neurochemistry International Butyrylcholinesterase : K variant, plasma activity, molecular forms and rivastigmine treatment in Alzheimer's disease in a Southern Brazilian population. *Neurochemistry International*, 81, 57–62.

CAPURRO, V., BUSQUET, P., LOPES J P., BERTORELLI, R.,TAROZZO G., BOLOGNESI, M.L., PIOMELLI, D., REGGIANI, A. and CAVALLI, A. (2013). Pharmacological Characterization of Memoquin, a Multi- Target Compound for the Treatment of Alzheimer's disease. *Public Library of Science One,* 8(2), 1-8.

CARTER, C. L., RESNICK, E. M., MALLAMPALLI, M. and KALBARCZYK, A. (2012). Sex and gender differences in Alzheimer's disease: recommendations for future research. *Journal of Women's Health*, *21*(10), 1018-1023.

CAVALLI, A., BOLOGNESI, M. L., MINARINI, A., ROSINI, M., TUMIATTI, V., RECANATINI, M. and MELCHIORRE, C. (2008). Multi-target-directed ligands to combat neurodegenerative diseases. *Journal of Medicinal Chemistry*, 51(3), 347-372.

CELL BIOLOGY OF DISEASE AND EXERCISE, (2012). *Alzheimer's disease cell bio.*Available from: http://pt851.wikidot.com/alzheimer-s-disease-cell-bio, 30 November 2015.

CHACKO, L. W. and CERF, J. A. (1960). Histochemical localization of cholinesterase in the amphibian spinal cord and alterations following ventral root section. *Journal of Anatomy*, 94(Pt 1), 74.

CHAO, X., HE, X., YANG, Y., ZHOU, X., JIN, M., LIU, S. and TAN, Y. (2012). Design, synthesis and pharmacological evaluation of novel tacrine–caffeic acid hybrids as multi-targeted compounds against Alzheimer's disease. *Bioorganic and Medicinal Chemistry Letters*, *22*(20), 6498-6502.

CHESSER, A. S., PRITCHARD, S. M. and JOHNSON, G. V. (2013). Tau clearance mechanisms and their possible role in the pathogenesis of Alzheimer disease. *Frontiers in Neurology*, 4(122), 1-12.

CHETELAT and. BARON, J-C. (2003). Early diagnosis of alzheimer's disease: contribution of structural neuroimaging. *NeuroImage*, 18(2), 525–541.

69

CHUNG, S. H. (2009). Aberrant phosphorylation in the pathogenesis of Alzheimer's disease. *Biochemistry and Molecular Biology Reports*, 42(8), 467-474.

CONTESTABILE, A. (2011). The history of the cholinergic hypothesis. *Behavioural Brain Research*, 221(2), 334-340.

CRAIG, L. A., HONG, N. S. and MCDONALD, R. J. (2011). Revisiting the cholinergic hypothesis in the development of Alzheimer's disease. *Neuroscience and Biobehavioral Reviews*, 35(6), 1397-1409.

CREWS, L. and MASLIAH, E. (2010). Molecular mechanisms of neurodegeneration in Alzheimer's disease. *Human Molecular Genetics*, ddq160.

DARREH-SHORI, T. and SOININEN, H. (2010). Effects of cholinesterase inhibitors on the activities and protein levels of cholinesterases in the cerebrospinal fluid of patients with Alzheimer's disease: a review of recent clinical studies. *Current Alzheimer Research*, *7*(1), 67-73.

DAWKINS, E. and SMALL, D. H. (2014). Insights into the physiological function of the β-amyloid precursor protein: beyond Alzheimer's disease. *Journal of Neurochemistry*, 129(5), 756-769.

DE STROOPER, B. and ANNAERT, W. (2000). Proteolytic processing and cell biological functions of the amyloid precursor protein. *Journal of Cell Science*, *113*(11), 1857-1870.

DESAI, A. K. and CHAND, P. (2009). Tau-based therapies for Alzheimer's disease: wave of the future. *Primary Psychiatry*, *16*(7), 40-46.

DI CARLO, M., GIACOMAZZA, D. and SAN BIAGIO, P. L., (2012). Alzheimer's disease: biological aspects, therapeutic perspectives and diagnostic tools, *Journal of Physics: Condensed Matter*, 24(24), 244102.

DIAS, K. S. T. and VIEGAS JR, C. (2014). Multi-target directed drugs: a modern approach for design of new drugs for the treatment of Alzheimer's disease. *Current Neuropharmacology*, *12*(3), 239-255.

DREWES, G. (2004). Marking tau for tangles and toxicity. *Trends in Biochemical Sciences*,

70

29(10), 548-555.

DRIES, D. R., YU, G. and HERZ, J. (2012). Extracting β-amyloid from Alzheimer's disease. *Proceedings of the National Academy of Sciences*, *109*(9), 3199-3200.

DURRANT, J. D. and MCCAMMON, J. A. (2011). Molecular dynamics simulations and drug discovery. *Bioorganic and Medicinal Chemistry Biology*, *9*(1), 71.

DUTHEY, B. (2013). Background paper 6.11: Alzheimer disease and other dementias. *A Public Health Approach to Innovation*, 1-74.

DVIR, H., SILMAN, I., HAREL, M., ROSENBERRY, T. L. and SUSSMAN, J. L. (2010). Acetylcholinesterase: from 3D structure to function. *Chemico-Biological Interactions*, 187(1), 10-22.

ELDER, G. A., GAMA SOSA, M. A. and DE GASPERI, R. (2010). Transgenic mouse models of Alzheimer's disease. *Mount Sinai Journal of Medicine: A Journal of Translational and Personalized Medicine*, *77*(1), 69-81.

FERNÁNDEZ-BACHILLER, M. I., PÉREZ, C., GONZÁLEZ-MUNOZ, G. C., CONDE, S., LÓPEZ, M. G., VILLARROYA, M. and RODRÍGUEZ-FRANCO, M. I. (2010). Novel Tacrine− 8-hydroxyquinoline hybrids as multifunctional agents for the treatment of alzheimer's disease, with neuroprotective, cholinergic, antioxidant, and copper-complexing properties. *Journal of Medicinal Chemistry*, *53*(13), 4927-4937.

FERREIRA, L. G., DOS SANTOS, R. N., OLIVA, G. and ANDRICOPULO, A. D. (2015). Molecular docking and structure-based drug design strategies. *Molecules*, *20*(7), 13384-13421.

FRANCIS, P. T., PALMER, A. M., SNAPE, M. and WILCOCK, G. K. (1999). The cholinergic hypothesis of Alzheimer's disease: a review of progress. *Journal of Neurology, Neurosurgery and Psychiatry*, *66*(2), 137-147.

FROST, D., MEECHOOVET, B., WANG, T., GATELY, S., GIORGETTI, M., SHCHERBAKOVA, I. and DUNCKLEY, T. (2011). β-carboline compounds, including harmine, inhibit DYRK1A and tau phosphorylation at multiple Alzheimer's disease-

related sites. *Public Library of Sciences One*, *6*(5), e19264.

GERVAIS, F., PAQUETTE, J., MORISSETTE, C., KRZYWKOWSKI, P., YU, M., AZZI, M. and SZAREK, W. A. (2007). Targeting soluble Aβ peptide with Tramiprosate for the treatment of brain amyloidosis. *Neurobiology of Aging*, 28(4), 537-547.

GONG, C. X., LIU, F., GRUNDKE-IQBAL, I. and IQBAL, K. (2006). Dysregulation of protein phosphorylation/dephosphorylation in Alzheimer's disease: a therapeutic target. *BioMedicinal Research International*, *2006*.

GOURI, A. (2004). Acetylcholinesterase activity and isozyme pattern in normal and lithium-treated developing chick brain.

GREIG, N. H., UTSUKI, T., YU, Q., ZHU, X., HOLLOWAY, H. W., PERRY, T. and LAHIRI, D. K. (2001). Butyrylcholinesterase: a new therapeutic target in AD treatment. *Alzheimer Insights*, *7*(2), 1-6.

HALLIWELL, B. (2001). Free Radicals and other reactive species in Disease. 1–7.

HAMAD, I., ARDA, N., PEKMEZ, M., KARAER, S. and TEMIZKAN, G. (2010). Intracellular scavenging activity of Trolox (6-hydroxy-2, 5, 7, 8-tetramethylchromane-2-carboxylic acid) in the fission yeast, Schizosaccharomyces pombe. *Journal of Natural Science, Biology, and Medicine*, 1(1), 16.

HERCZENIK, E. and GEBBINK, M. F. (2008). Molecular and cellular aspects of protein misfolding and disease. *The Federation of American Societies for Experimental Biology Journal*, *22*(7), 2115-2133.

HERRAIZ, T., GONZÁLEZ, D., ANCÍN-AZPILICUETA, C., ARÁN, V. J. and GUILLÉN, H. (2010). β-Carboline alkaloids in Peganum harmala and inhibition of human monoamine oxidase (MAO). *Food and Chemical Toxicology*, *48*(3), 839-845.

HINDLE, J. V. (2010). Ageing, neurodegeneration and Parkinson's disease. *Age and Ageing*, *39*(2), 156-161.

HONG-QI, Y., ZHI-KUN, S. and SHENG-DI, C. (2012). Current advances in the treatment of Alzheimer's disease: focused on considerations targeting Aβ and tau. *Translational*

72

Neurodegeneration, *1*(1), 1-12.

INESTROSA, N. C., ALVAREZ, A., PEREZ, C. A., MORENO, R. D., VICENTE, M., LINKER, C. and GARRIDO, J. (1996). Acetylcholinesterase accelerates assembly of amyloid-β-peptides into Alzheimer's fibrils: possible role of the peripheral site of the enzyme. *Neuron*, *16*(4), 881-891.

JACKSON-SIEGAL, J. (2005). Our current understanding of the pathophysiology of Alzheimer's disease. *Advanced Studies in Pharmcy*, *2*(4), 126-135.

JOHNSON, G. V. and STOOTHOFF, W. H. (2004). Tau phosphorylation in neuronal cell function and dysfunction. *Journal of Cell Science*, *117*(24), 5721-5729.

KÁSA, P., RAKONCZAY, Z. and GULYA, K. (1997). The cholinergic system in Alzheimer's disease. *Progress in Neurobiology*, *52*(6), 511-535.

KELLER, T. H., PICHOTA, A. and YIN, Z. (2006). A practical view of 'druggability'. *Current Opinion in Chemical Biology*, *10*(4), 357-361.

KENT, S. (1983). What causes Alzheimer's? *Geriatrics*, 38(2), 33, 36, 41.

KOZURKOVA, M., HAMULAKOVA, S., GAZOVA, Z., PAULIKOVA, H. and KRISTIAN, P. (2011). Neuroactive multifunctional tacrine congeners with cholinesterase, anti-amyloid aggregation and neuroprotective properties. *Pharmaceuticals*, *4*(2), 382-418.

LAFERLA, F.M., GREEN, K.N. and ODDO, S. (2007). Intracellular amyloid-β in Alzheimer's disease. *Nature Reviews Neuroscience*, 8(7), 499–509.

LAN, J-S., SAI-SAI X., SU-YI, L., LONG-FEI, P., XIAO-BING, W. and LING-YI, K. (2014). Synthesis and Evaluation of Novel Tacrine- (B -Carboline) Hybrids as Multifunctional Agents for the Treatment of Alzheimer ' S Disease. *Bioorganic and Medicinal Chemistry Design,* 22, 6089–6104.

LANE, R. M., POTKIN, S. G. and ENZ, A. (2006). Targeting acetylcholinesterase and butyrylcholinesterase in dementia. *The International Journal of Neuropsychopharmacology*, *9*(01), 101-124.

73

LIM, S., HAQUE, M. M., KIM, D., KIM, D. J. and KIM, Y. K. (2014). Cell-based Models to Investigate Tau Aggregation. *Computational and Structural Biotechnology Journal*, *12*(20), 7-13.

LIU, C. C., KANEKIYO, T., XU, H. and BU, G. (2013). Apolipoprotein E and Alzheimer disease: risk, mechanisms and therapy. *Nature Reviews Neurology*, *9*(2), 106-118.

LÜ, J. M., LIN, P. H., YAO, Q. and CHEN, C. (2010). Chemical and molecular mechanisms of antioxidants: experimental approaches and model systems. *Journal of Cellular and Molecular Medicine*, *14*(4), 840-860.

MAHER, P. and DAVIS, J. B. (1996). The role of monoamine metabolism in oxidative glutamate toxicity. *The Journal of Neuroscience*, *16*(20), 6394-6401.

MANDELKOW, E. M. and MANDELKOW, E. (2012). Biochemistry and cell biology of tau protein in neurofibrillary degeneration. *Cold Spring Harbor Perspectives in Medicine*, *2*(7), a006247.

MAO, P. and REDDY, P. H. (2011). Aging and amyloid beta-induced oxidative DNA damage and mitochondrial dysfunction in Alzheimer's disease: implications for early intervention and therapeutics. *Biochimica et Biophysica Acta (BBA)-Molecular Basis of Disease*, *1812*(11), 1359-1370.

MASSOULIÉ, J., PEZZEMENTI, L., BON, S., KREJCI, E. and VALLETTE, F. M. (1993). Molecular and cellular biology of cholinesterases. *Progress in Neurobiology*, *41*(1), 31-91.

MEHTA, M., ADEM, A. and SABBAGH, M. (2011). New acetylcholinesterase inhibitors for Alzheimer's disease. *International Journal of Alzheimer's Disease*, *2012*.

MIETELSKA-POROWSKA, A., WASIK, U., GORAS, M., FILIPEK, A. and NIEWIADOMSKA, G. (2014). Tau protein modifications and interactions: their role in function and dysfunction. *International Journal of Molecular Sciences*, *15*(3), 4671-4713.

MONDRAGÓN-RODRÍGUEZ, S., PERRY, G., ZHU, X. and BOEHM, J. (2012). Amyloid

beta and tau proteins as therapeutic targets for Alzheimer's disease treatment: rethinking the current strategy. *International Journal of Alzheimer's disease*, *2012*.

MORLEY, J. E. and FARR, S. A. (2014). The role of amyloid-beta in the regulation of memory. *Biochemical pharmacology*, *88*(4), 479-485.

MORRISON, A.S. and LYKETSOS, C. (2005). Review the pathophysiology of Alzheimer's disease. *Advanced Studies in Nursing*, 3(8), 256–270.

MÜLLER, U.C. and ZHENG, H. (2013). Physiological functions of APP family proteins. *Cold Spring Harbor Perspectives in Medicine*, 2(2), 1–17.

MUÑOZ, F. J., OPAZO, C., GIL-GÓMEZ, G., TAPIA, G., FERNÁNDEZ, V., VALVERDE, M. A. and INESTROSA, N. C. (2002). Vitamin E but not 17β-estradiol protects against vascular toxicity induced by β-amyloid wild type and the Dutch amyloid variant. *The Journal of Neuroscience*, *22*(8), 3081-3089.

NEPOVIMOVA, E., KORABECNY, J., DOLEZAL, R., BABKOVA, K., ONDREJICEK, A., JUN, D. and BUKUM, N. (2015). Tacrine–trolox hybrids: A Novel Class of Centrally Active, Nonhepatotoxic Multi-Target-Directed Ligands Exerting Anticholinesterase and Antioxidant Activities with Low In Vivo Toxicity. *Journal of Medicinal Chemistry*, *58*(22), 8985-9003.

NEPOVIMOVA, E., ULIASSI, E., KORABECNY, J., PEÑA-ALTAMIRA, L. E., SAMEZ, S., PESARESI, A. and FATO, R. (2014). Multitarget drug Design srategy: quinone–tacrine hybrids designed to block amyloid-β aggregation and to exert anticholinesterase and antioxidant effects. *Journal of Medicinal Chemistry*, 57(20), 8576-8589.

NICOLET, Y., LOCKRIDGE, O., MASSON, P., FONTECILLA-CAMPS, J. C. and NACHON, F. (2003). Crystal structure of human butyrylcholinesterase and of its complexes with substrate and products. *Journal of Biological Chemistry*, *278*(42), 41141-41147.

NIMSE, S. B. and PAL, D. (2015). Free radicals, natural antioxidants, and their reaction mechanisms. *Royal Society of Chemistry Advances*, *5*(35), 27986-28006.

75

O'BRIEN, R. J. and WONG, P. C. (2011). Amyloid precursor protein processing and Alzheimer's disease. *Annual Review of Neuroscience*, *34*, 185-204.

OUTCOMES, B. and MONOAMINE, O.F. (2012). NIH Public Access. , pp.1–27.

PACHAIYAPPAN, B., (2011). Structure-and Ligand-Based Modeling of Beta-Secretase 1 (BACE1) Inhibitors (*Doctoral Dissertation, University of Illinois at Chicago*).

PARSONS, C. G., DANYSZ, W., DEKUNDY, A. and PULTE, I. (2013). Memantine and cholinesterase inhibitors: complementary mechanisms in the treatment of Alzheimer's disease. *Neurotoxicity Research*, *24*(3), 358-369.

PEREIRA, C., AGOSTINHO, P., MOREIRA, P. I., CARDOSO, S. M. and OLIVEIRA, C. R. (2005). Alzheimer's disease-associated neurotoxic mechanisms and neuroprotective strategies. *Current Drug Targets-CNS and Neurological Disorders*, *4*(4), 383-403.

PERLUIGI, M. and BUTTERFIELD, D. A. (2011). Oxidative stress and Down syndrome: a route toward Alzheimer-like dementia. *Current Gerontology and Geriatrics Research*, *2012*.

POHANKA, M. (2011). Cholinesterases, a target of pharmacology and toxicology. *Biomedical Papers*, *155*(3), 219-223.

RADESÄTER, A. C., JOHANSSON, S., ÖBERG, C. and LUTHMAN, J. (2003). The vitamin-E analog trolox and the NMDA antagonist MK-801 protect pyramidal neurons in hippocampal slice cultures from IL-1β-induced neurodegeneration. *Neurotoxicity Research*, *5*(6), 433-441.

RAMBARAN, R.N. and SERPELL, L.C. (2008). Amyloid fibrils: abnormal protein assembly. *Prion*, 2(3), 112-117.

RANG, H.P., DALE, M.M., RITTER, J.M. and FLOWER, R.J. (2007). Neurodegenerative disease Stephen McGrath / Louise Cook. Rang and Dale Pharmacology philadelphia, PA: Churchill Livingstone / Elsevier, Six edition, 514-515.

REITZ, C., WAY, R. and CB, C. (2012). Epidemiology of Alzheimer disease. , 7(3), 137–152.

RICERCA, D.D.I. (2009). Design and Synthesis of Multi Target Compounds for the Treatment of Alzheimer's disease, 1–81.

ROOK, Y., SCHMIDTKE, K. U., GAUBE, F., SCHEPMANN, D., WÜNSCH, B., HEILMANN, J. and WINCKLER, T. (2010). Bivalent β-carbolines as potential multitarget anti-Alzheimer agents. *Journal of Medicinal Chemistry*, *53*(9), 3611-3617.

ROTHENBERG, M. A. and NACHMANSOHN, D. (1947). Studies on cholinesterase III. Purification of the enzyme from electric tissue by fractional ammonium sulfate precipitation. *Journal of Biological Chemistry*, *168*(1), 223-231.

SAVINI, L., GAETA, A., FATTORUSSO, C., CATALANOTTI, B., CAMPIANI, G., CHIASSERINI, L. and SAXENA, A. (2003). Specific targeting of acetylcholinesterase and butyrylcholinesterase recognition sites. Rational design of novel, selective, and highly potent cholinesterase inhibitors. *Journal of Medicinal Chemistry*, *46*(1), 1-4.

SCHOTT, Y., DECKER, M., ROMMELSPACHER, H. and LEHMANN, J. (2006). 6-Hydroxy- and 6-methoxy-β-carbolines as acetyl- and butyrylcholinesterase inhibitors, Bioorganic. *Medicinal Chemistry Letter*, 16, 5840–5843

SHALABY, EMAD A. and SANAA M M SHANAB. (2013). "Comparison of DPPH and ABTS Assays for Determining Antioxidant Potential of Water and Methanol Extracts of Spirulina Platensis." *Indian Journal of Marine Sciences* 42 (5): 556–64.

SHIMIZU, H., TOSAKI, A., KANEKO, K., HISANO, T., SAKURAI, T. and NUKINA, N. (2008). Crystal structure of an active form of BACE1, an enzyme responsible for amyloid β protein production. *Molecular and Cellular Biology*, 28(11), 3663-3671.

SILVESTRELLI, G., LANARI, A., PARNETTI, L., TOMASSONI, D. and AMENTA, F. (2006). Treatment of Alzheimer's disease: from pharmacology to a better understanding of disease pathophysiology. *Mechanisms of Ageing and Development*, *127*(2), 148-157.

SIMONE TRANCHES DIAS, K. and VIEGAS, C. (2014). Multi-target directed drugs: a modern approach for design of new drugs for the treatment of Alzheimer's disease. *Current Neuropharmacology*, *12*(3), 239-255.

SIMONI, E., DANIELE, S., BOTTEGONI, G., PIZZIRANI, D., TRINCAVELLI, M. L., GOLDONI, L. and MELCHIORRE, C. (2012). Combining galantamine and memantine in multitargeted, new chemical entities potentially useful in Alzheimer's disease. *Journal of Medicinal Chemistry*, *55*(22), 9708-9721.

SIMPKINS, J. W., PEREZ, E., WANG, X., YANG, S., WEN, Y. and SINGH, M. (2009). Review: The potential for estrogens in preventing Alzheimer's disease and vascular dementia. *Therapeutic Advances in Neurological Disorders*, *2*(1), 31-49.

SIPE, J. D. and COHEN, A. S. (2000). Review: history of the amyloid fibril. *Journal of Structural Biology*, *130*(2), 88-98.

SKOVRONSKY, D. M., LEE, V. M. Y. and TROJANOWSKI, J. Q. (2006). Neurodegenerative diseases: new concepts of pathogenesis and their therapeutic implications. *Annual Review of Pathology: Mechanism of Disease*, *1*, 151-170.

SONG, Y., WANG, J., TENG, S. F., KESUMA, D., DENG, Y., DUAN, J. and SIM, M. M. (2002). β-Carbolines as specific inhibitors of cyclin-Dependent kinases. *Bioorganic and Medicinal Chemistry Letters*, *12*(7), 1129-1132.

STURZA, A., LEISEGANG, M. S., BABELOVA, A., SCHRÖDER, K., BENKHOFF, S., LOOT, A. E. and BRANDES, R. P. (2013). Monoamine oxidases are mediators of endothelial dysfunction in the mouse aorta. *Hypertension*, *62*(1), 140-146.

SUSSMAN, J. and SILMAN, I., (2009). Structural Studies on Acetylcholinesterase. *Springer Sciences*. 183–199.

SWERDLOW, R.H. (2011). Brain aging, Alzheimer's disease, and mitochondria. *Biochimica et Biophysica Acta (BBA) - Molecular Basis of Disease*, 1812(12), 1630–1639.

SZYMAŃSKI, P., SKIBIŃSKI, R., INGLOT, T., BAJDA, M., JOŃCZYK, J., MALAWSKA, B. and MIKICIUK-OLASIK, E. (2013). New Tacrine Analogs as Acetylcholinesterase Inhibitors—Theoretical Study with Chemometric Analysis. *Molecules*, *18*(3), 2878-2894.

TANZI, R. E., MOIR, R. D. and WAGNER, S. L. (2004). Clearance of Alzheimer's Aβ

peptide: the many roads to perdition. *Neuron*, *43*(5), 605-608.

TEDWILLIAMS, (2006). *Acetylcholinesterase*. Available from: http://drtedwilliams.net/kb/index.php?pagename=Acetylcholinesterase. October 7th 2015.

TENREIRO, S., ECKERMANN, K. and OUTEIRO, T. F. (2014). Protein phosphorylation in neurodegeneration: friend or foe?. *Frontiers in Molecular Neuroscience*, *7*.

THIRATMATRAKUL, S., YENJAI, C., WAIWUT, P., VAJRAGUPTA, O., REUBROYCHAROEN, P., TOHDA, M. and BOONYARAT, C. (2014). Synthesis, biological evaluation and molecular modeling study of novel tacrine–carbazole hybrids as potential multifunctional agents for the treatment of Alzheimer's disease. *European Journal of Medicinal Chemistry*, *75*, 21-30.

TRIPATHI, A. and SRIVASTAVA, U. C. (2010). Acetylcholinesterase: a versatile enzyme of nervous system. *Annals of Neurosciences*, *15*(4), 106-111.

TYAS, S. L., MANFREDA, J., STRAIN, L. A., AND MONTGOMERY, P. R. (2001). Risk factors for Alzheimer's disease: a population-based, longitudinal study in Manitoba, Canada. *International Journal of Epidemiology*, *30*(3), 590-597.

UTTARA, B., SINGH, A. V., ZAMBONI, P. and MAHAJAN, R. T. (2009). Oxidative stress and neurodegenerative diseases: a review of upstream and downstream antioxidant therapeutic options. *Current Neuropharmacology*, *7*(1), 65.

VALASANI, K. R., CHANEY, M. O., DAY, V. W. and SHIDU YAN, S. (2013). Acetylcholinesterase inhibitors: structure based design, synthesis, pharmacophore modeling, and virtual screening. *Journal of Chemical Information and Modeling*, *53*(8), 2033-2046.

VENAULT, P. and CHAPOUTHIER, G. (2007). From the behavioral pharmacology of beta-carbolines to seizures, anxiety, and memory. *The Scientific World Journal*, *7*, 204-223.

WANG, L., ZANG, Y., HE, Y., LIANG, M., ZHANG, X., TIAN, L. and LI, K. (2006). Changes in hippocampal connectivity in the early stages of Alzheimer's disease:

79

evidence from resting state fMRI. *Neuroimage*, *31*(2), 496-504.

WOREK, F., EYER, P. and THIERMANN, H. (2012). Determination of acetylcholinesterase activity by the Ellman assay: a versatile tool for in vitro research on medical countermeasures against organophosphate poisoning. *Drug Testing and Analysis*, *4*(3-4), 282-291.

XU, Y., COLLETIER, J. P., WEIK, M., JIANG, H., MOULT, J., SILMAN, I. and SUSSMAN, J. L. (2008). Flexibility of aromatic residues in the active-site gorge of acetylcholinesterase: X-ray versus molecular dynamics. *Biophysical Journal*, *95*(5), 2500-2511.

YAMASAKI, T., MURANAKA, H., KASEDA, Y., MIMORI, Y. and TOBIMATSU, S. (2011). Understanding the pathophysiology of Alzheimer's disease and mild cognitive impairment: A mini review on fMRI and eRP studies. *Neurology Research International*, 1-9.

YAN, Z. and FENG, J. (2004). Alzheimer's disease: interactions between cholinergic functions and β-amyloid. *Current Alzheimer Research*, *1*(4), 241-248.

ZHAO, Y. and ZHAO, B. (2013). Oxidative stress and the pathogenesis of Alzheimer's disease. *Oxidative Medicine and Cellular Longevity*, 1-10.

ZHENG, H. and KOO, E. H. (2011). Biology and pathophysiology of the amyloid precursor protein. *Molecular Neurodegeneration*, *6*(1), 27.

ZHENG, H., FRIDKIN, M. and YOUDIM, M. (2014). From single target to multitarget/network therapeutics in Alzheimer's therapy. *Pharmaceuticals*, *7*(2), 11

ZHOU, Y., WANG, S. and ZHANG, Y. (2010). Catalytic Reaction Mechanism of Acetylcholinesterase Determined by Born− Oppenheimer Ab Initio QM/MM Molecular Dynamics Simulations. *The Journal of Physical Chemistry B*,*114*(26), 8817-8825.

ANNEXURE:

SPECTRAL DATA ^{1}HNMR, ^{13}C, MS AND IR

Spectrum 1: *6-Hydroxy-2,5,7,8-tetramethyl-N-{2-[(1,2,3,4-tetrahydroacridin-9-yl)amino]ethyl}-3,4-dihydro-2H-1-benzopyran-2-carboxamide* (**8a**).
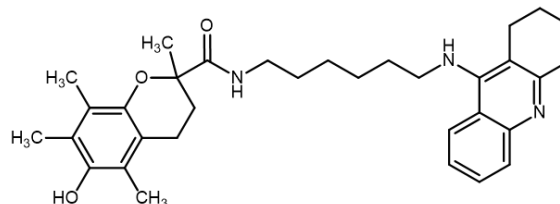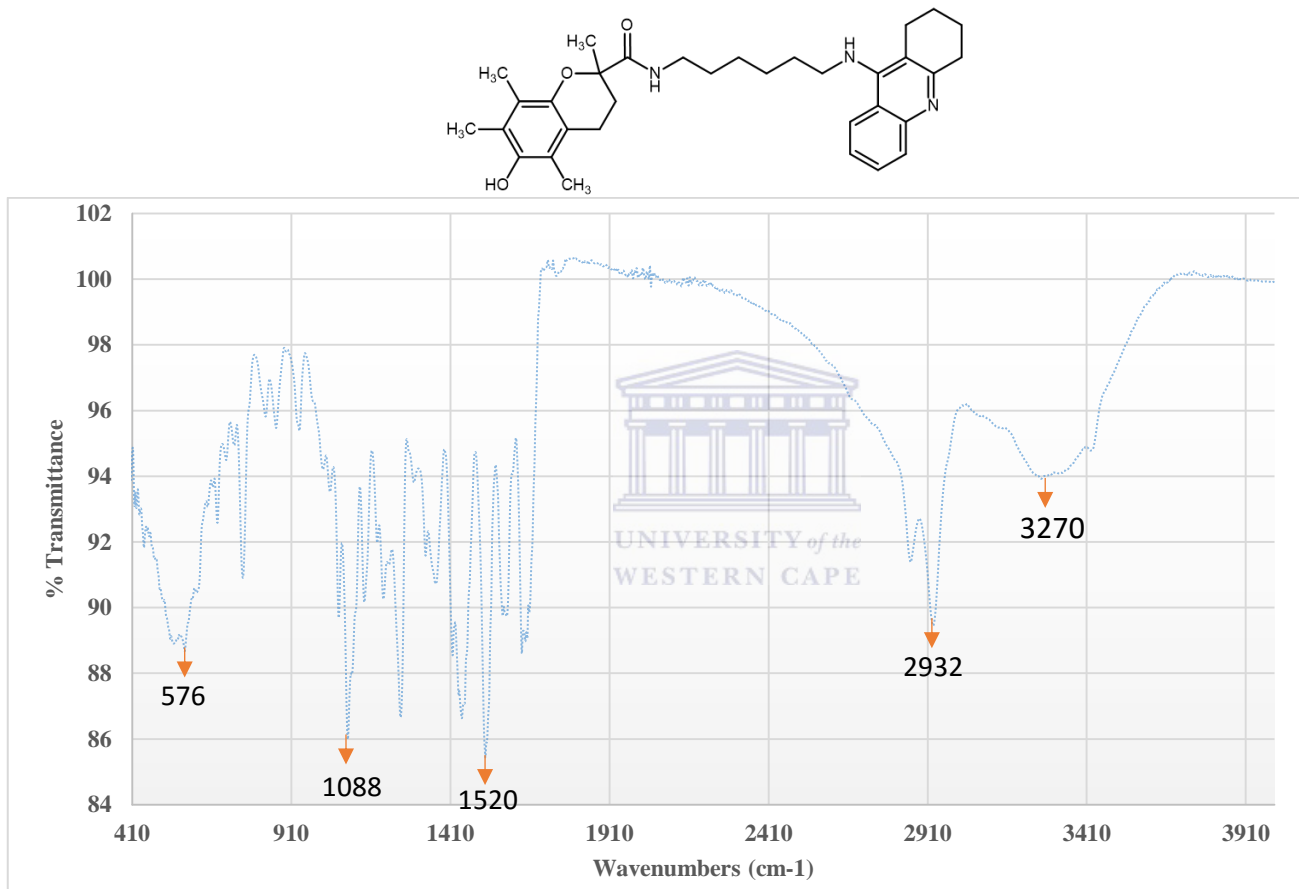
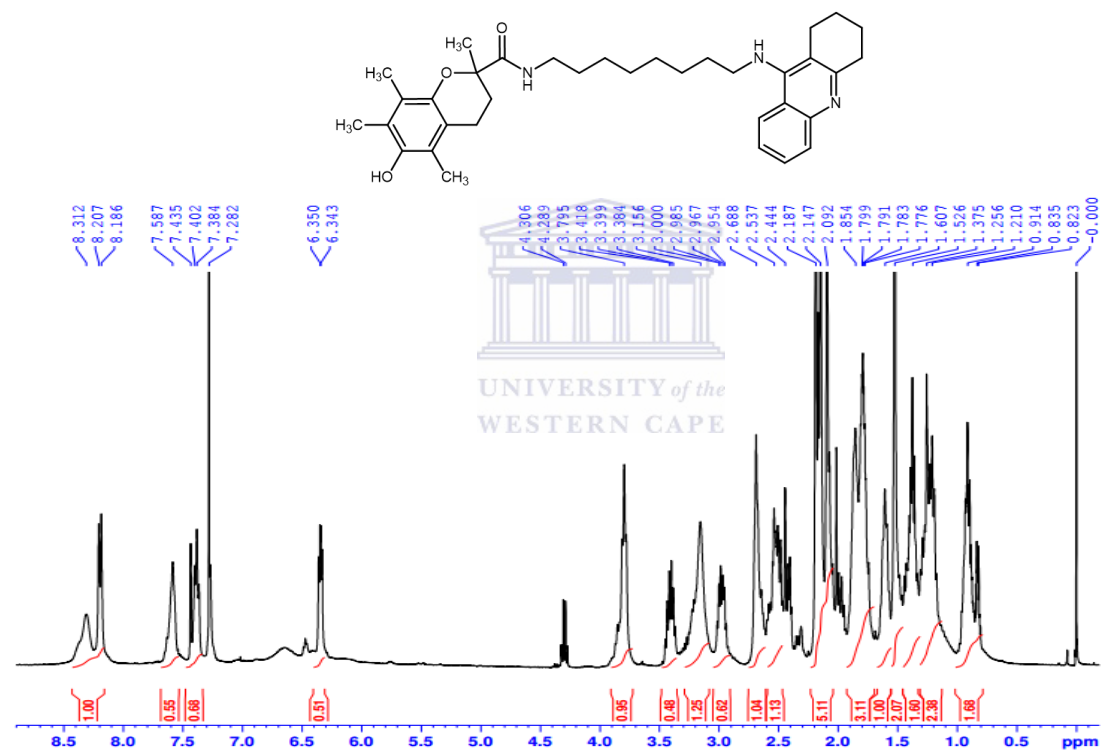**Spectrum 1a:**^{1}H-NMR

82
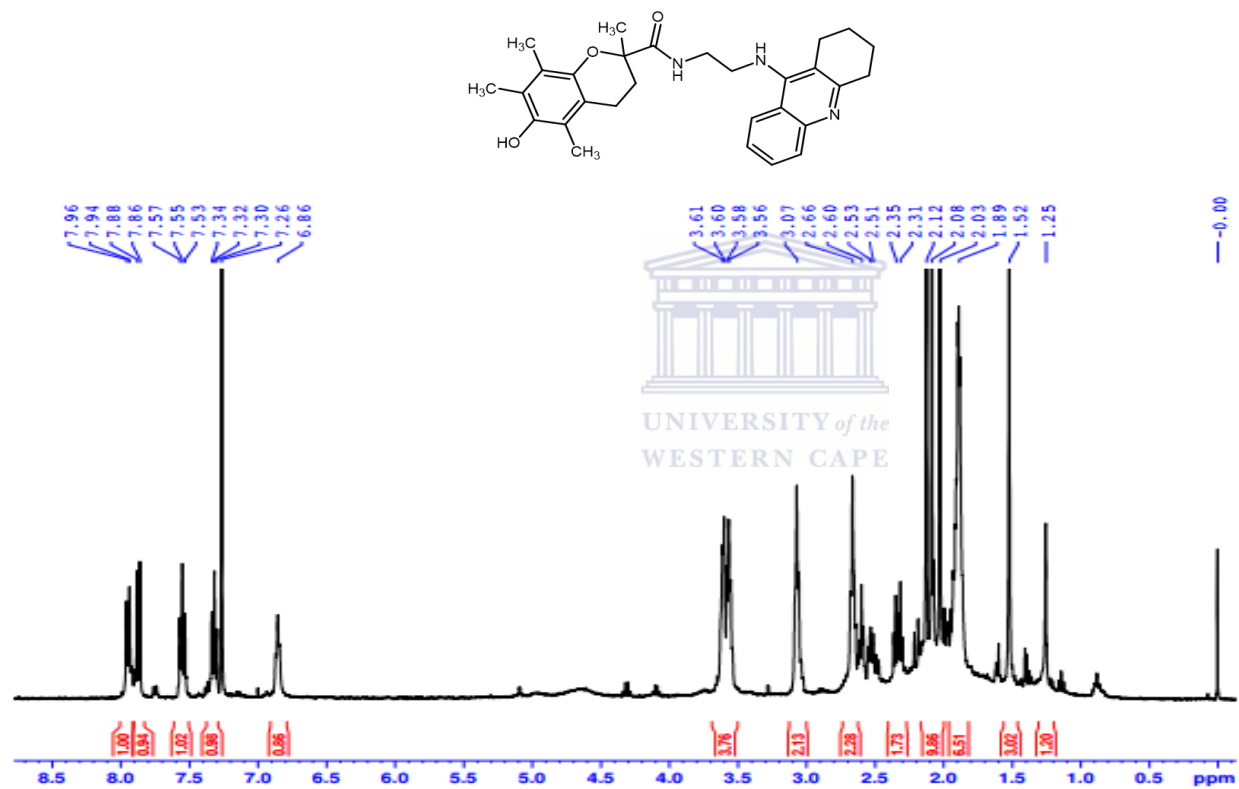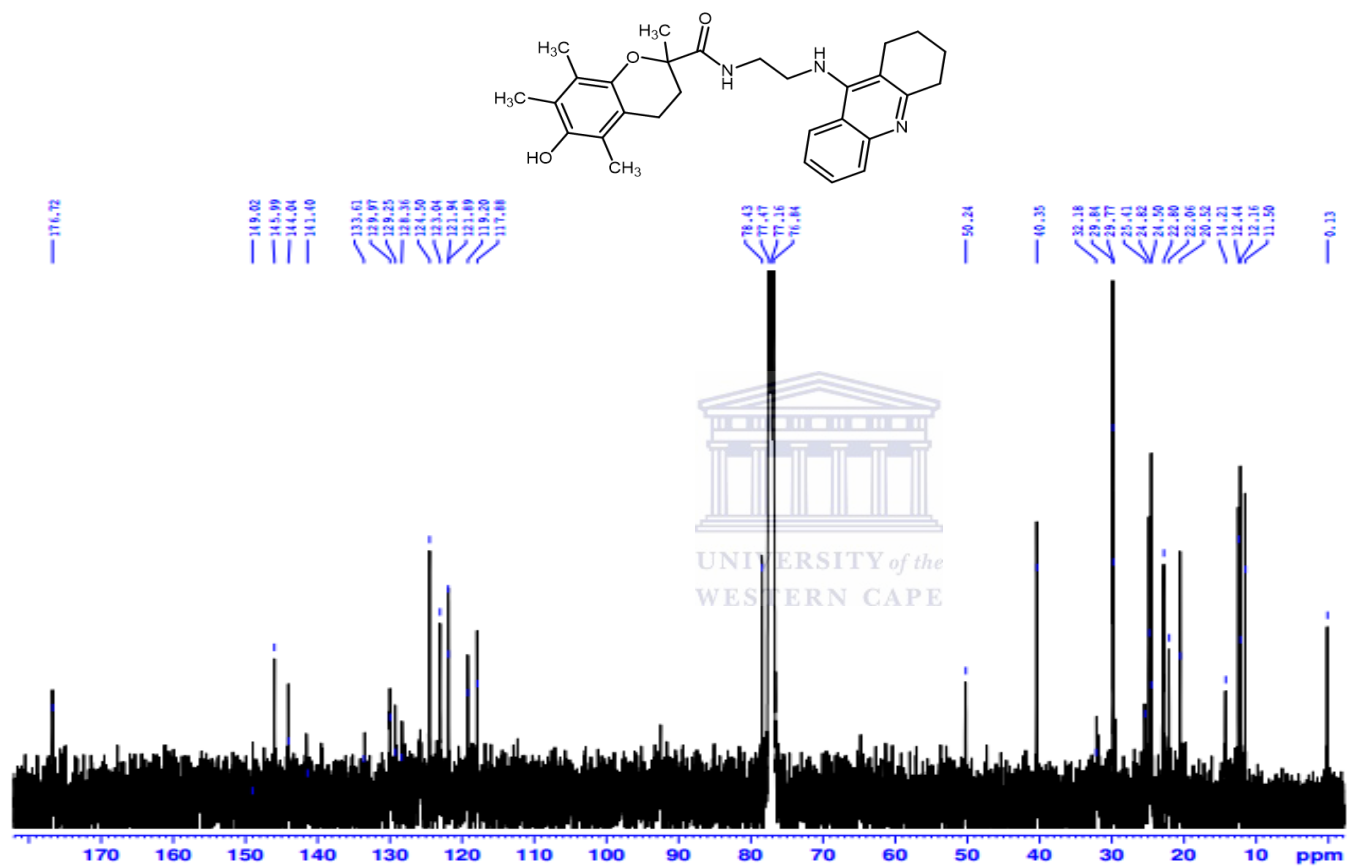
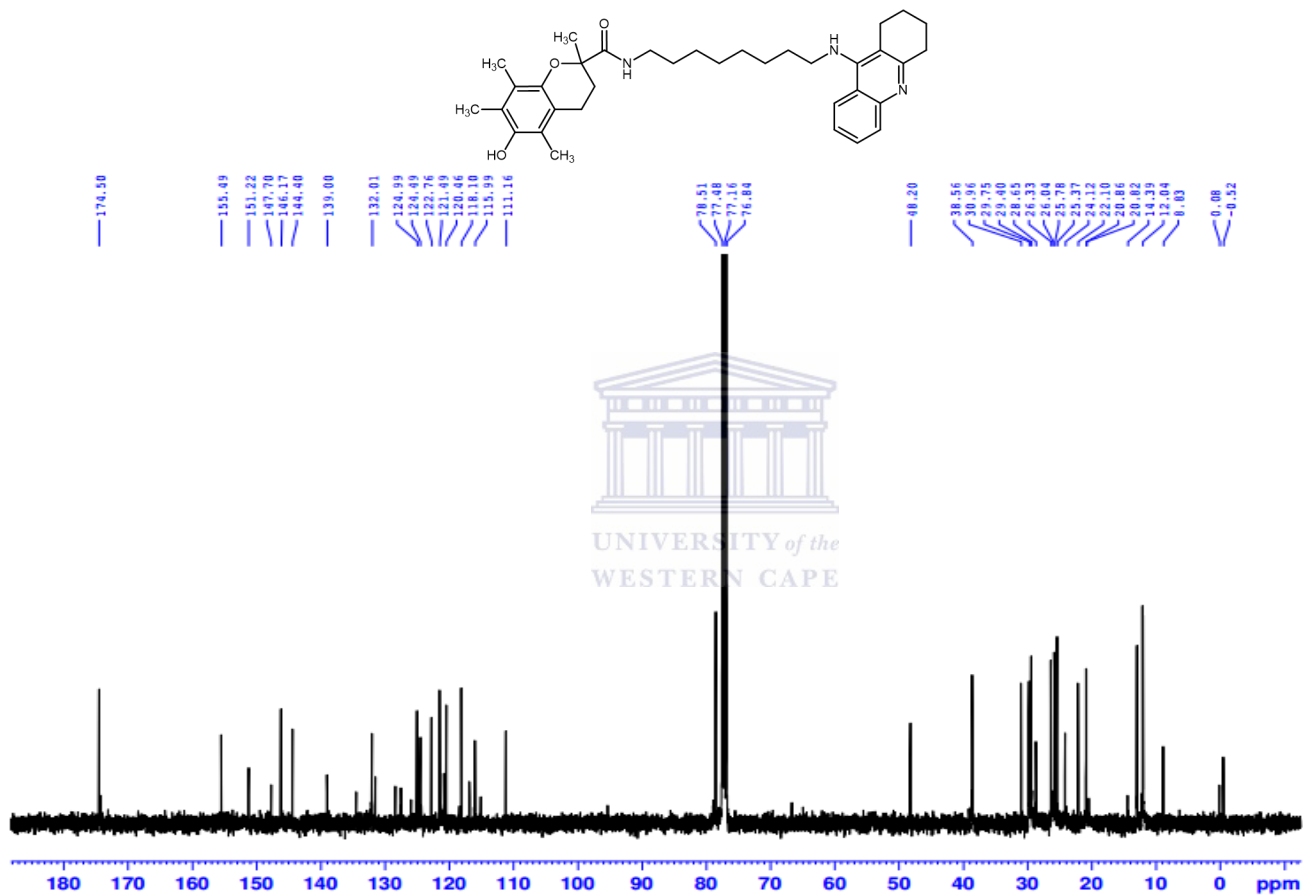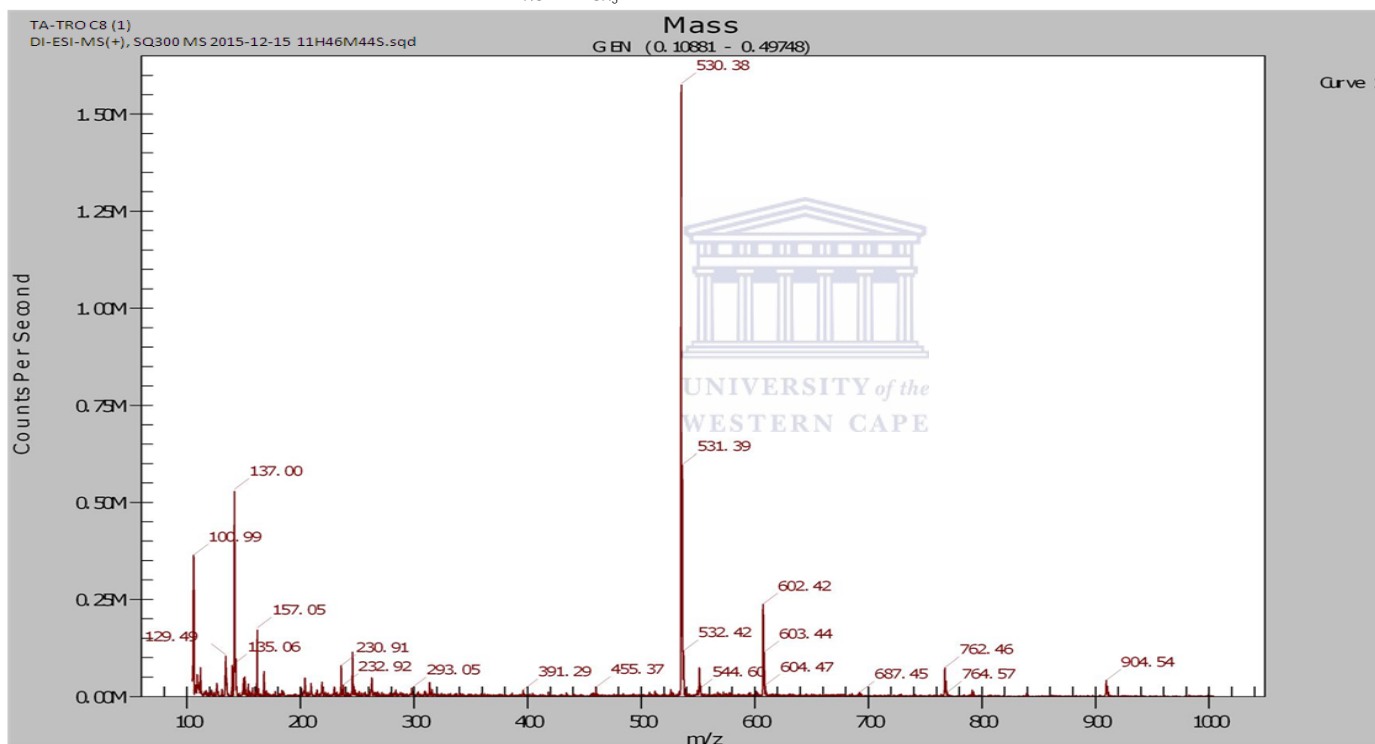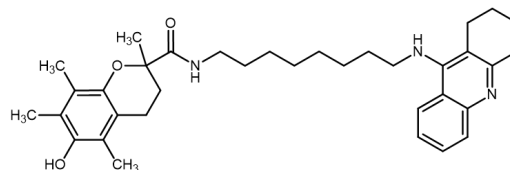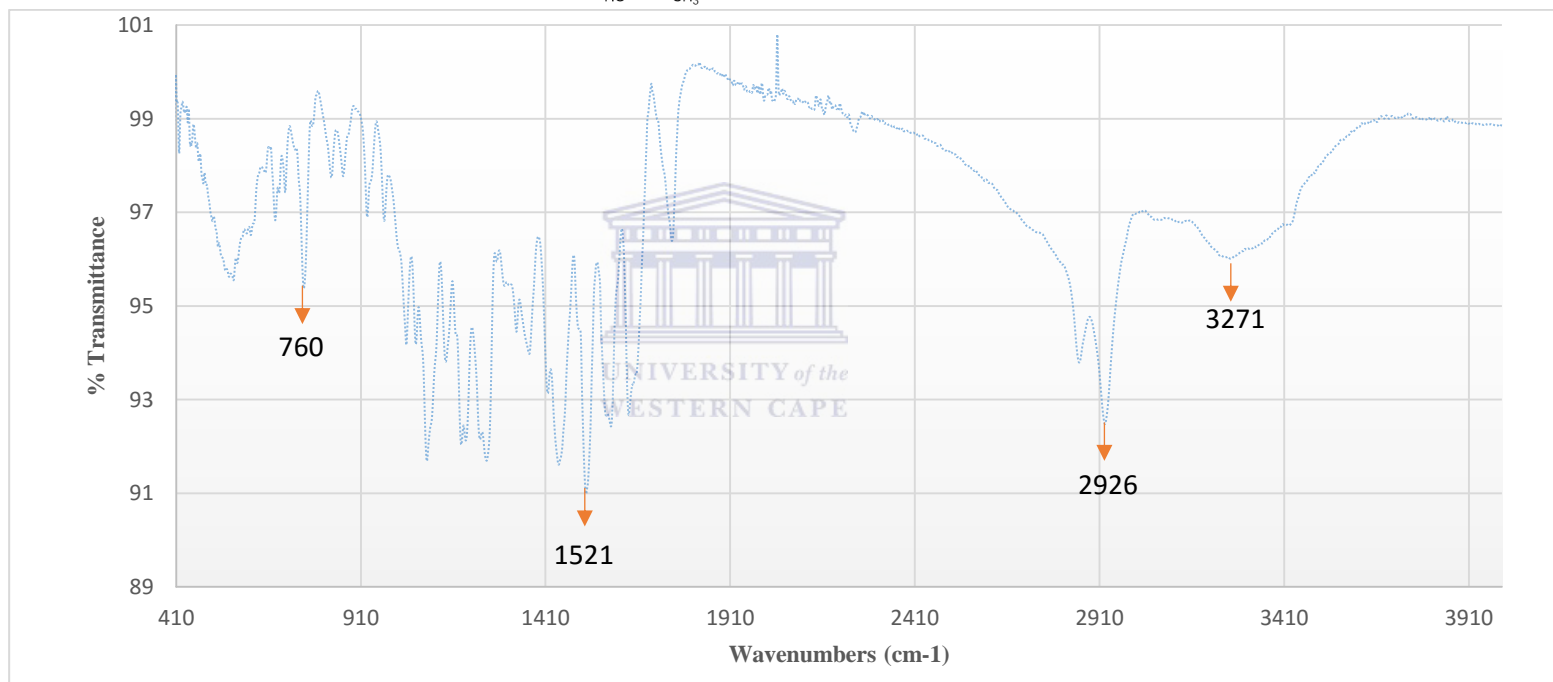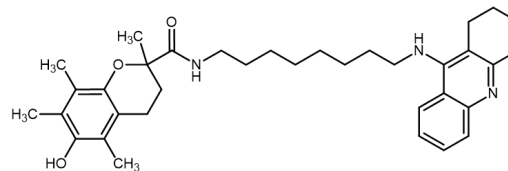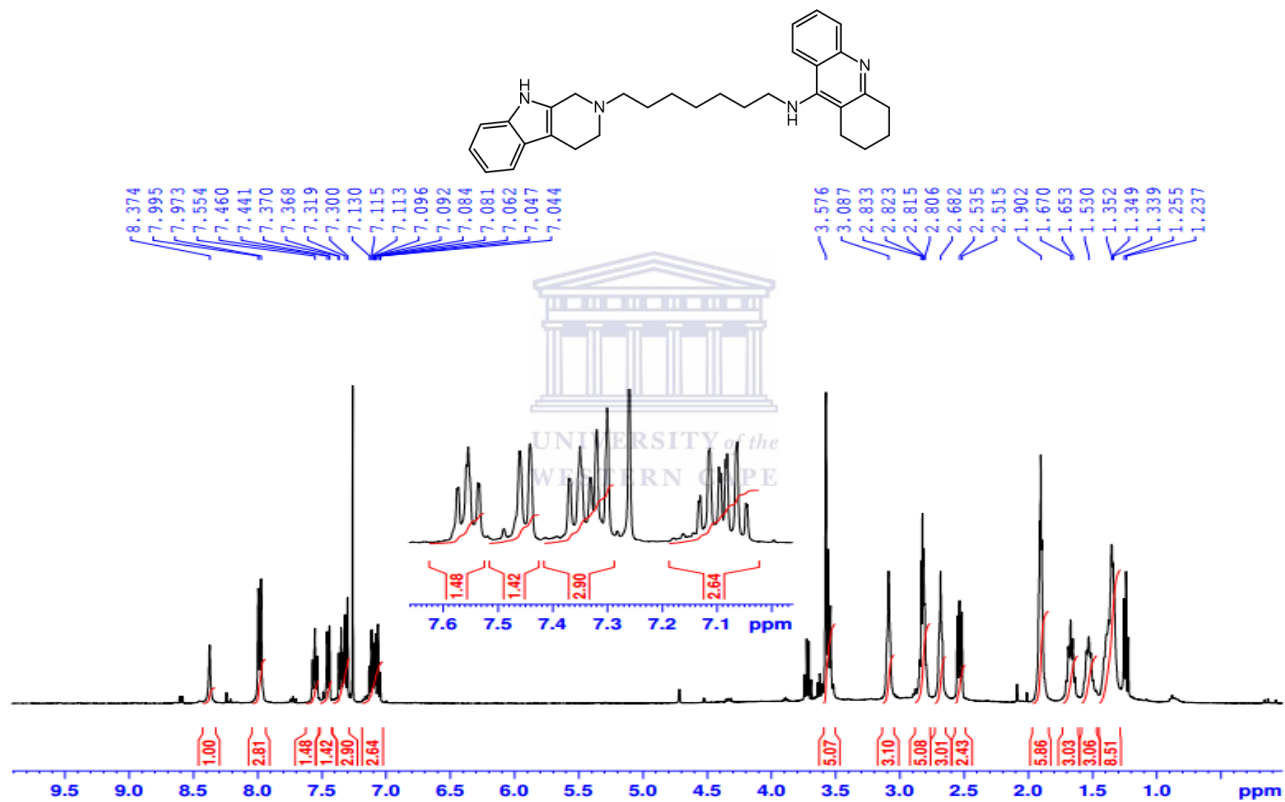**Spectrum 1b: ¹³C**

Spectrum 1c: MS
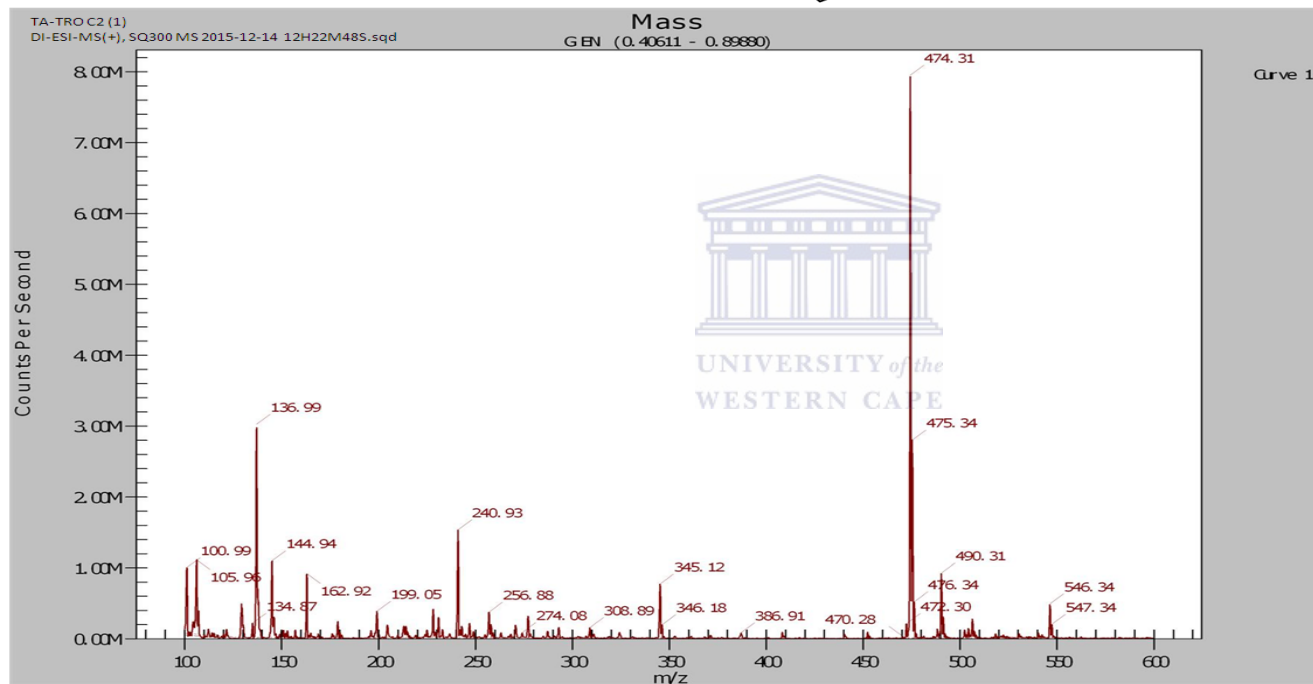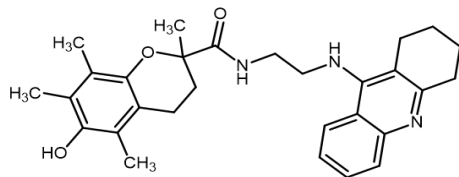
Spectrum 1d: IR
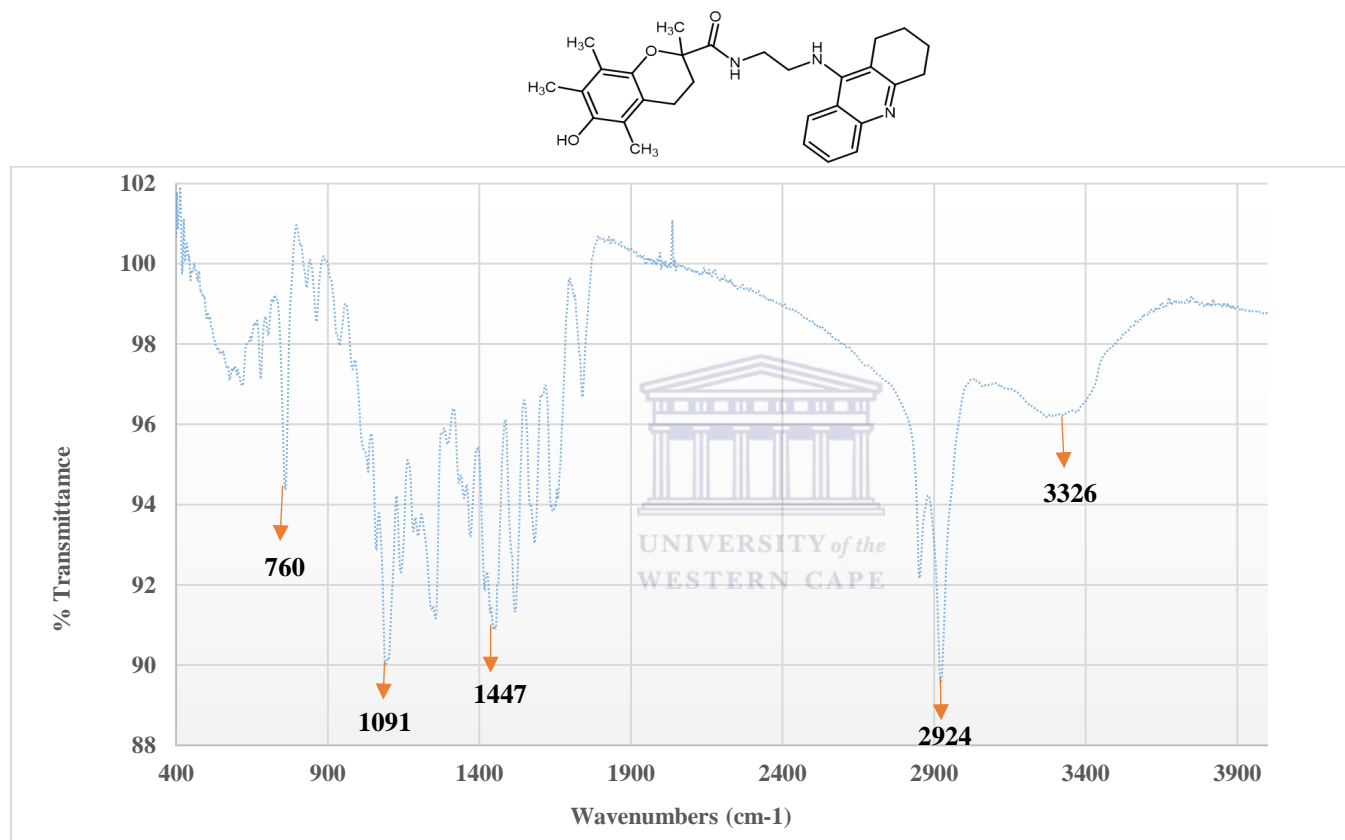
Spectrum 2: *6-Hydroxy-2,5,7,8-tetramethyl-N-{3-[(1,2,3,4-tetrahydroacridin-9-yl)amino]propyl}-3,4-dihydro-2H-1-benzopyran-2-carboxamide* (**8b**).

Spectrum 2a: ^{1}H NMR
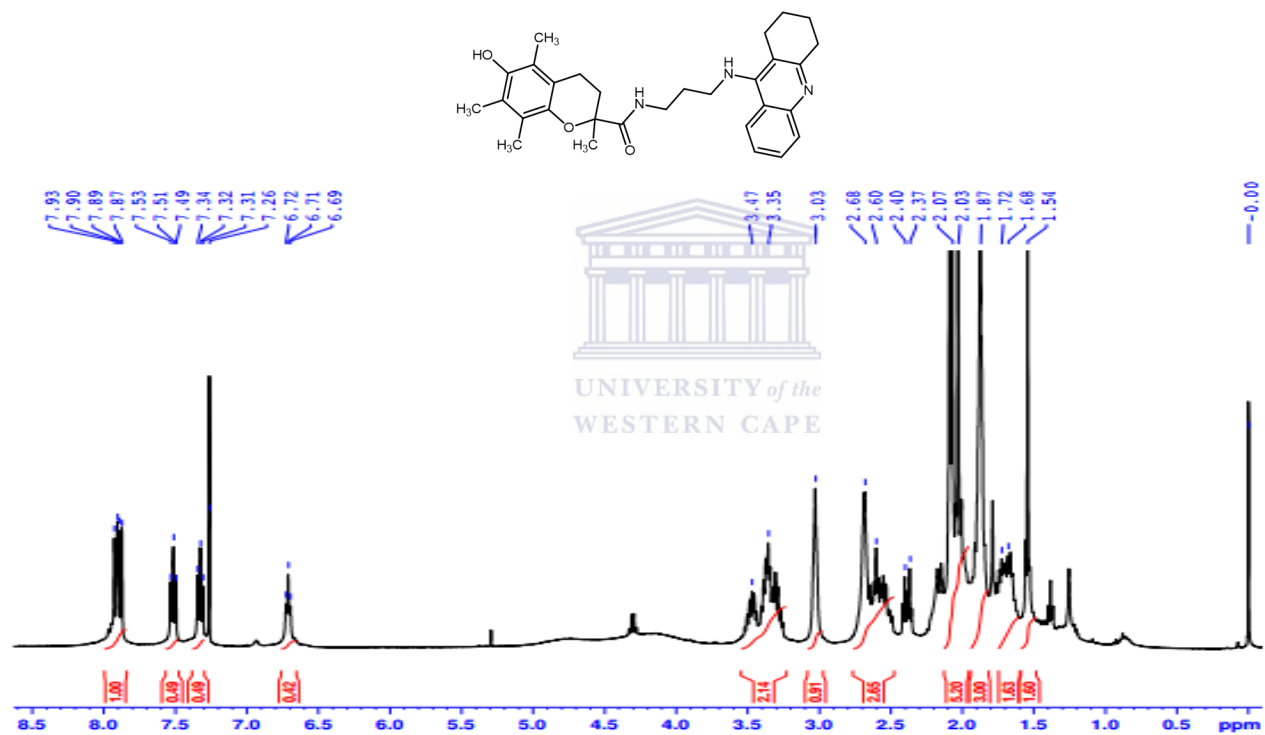
Spectrum 2b: ^{13}C NMR
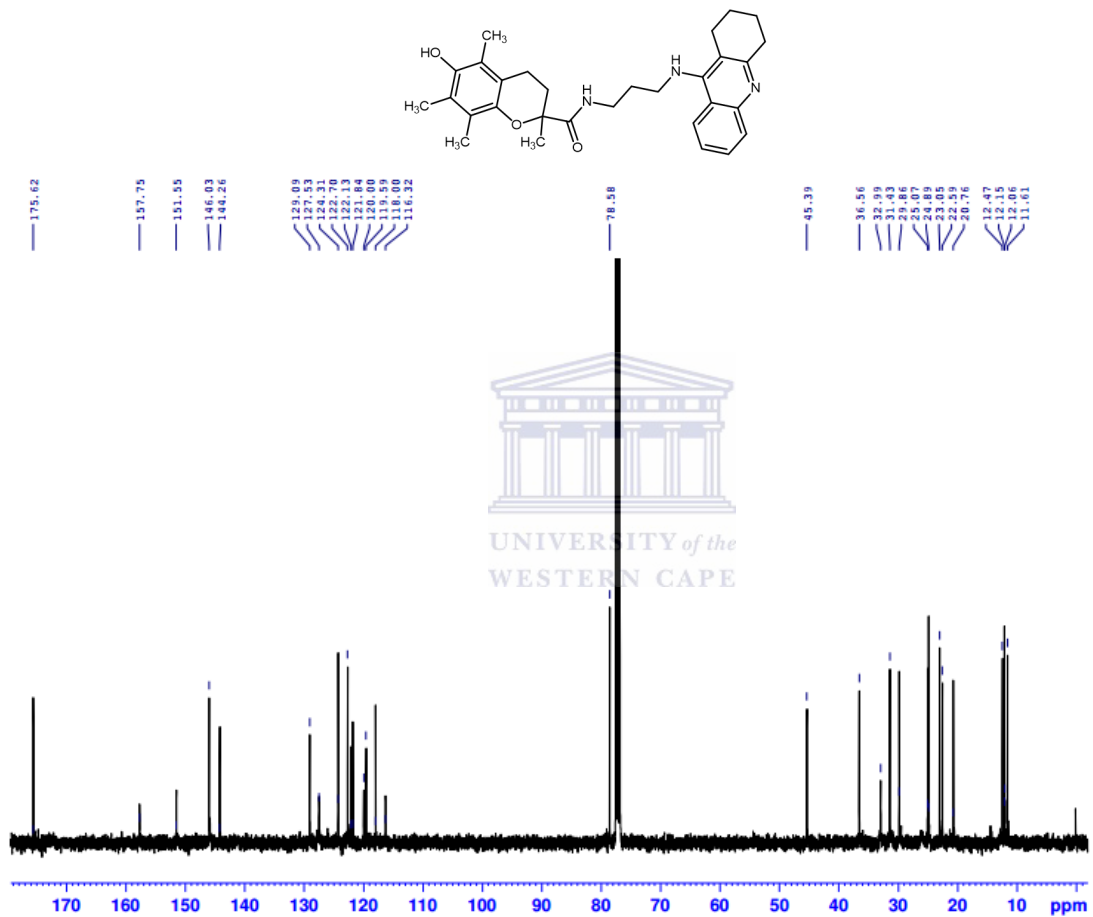
Spectrum 2c: MS
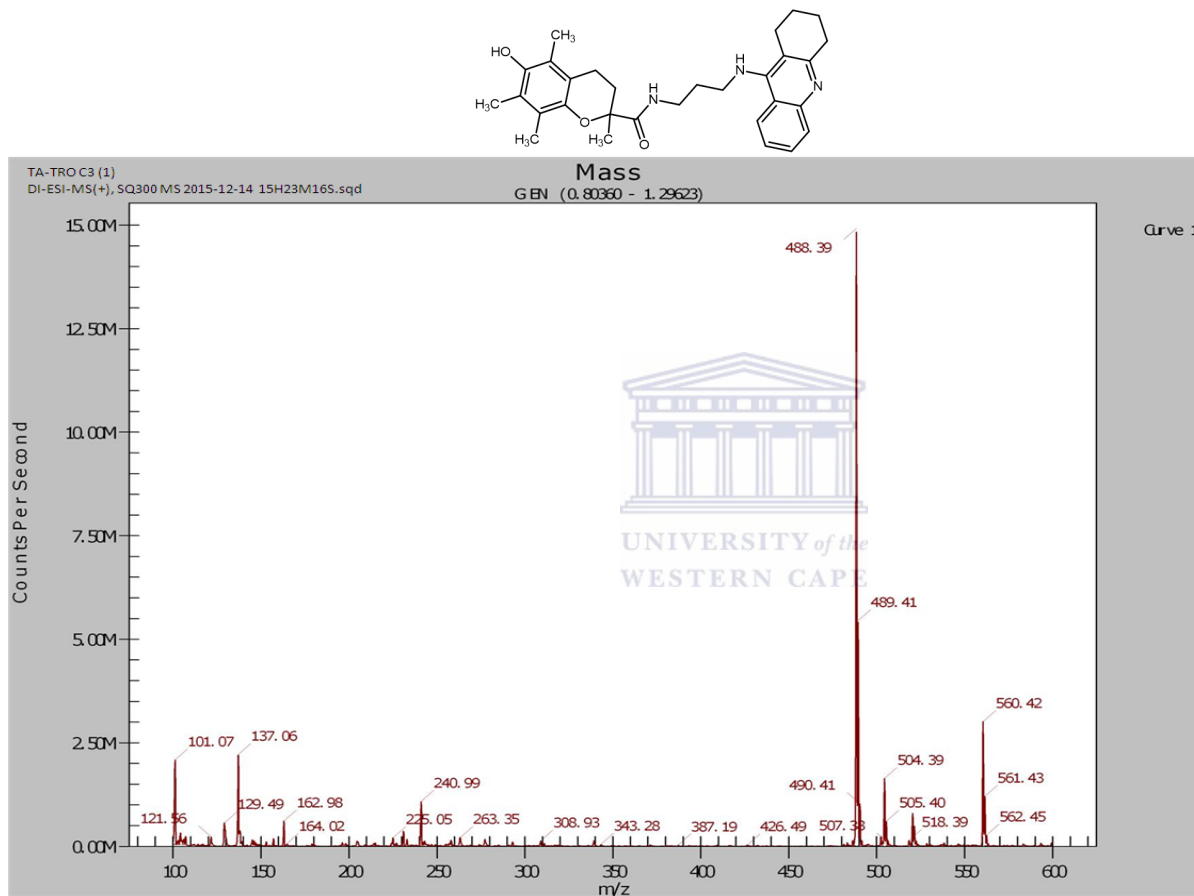
Spectrum 2d: IR
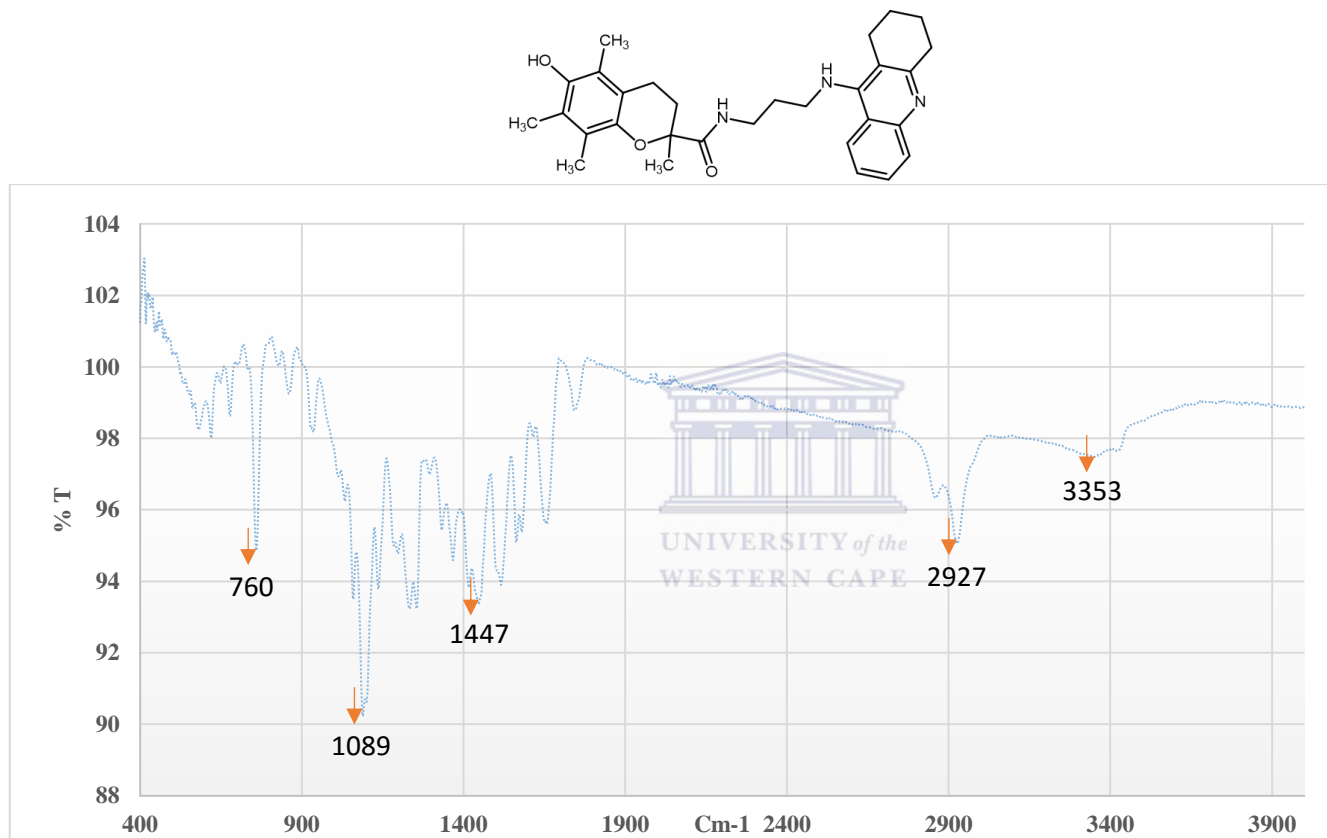
Spectrum 3: *6-Hydroxy-2,5,7,8-tetramethyl-N-{4-[(1,2,3,4-tetrahydroacridin-9-yl)amino]butyl}-3,4-dihydro-2H-1-benzopyran-2-carboxamide* (**8c**).

Spectrum 3a: ^{1}H NMR
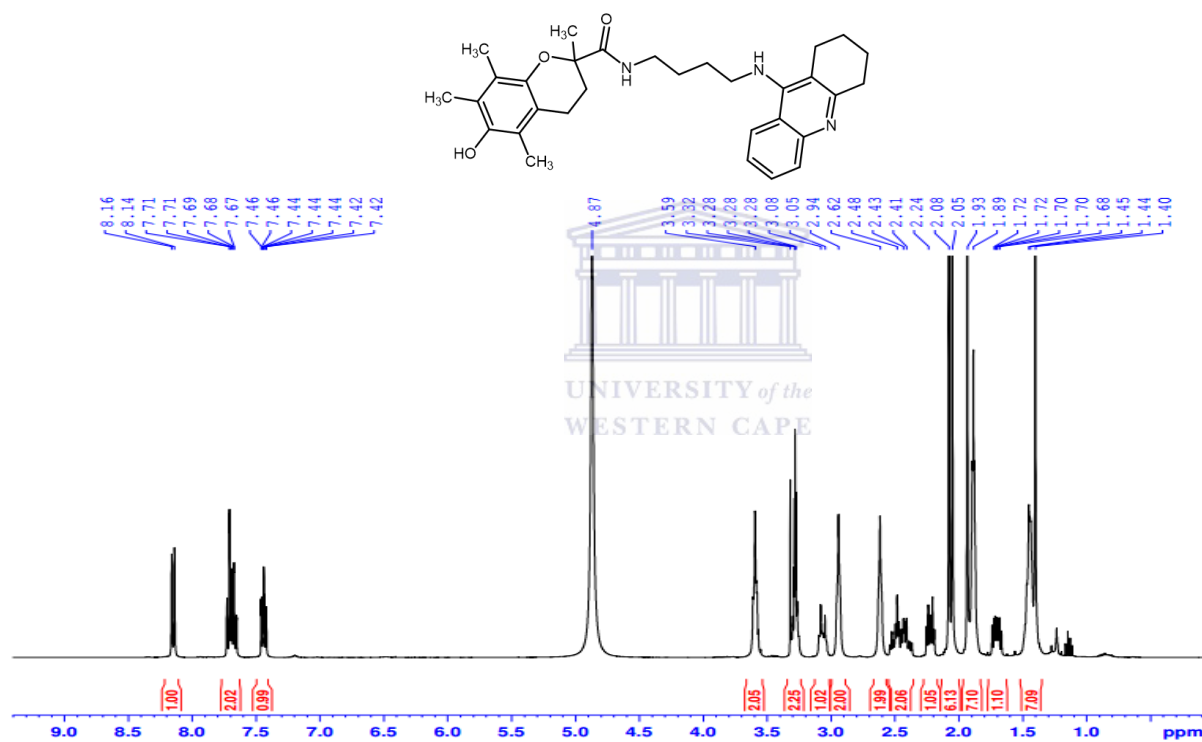
Spectrum 3b: ^{13}C NMR
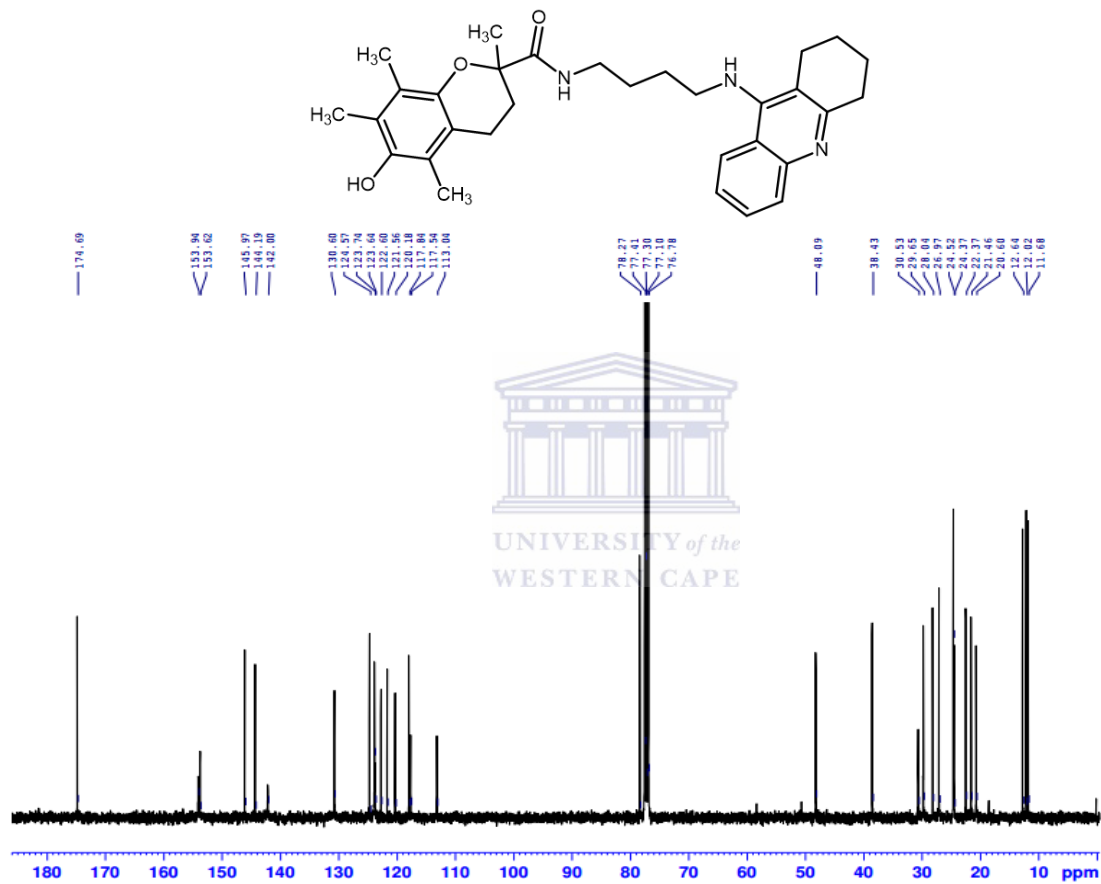
Spectrum 3c: MS
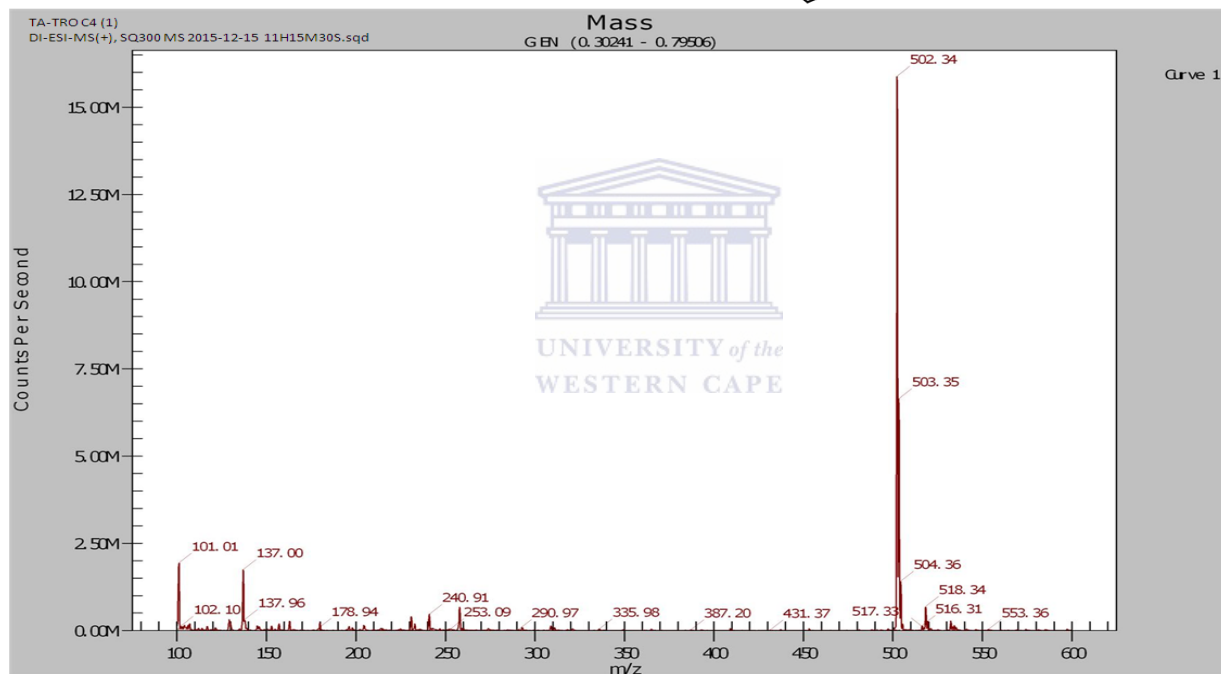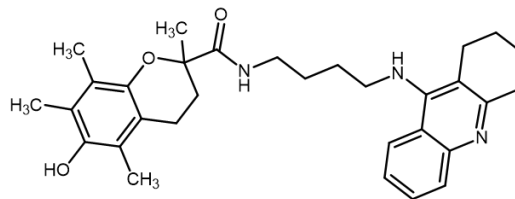
Spectrum 3d: IR
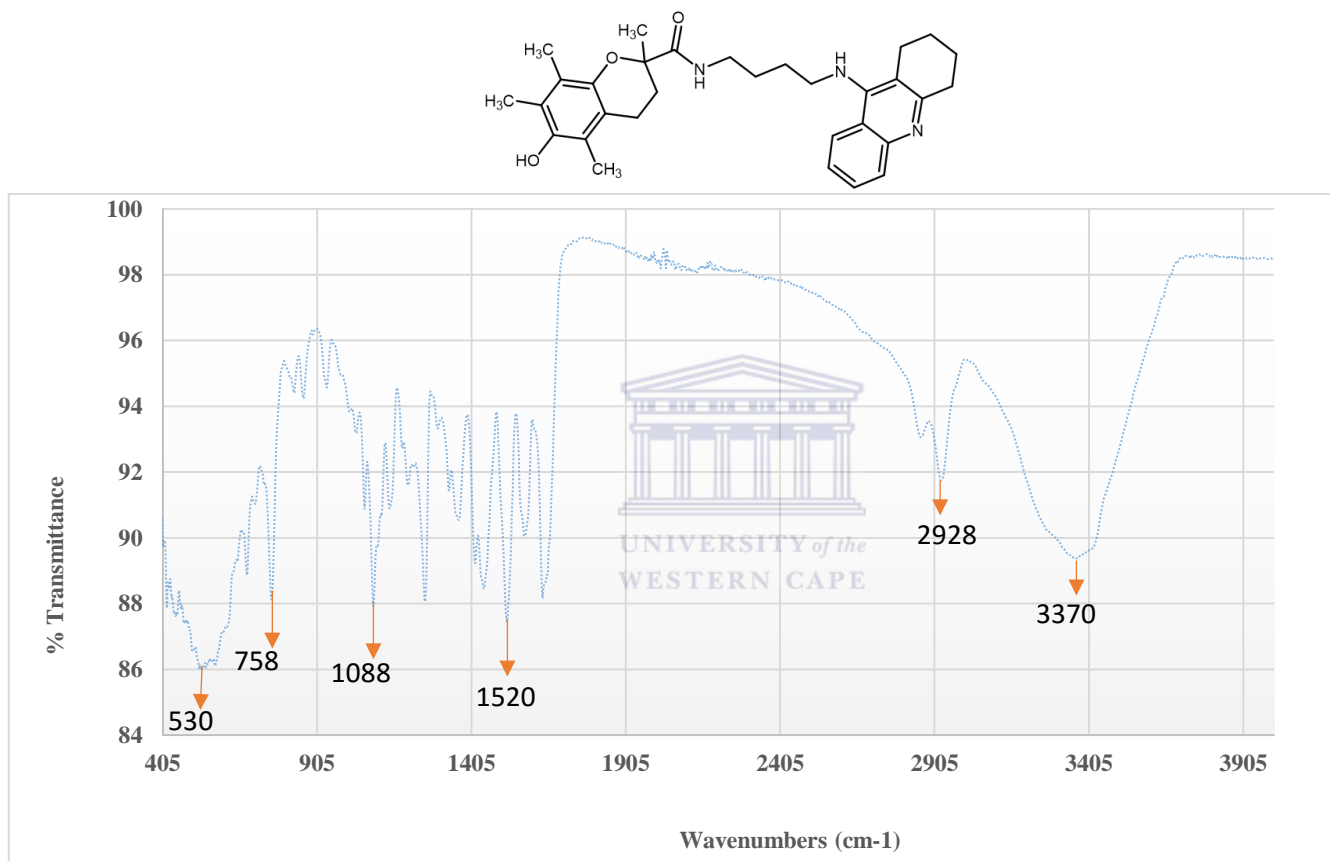
Spectrum 4: *6-Hydroxy-2,5,7,8-tetramethyl-N-{6-[(1,2,3,4-tetrahydroacridin- 9-yl)amino]hexyl}-3,4-dihydro-2H-1-benzopyran-2-carboxamide* (**8d**).

Spectrum 4a: ^{1}H NMR
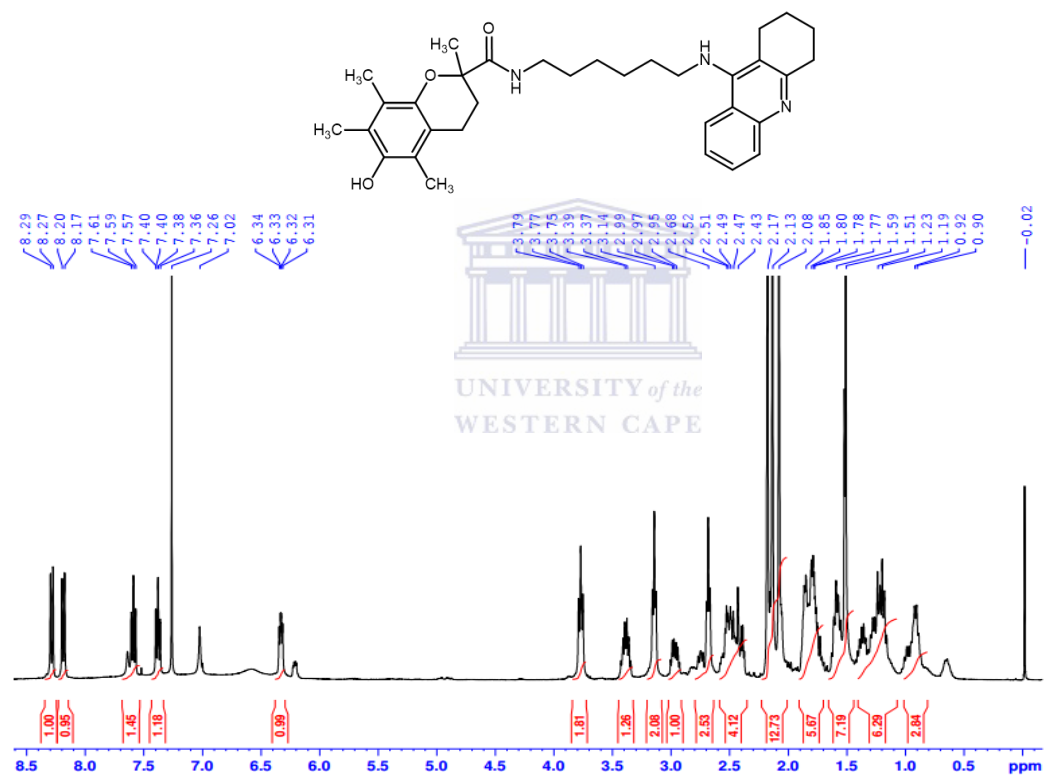
Spectrum 4b: ^{13}C NMR
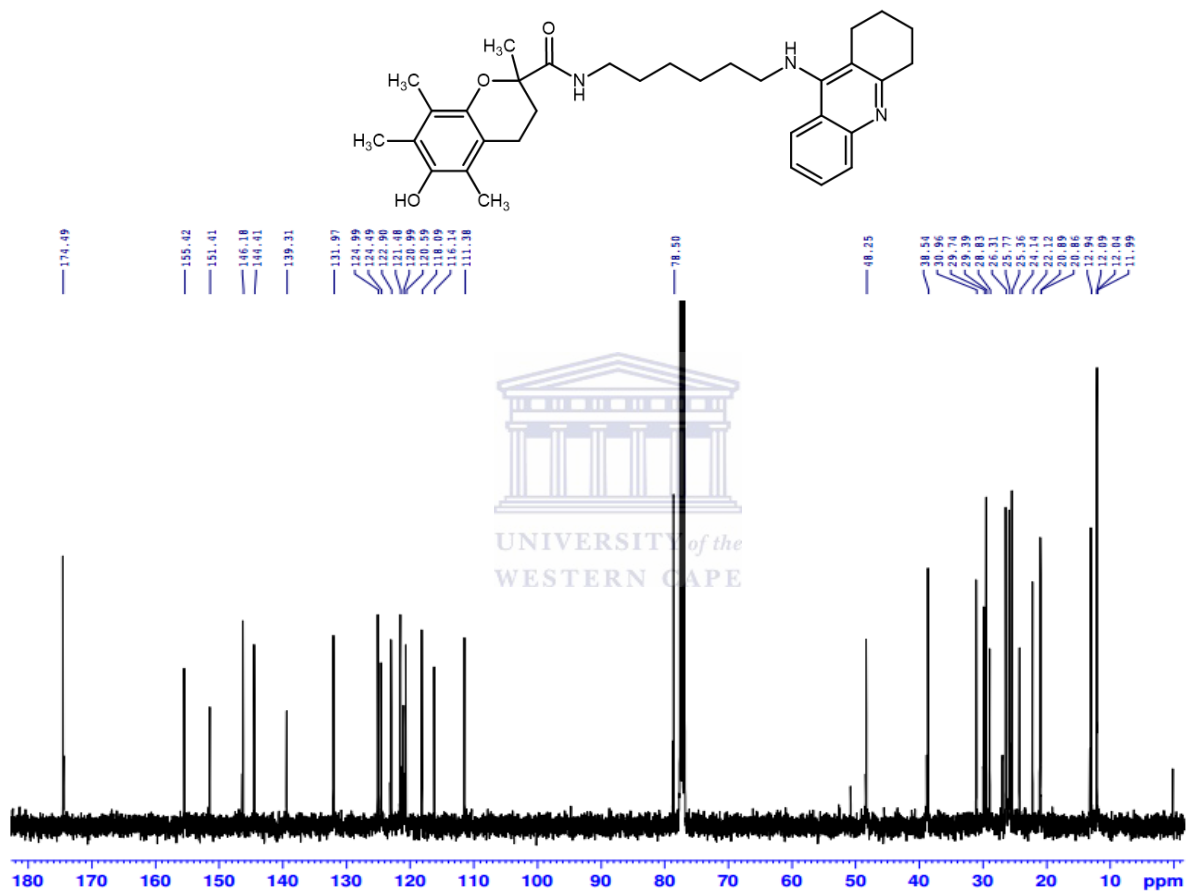
Spectrum 4c: MS
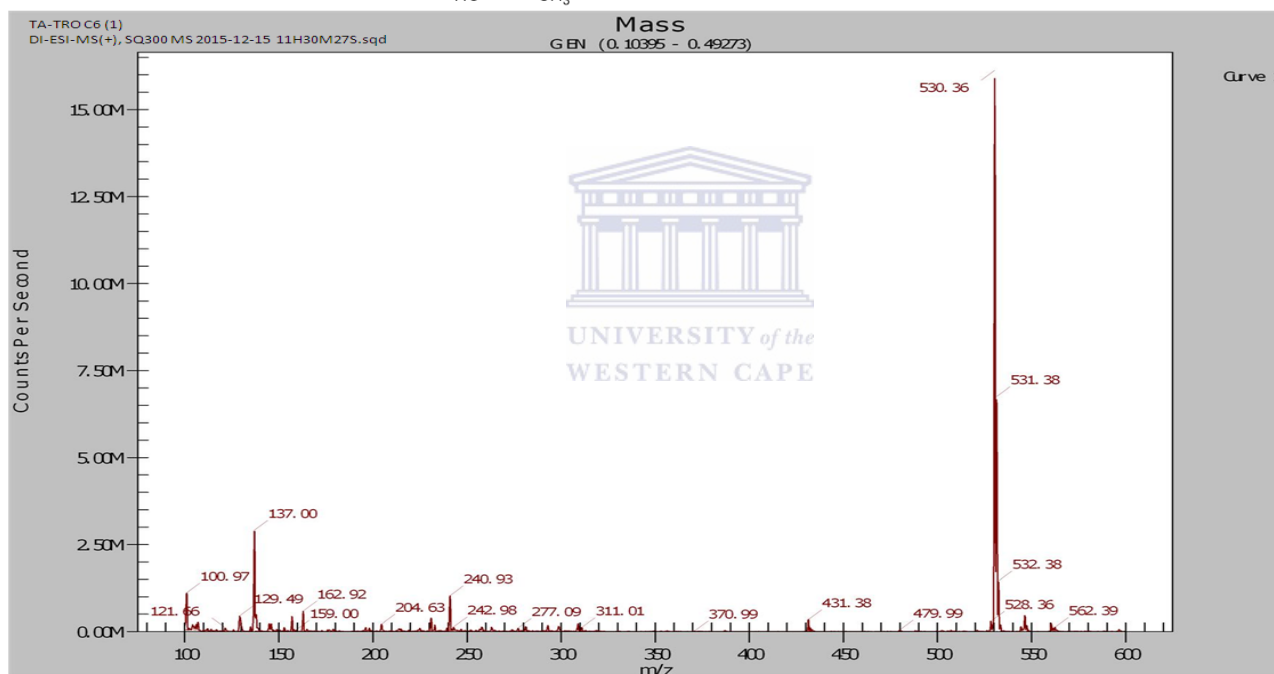
Spectrum 4d: IR

Spectrum 5: *6-Hydroxy-2,5,7,8-tetramethyl-N-{8-[(1,2,3,4-tetrahydroacridin- 9-yl)amino]octyl}-3,4-dihydro-2H-1-benzopyran-2-carboxamide* (**8e**).

Spectrum 5a: ^{1}H NMR

Spectrum 5b: ^{13}C NMR

Spectrum 5c: MS

Spectrum 5d: IR

Spectrum 6: *N-(7-(3,4-dihydro-1H-pyrido[3,4-b]indol-2(9H)-yl)heptyl)-1,2,3,4-tetrahydroacridin-9-amine* (**14**).
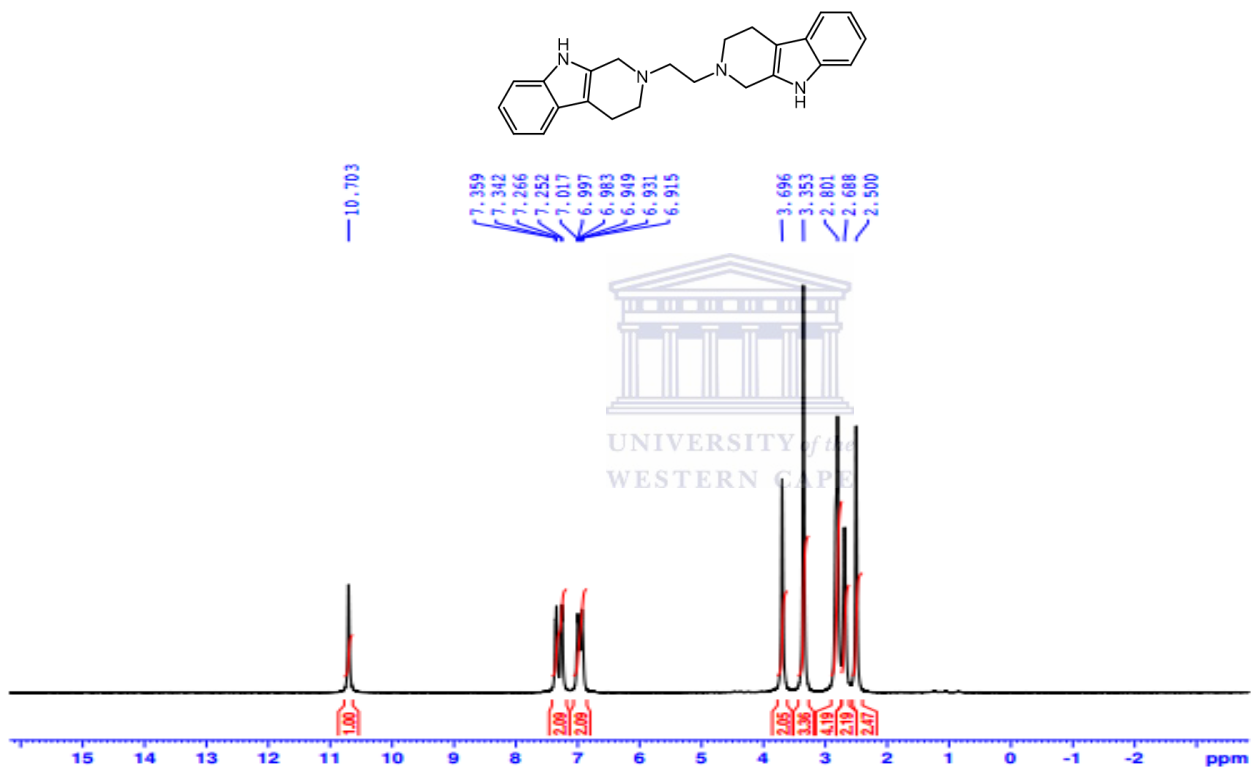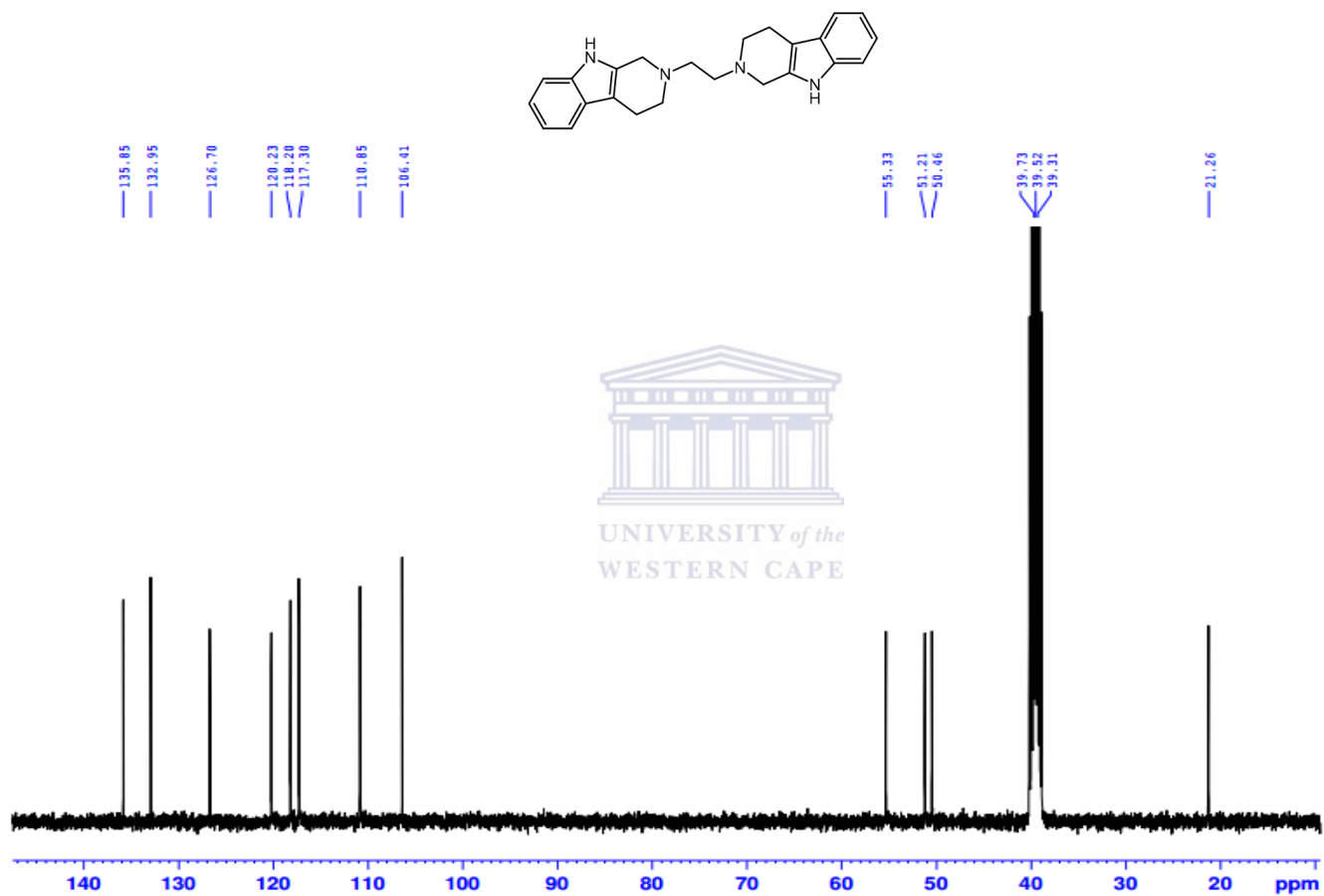
Spectrum 6a: ^{1}H NMR
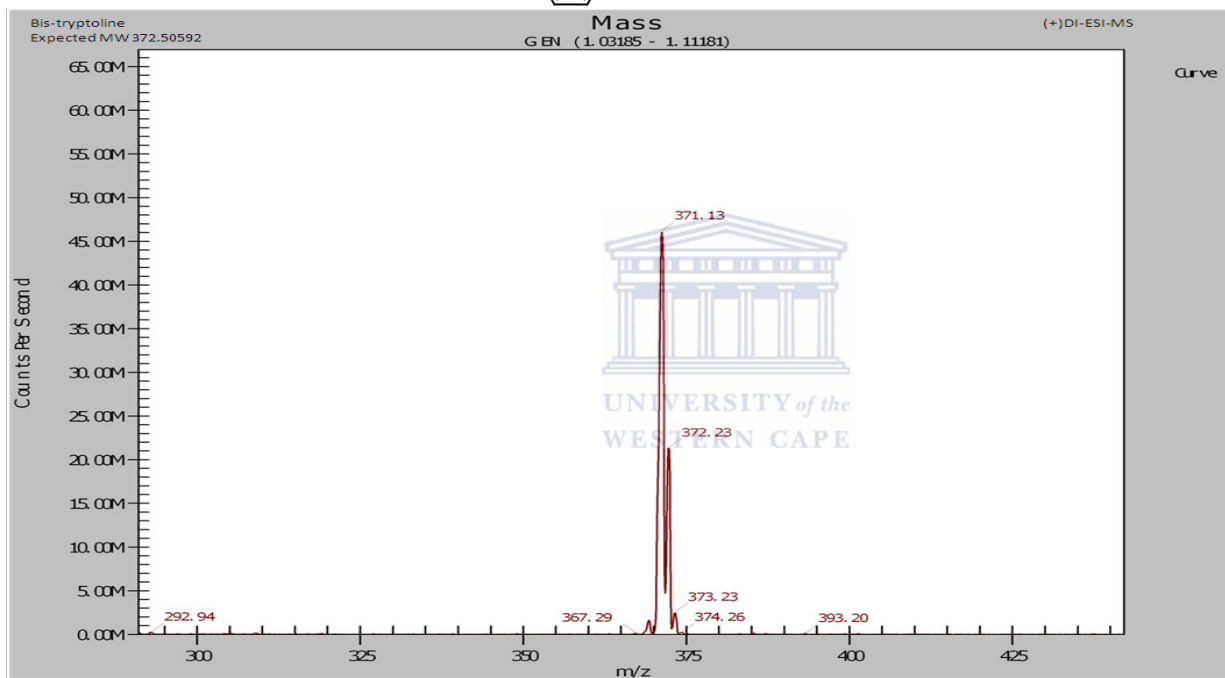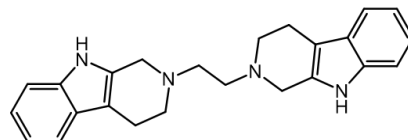
Spectrum 6b: ¹³C NMR
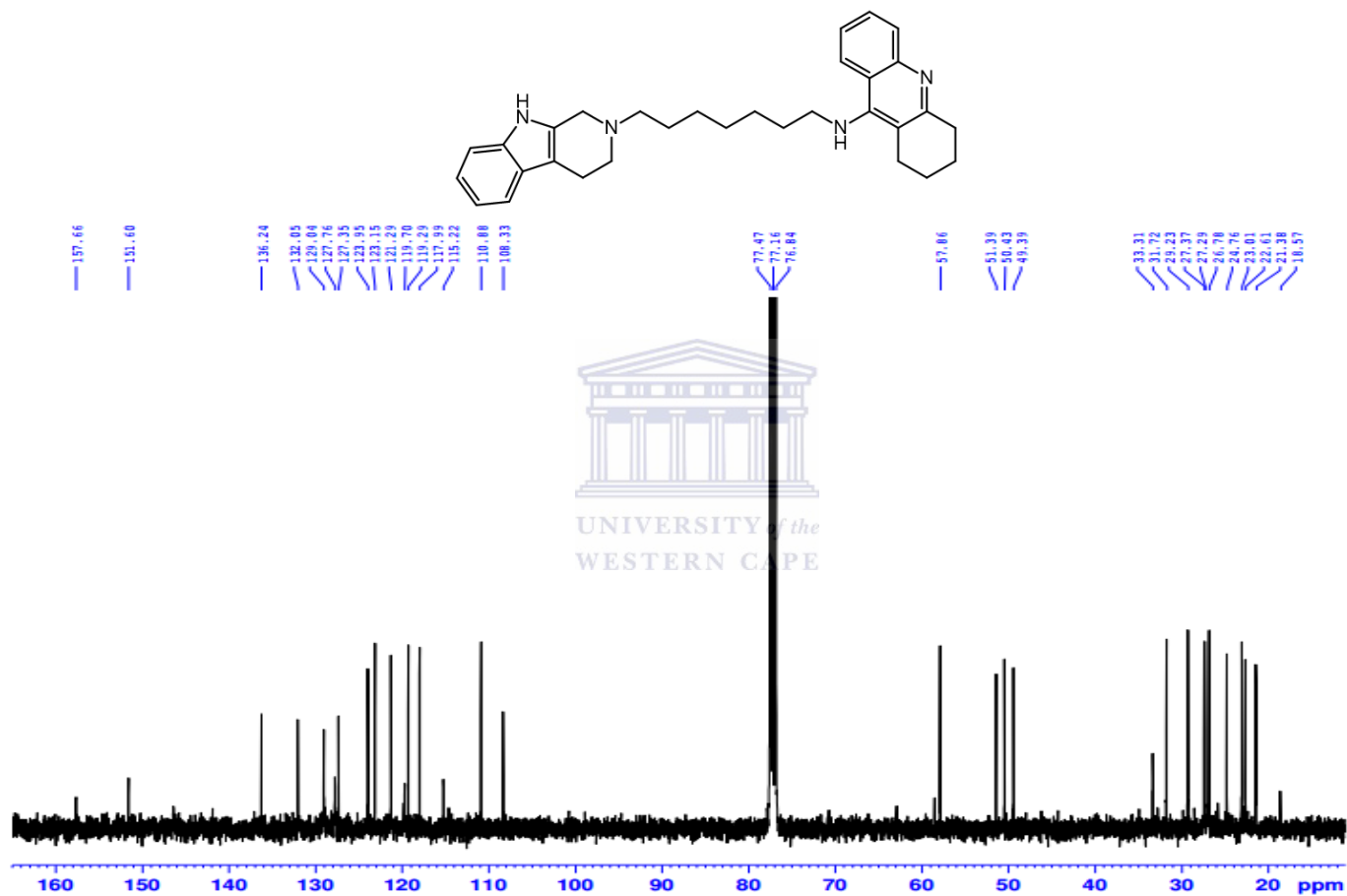
Spectrum 6c: MS
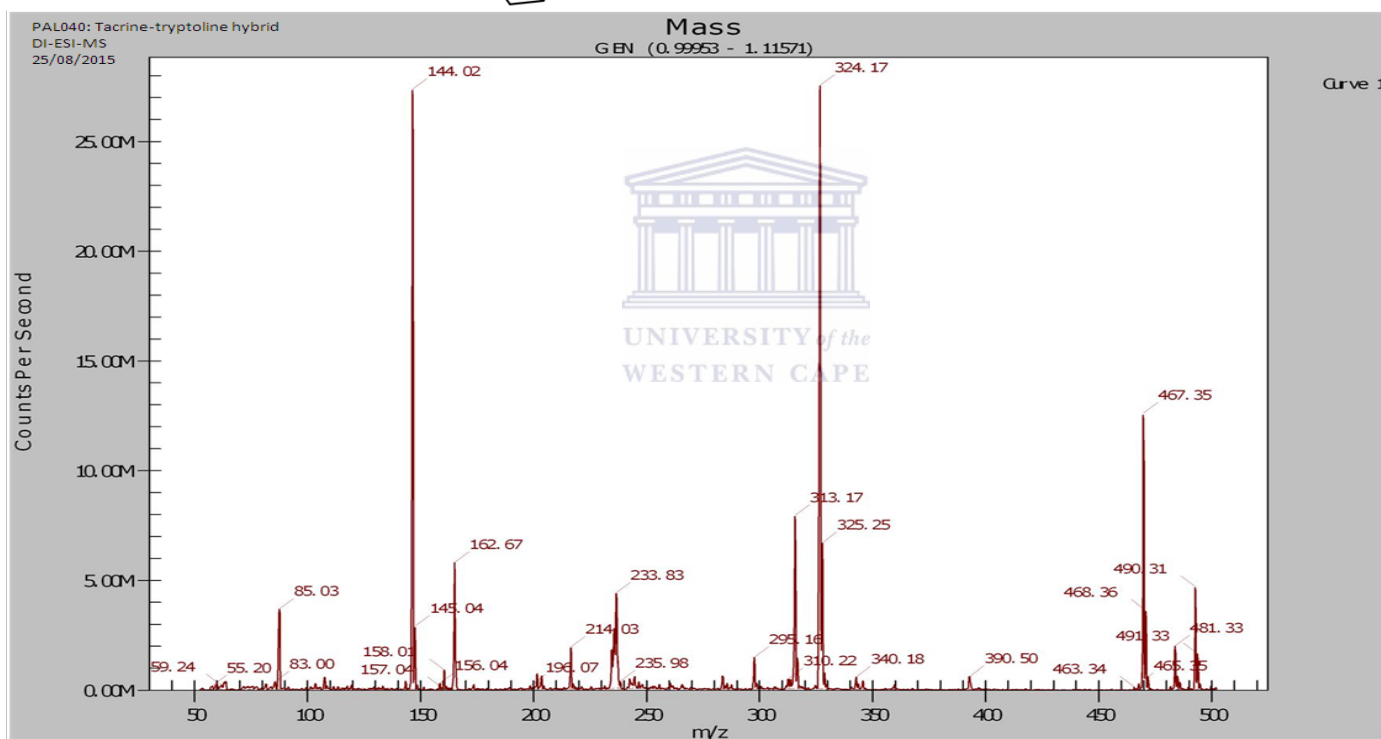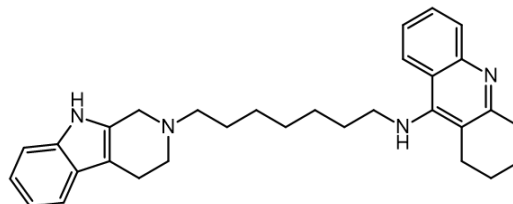
Spectrum 6d: IR
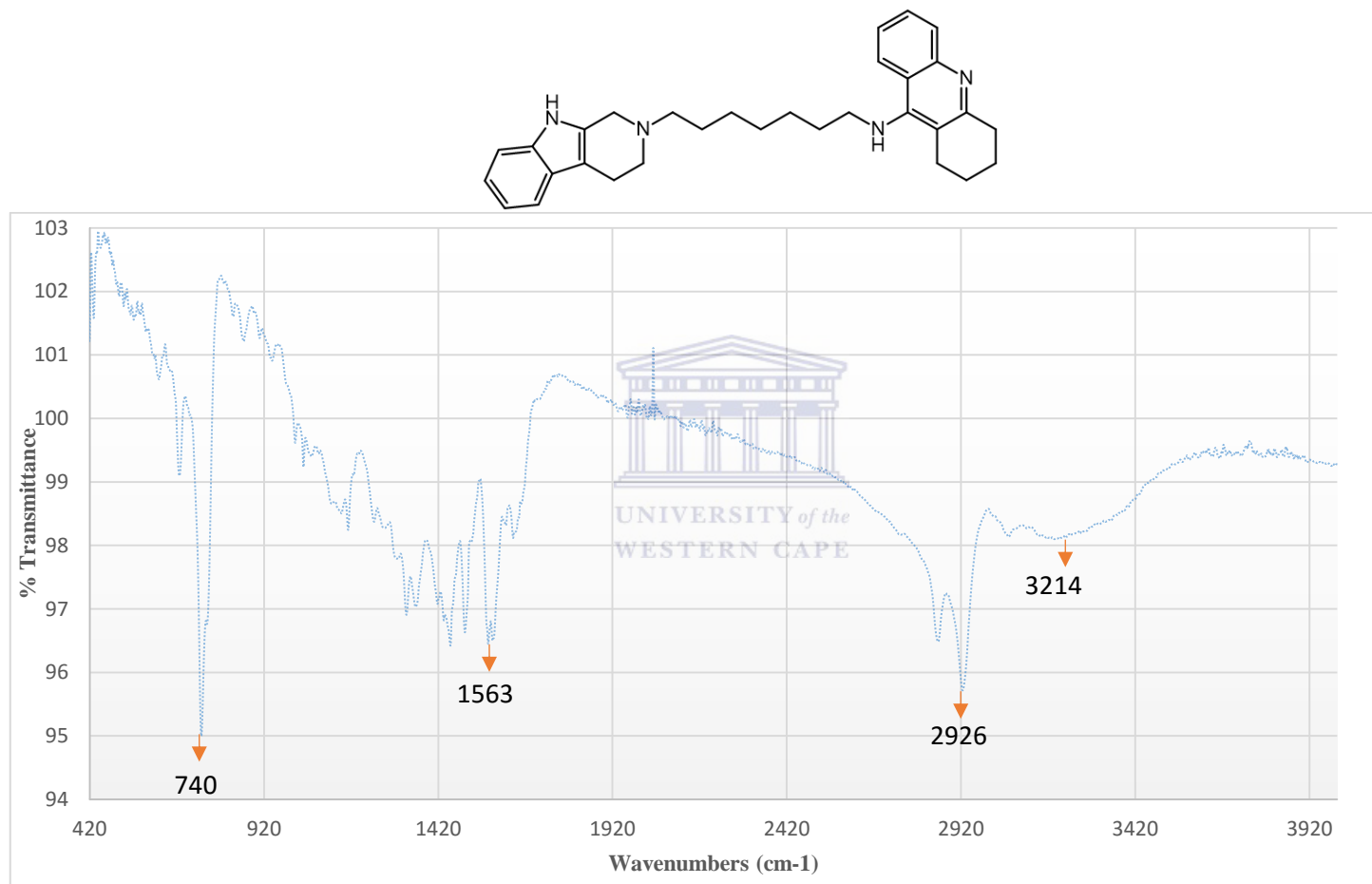
Spectrum 7: *1,2-bis(3,4-dihydro-1H-pyrido[3,4-b]indol-2(9H)-yl)ethane* (**16**).

Spectrum 7a: ^{1}H NMR

Spectrum 7b: ^{13}C NMR

Spectrum 7c: MS

Spectrum 7d: IR